IDENTIFICATION OF HIGH PERFORMANCE AND COMPONENT TECHNOLOGY FOR SPACE ELECTRICAL POWER SYSTEMS FOR USE BEYOND THE YEAR 2000

FINAL TECHNICAL REPORT

NASA GRANT NO. NAG-3-714

PRINCIPAL INVESTIGATOR: JAMES E. MAISEL

PERIOD COVERED: 5-16-86 TO 12-15-88

(NASA-CR-183003) IDENTIFICATION OF HIGH PERFORMANCE AND COMPONENT TECHNOLOGY FOR SPACE ELECTRICAL POWER SYSTEMS FOR USE BEYOND THE YEAR 2000 Final Technical Report, 16 May 1986 - 15 Dec. 1988 (Arizona State
N89-11807
Unclas
G3/20 0174642

ARIZONA STATE UNIVERSITY
TEMPE, ARIZONA 85287-6606

TABLE OF CONTENTS

	Page
Abstract	i
Preface	ii
A Brief Historical Overview of Some U.S. Manned/Unmanned Spacecraft Power Systems	1.1
General Topological Characteristics of Terrestrial/Space Power Systems	2.1
Radiator Mass Trade-Off With System Temperature	3.1
General Electrical Characteristics of Terrestrial/Space Power Systems	4.1
Adaptive/Expert Power Systems	5.1
Radiator Surface Area Reduction By Increasing System Efficiency or Operating Temperature	6.1
The Behavior of Transmission Line Mass and Temperature As a Function of Transmission Line Efficiency	7.1
Voltage Regulation and Its Effect on Transmission Line Parameters	8.1
High Temperature Electronic Materials	9.1
High Power Vacuum Switching Devices	10.1
Optimal Operation of Electric Power Systems	11.1
System Reliability	12.1
Effect of Reducing The Spatial Separation Between The Electrical Heat Source and The Electronic Power Converter	13.1
System Specific Mass, Reliability and Operational Temperature and Their Interactions	14.1
Tradeoffs In System Availability	15.1
Concluding Remarks	16.1
Bibliography	17.1

ABSTRACT

This report addresses some of the space electrical power system technologies that should be developed for the U.S. space program to remain competitive in the 21st century. A brief historical overview of some U.S. manned/unmanned spacecraft power systems is discussed to establish the fact that electrical systems are and will continue to become more sophisticated as the power levels approach levels comparable to terrestrial electrical power systems.

Adaptive/Expert power systems that can function in an extraterrestrial environment will be required to take the appropriate action during electrical faults so that the fault impact is minimal. Manhours can be reduced significantly by relinquishing tedious routine system component maintenance to the adaptive/expert system. By cataloging component signatures over time this system can set a flag for a premature component failure and thus possibly avoid a major fault. High frequency operation is important if the electrical power system mass is to be reduced significantly. High power semiconductor or vacuum switching components will be required to meet future power demands.

System mass tradeoffs have been investigated in terms of operating at high temperature, efficiency, voltage regulation, and system reliability. It appears that high temperature semiconductors will be required. Silicon carbide materials will operate at temperature around 1000°K and the diamond material up to 1300°K. The driver for elevated temperature operation is that radiator mass is reduced significantly because of inverse temperature to the fourth power.

This report includes a comprehensive bibliography on the various topics covered.

PREFACE

One of the earliest unmanned space programs involved the Pioneer Project. The electrical power system was capable of delivering approximately 150 watts of electrical power that derived its energy from a set of radioisotope thermoelectric generators that were mounted in pairs at the end of each of two extended booms.

More than thirty years later a space station will be launched with an initial power system capable of generating approximately 75 kw using a photovoltaic system for the energy source. As the station develops to its full potential, a set of solar dynamic generators will be added. Focusing the sun's energy to heat a fluid that will drive turbine-alternator systems, the power output level of the combined electrical systems will eventually reach a power level of approximately 300 kw. Thus within a relatively short time frame of approximately thirty years the power demand has increased by a factor of 2000. This power increase trend will accelerate beyond the year 2000.

Because personnel will be part of the space vehicle system, their welfare will be strongly coupled to the reliability of the power system. A space colony located on another heavenly body, such as the Moon, will demand electrical power that has characteristics similar or better than provided by terrestrial power systems. As the power output increases the power system will adopt features that is found in terrestrial electrical systems. Higher operating voltage and frequency are two drivers needed to reduce the electrical power system mass.

Like its Earth's counterpart, the extra-terrestrial system will experience user power demands and component failures. However, a catastrophic failure in space could be tantamount to loss of personnel and the entire system, so extra precautions must be taken to ensure the best reliable power system possible. Because the power system is at the focal point of importance, it must be designed to operate in an almost autonomous mode with a minimum number of personnel involved with its daily operation. Using appropriate fault and premature signature failure detectors that are coupled to a computer network, expert computer software will continuously observe the power system for any telltale signs of impending failures and develop an appropriate strategy to minimize any impact that may occur. Personnel will be notified before any major decision is made by the expert system. It is to be noted that if the power system's operating frequency is approximately 20 KHZ or higher, the expert system, failure detectors, premature signature failure analysis will have to have a fast response to ward off serious power system failures.

There is a design trend to operate space systems, whether electrical or not, at higher temperatures in order to reduce the size of the radiator's surface. Unless technology raises the boundries of high temperature materials, the impact of mass savings may not be as great as anticipated. Also, system reliability tends to decrease with increasing system temperatures. Great effort must be made to maintain or increase system reliability at high temperatures.

Since it is important to have that portion of the electric power system consisting of the energy source and power frequency converter as close to each other as possible, semiconductor electronic devices will have to operate at temperatures much higher than today's standards. Wide-bandgap materials, such as the carbide and diamond family, will have to be developed, not only to withstand the high temperature environment, but also to be insensitive to all forms of radiation damage.

For power systems approaching the typical power level on Earth, high power vacuum switching should be developed as an option since there is no crystalline structure to be damaged by heat or radiation. Results show that it is possible to interrupt several thousand amperes with less than 50-volt switch voltage with a frequency approaching 1 MHZ.

The structure of this report consists of a set of chapters that addresses topics that this author deems important for a successful space program in the 21st century. The author is also aware of the fact that these topics are not all inclusive and that they should be treated as topics that must be expanded upon to enhance the necessary technology that would be developed by experts in their respective fields. A bibliography was added for those who care to learn more about a particular topic.

Chapter 1

A BRIEF HISTORICAL OVERVIEW OF SOME U.S. MANNED/UNMANNED SPACECRAFT POWER SYSTEMS

As the Space Program moves towards the 21st century, space power levels will increase dramatically with levels reaching multi-kilowatts to megawatts. The transmission distances between the power sources and electrical loads will increase correspondingly with increased power demand.

In order to accommodate these high power levels, Power Management and Distribution (PMAD) architecture designers will have to focus their attention on the following important design considerations:

- Systems operating voltage
- Power systems frequency
- Power system loss
- Power system cost
- Power system reliability
- Total power system mass
- Total PMAD volume
- Power system operating temperature.

The above listing is obviously not complete, but does reflect the fact that in the end, the PMAD architecture is a multi-dimensional problem and each dimension must be considered in order to maintain a reasonable specific mass (kg/kw) for the PMAD system.

Looking back in time, the evolution of power sources for space applications came in a series of steps depending on the available technology at the time of demand. Initially, PMAD was strongly influenced by the design philosophy used in the aviation industry where most of the electrical loads were dedicated. Electrical power system design changed as the planes increased in size. However, the electrical system operating voltage remained at approximately the same value (28 volts dc) for a long time. The voltage level remained in this range because the total plane's power demand was relatively low compared to the projected space station need that is anticipated in the 21st century.

In order to better understand what will be required for the future PMADs, a brief historical look at PMAD's that were used in some of the U.S. manned and unmanned missions or projects will be reviewed. Not all U.S. power systems used in the space programs could be investigated because this would involve hundreds of different missions, especially in the unmanned segment of the space program. The unmanned space missions that were chosen were based on the impact their electrical power systems had on the manned mission. This is not to say, that other U.S. unmanned missions did not contribute to the overall manned space program. Each space mission expanded our knowledge of the universe and permitted technological barriers to be crossed.

A summary is presented in Table 1.1 to bring the results into focus. Details of the electrical power system structure of U.S. manned and unmanned spacecraft are presented elsewhere [1.1]. The summary lists the U.S. manned space program first, because it will be the greatest driver in the design of manned future space station PMAD systems.

A brief description of the electrical system will be given for each mission or project listed in TABLE 1.1. The descriptions and the summary in TABLE 1.1 should aid the reader in understanding how the salient features of a spacecraft power system grew over the last quarter of a century.

Project Mercury had silver-zinc batteries that were non-rechargeable as the prime source of power. This configuration is very expedient at a time when it was of paramount importance to have a spacecraft reach and maintain an orbital path. Because the flight time duration was short and the power demand was low, it was not necessary to have a secondary source of power on board the spacecraft. Conversion from dc to ac was necessary in order to operate the gyro motors and other motors aboard the spacecraft.

In the early stages of Project Gemini, the main power source was silver-zinc batteries because fuel cells were not reliable at the time. In later missions, however, fuel cells replaced the batteries allowing the flight duration to be increased from hours to days. Besides providing electrical power, the fuel cells supplied, in the form of a by-product, he required water needed to sustain the crew during the mission.

Fuel cells were the main source of electrical energy for the Apollo Program, with silver oxide-zinc batteries serving as the secondary power source. Again, inverters were necessary for the electrical motors in the spacecraft. The combination of fuel cells and batteries on the Apollo spacecraft provided an ample amount of electrical power for the round trip to the Moon.

Projects Mercury and Gemini and the Apollo Program were the underpinnings for the Skylab Project. This spacecraft used the fuel cell technology from the two previous programs and solar arrays for the main source of electrical power with nickel-cadmium batteries serving as the secondary power source. This combination of electrical sources allowed for extended flight duration, well over 150 days.

Finally, the Space Shuttle Program, plus Spacelab, moved PMAD technology one step closer to the PMADs that will be used on future space stations. Because the Space Shuttle was designed to have long flight durations, fuel cells became the main source of power. Two of the three fuel cells on board the Shuttle had sufficient power capacity to supply all the required power. The third fuel cell supplied dc power to Spacelab. Using a set of inverters, Spacelab provided 220 and 115 volts at 50 and 60 hertz, respectively, as well as 115 volts at 400 hertz.

The culmination of the manned space programs may not have moved as rapidly in time if it were not for the parallel unmanned space program. These spacecrafts, acting as space probes, permitted measurements to be conducted on the kind of environment that the astronauts would face in the manned program. Since human life was not a primary concern in the design of an unmanned spacecraft, such items as life support during flight were not necessary. Also, the power level demand in the unmanned spacecraft was considerably lower as compared to a manned spacecraft.

The Pioneer Missions could be divided into two destinations both outer planetary, such as Jupiter/Saturn, and Venus Missions. Each had different primary power sources. For the case of the outer planetary missions, a radioisotope thermoelectric generator was used because the amount of sunlight in the vicinity of Jupiter and Saturn was far less than near Earth. Besides supplying electrical power, the radiosotope thermoelectric generator also provided a source of heat to control the temperature of the spacecraft.

The main source of power in the Mariner-Venus Program inner planetary destinations was the solar array, with silver-zinc or nickel-cadmium batteries as the secondary source, depending on the particular Mariner Mission. The number of solar array panels varied from mission to mission. For example, mariner 9 and 10 had 4 and 2 panels, respectively.

Ranger, Lunar Orbiter, and Surveyor Projects formed a group of missions to investigate the environment and surface characteristics of the Moon. These three missions laid the foundation for the Apollo Program. Because of the ample amount of sunlight near the Moon, solar arrays were used in all three missions with the secondary source being silver-zinc and nickel-cadmium batteries for the Ranger/Surveyor Projects and Lunar Orbiter Program, respectively.

The spacecraft used in the Viking Project consisted of the Viking Orbiter and Lander. The main and secondary power sources for the Orbiter were, respectively, solar panels and nickel-cadmium batteries. The main source of power for the Viking Lander was the Radioisotope thermoelectric generator which supplied the necessary electrical power as well as thermal energy to control the temperature of the Lander.

Likewise, the Voyager spacecraft received its main power from a radioisotope thermoelectrical source. Instead of using batteries as a secondary source, charged capacitors served as energy storage. This increased the life span of the secondary source almost indefinitely.

Results indicate that the main distribution voltage for the manned spacecraft was regulated/unregulated 28 volts dc with inverters supplying 115 or 220 volts, 50/60/400 Hertz, and single or three phase. Batteries, fuel cells, and solar arrays were the main power sources and batteries the backup or secondary sources. The unmanned spacecraft main operating distribution voltage was below 60 volts dc with inverters to supplying the necessary ac voltage. Solar arrays and radioisotope thermoelectric generators were the main electrical power sources and silver-zinc/nickel-cadmium batteries were the secondary sources.

TABLE 1.1. SUMMARY OF ELECTRICAL POWER SYSTEMS USED IN MANNED/SOME UNMANNED SPACECRAFTS

I. MANNED SPACECRAFTS

Project Mercury

Main Power Source: silver-zinc batteries (non-rechargeable)
D.C. Bus Voltage: 24 volts
Inverters: 115 volts, 400 hertz, single phase, 250 and 150 volt-amperes

Project Gemini

Main Power Source:

A. silver-zinc batteries (non-rechargeable)
D.C. Bus Voltage: 22/30 unregulated

B. fuel cells
D.C. Bus Voltage: 22/30 unregulated

Apollo Program

Main Power Source: fuel cells
Secondary Power Source: silver-oxide-zinc batteries (rechargeable)
D.C. Bus Voltage: 28 volts (nominal)
Inverters: 115/200 volt, 400 hertz, three-phase, 1250 volt-amperes

Space Shuttle Program

Main Power Source: fuel cells
D.C. Bus Voltage: 28 volts (unregulated)
Inverters: 117 volts at 400 hertz

Spacelab

Main Power Source: one fuel cell from Space Shuttle Orbiter
Secondary Power Source: Peak power battery (flown on request)
D.C. Bus Voltage: 27/32 volts dc (unregulated)
Inverters: 220 volts at 50 hertz, 115 volts at 60 hertz, 115 volts at 400 hertz

II. SOME UNMANNED SPACECRAFTS

Pioneer Missions

A. Pioneer Jupiter/Saturn Mission
Main Power Source: radioisotope thermoelectric generator
Secondary Power Source: silver-cadmium batteries (rechargeable)
D.C. Bus Voltage: 28±2% volts
Inverters: 30.5 volts, 2500 hertz, trapezoidal waveform

B. Pioneer Venus Mission
Main Power Source: solar array
Secondary Power Source: nickel-cadmium batteries rechargeable via a small solar array
D.C. Bus Voltage 28±10% volts (semiregulated)

Mariner Program

Main Power Source: solar array
Secondary Power Source: silver-zinc or nickel-cadmium batteries depending on particular mission
D.C. Bus Voltage: 30 or 56 volts depending on particular mission
Inverters: 50-volts, 2400 hertz, single-phase, square-wave
28-volts, 400 hertz, single-phase
27.2 volts, 400 hertz, three-phase depending on particular mission

Ranger Project

Main Power Source: solar arrays
Secondary Power Source: silver-zinc batteries
D.C. Bus Voltage: 25.5 volts regulated

Lunar Orbiter Program

Main Power Source: solar arrays
Secondary Power Source: nickel-cadmium batteries rechargeable
D.C. Bus Voltage: 20-volt regulated

Surveyor Project

Main Power Source: solar array
Secondary Power Source: silver-zinc batteries rechargeable
D.C. Bus Voltage: 29 volts±0.29 volts regulated; 17-27.3 unregulated

Viking Project

A. Viking Orbiter
Main Power Source: solar arrays
Secondary Power Source: nickel-cadmium batteries

D.C. Bus Voltages: 55.2±6% regulated
25 - 50 unregulated
30±5% regulated
A.C. Bus Voltages: 27.2±6% regulated
50+3% or -4% regulated
Inverters: 27.2-volt, 400 hertz, three-hase, 12 watts
50-volts, 2400 hertz, single-hase, 350 watts
Converter: 30-volts, 90 watts

B. Viking Lander
Main Power Source: radioisotope thermoelectric generator
Secondary Power Source: silver-zinc batteries
D.C. Bus Voltage: 35.25 - 37 regulated

Voyager Mission

Main Power Source: radioisotope thermoelectric generators
Secondary Power Source: charge capacitor energy
D.C. Bus Voltage: 30 volts regulated
Inverter: 50-volt, 2400 hertz, regulated square-wave

Reference

[1.1] Maisel, J.E., "A Historical Overview of the Electrical Power Systems in the U.S. Manned and Some U.S. Unmanned Spacecraft," NASA Grant No. NAG 3-547, 1985.

Chapter 2

GENERAL TOPOLOGICAL CHARACTERISTICS OF TERRESTRIAL/SPACE POWER SYSTEMS

I. Introduction

In a general sense, the electrical space and terrestrial power systems have much in common. They both have a myriad of interrelated technical problems, such as whether the present facilities will be adequate, or whether the present distribution voltage will meet future growth. However, there are some differences between the power systems. For example, the space system transportation is costlier and human life is directly tied to its reliability.

Terrestrial and space power distribution systems take on more similar features as the output power level increases (multi-kilowatts to megawatts). This chapter will investigate the terrestrial distribution system planning in order to gain insights about space power distribution system planning.

II. Electrical Distribution Objective

Terrestrial distribution system planning is very important to an electrical utility, because the distribution system is the interface between the electrical source/main transmission line and the electrical power user (customer). Failures occurring either at the generating level or on the main transmission line level can be made transparent to the user if faults are isolated and other generating and main transmission line systems are quickly directed to pickup the faulted power demand during the fault interruption. Likewise, a user fault must be isolated so as not to disturb other loads connected to the system. The objective of any electrical distribution system planning is to guarantee that the increase demand for electrical power can be satisfied in some optimum manner.

III. Drivers Affecting Terrestrial Distribution System Planning

Perhaps the most important driver for a terrestrial distribution system is the load demand of a geographical area that is, or will be, served by the power utility. The load demand forecasting can be divided into two time periods, near and far, which are approximately 5 and 20 years, respectively.

Table 2.1 lists some of the elements that effect load forecasting [2.1]. These drivers effect both the economic and technical characteristics of the distribution system. The more information that is known about each driver, the clearer the planning strategy. As forecasting looks further into the future, less is known about the exact behavior of each driver, causing the load forecasting uncertainty to increase.

IV. Important Features Required for Distribution System Planning

The distribution system planner must incorporate the items from section III in some manner in order to develop a mathematical model that would, with a degree of accuracy, indicate the results in the near or far future.

Essentially, the distribution designer must determine the future load densities (volt-ampere per unit area), develop a pattern of transmission main and lateral lines, and determine the most economical means of energizing the distribution system.

Distribution system planning is still a highly complex problem, even when the three items stated in the previous paragraph are known. Mathematical models having a regular geometrical configuration are used to illustrate the relationship between voltage regulation, load density, and the transmission line voltage.

V. Terrestrial Distribution System Planning Models

Because the number of variables involved in planning a distribution system is inordinately large, models are employed to aid the designer in arriving at a given objective. The designer can optimize such items as feeder routes and cable size to supply a given load demand, substation location, or whether a new substation is to be constructed or to expand an existing substation.

According to [2.1] the techniques shown in Table 2.2 are presently employed by many electric utilities utilizing computer programs. Future power distribution system designs will be heavily impacted by several economic drivers such as inflation, increasing expense of acquiring new capital money, which is fueled by inflation, and the reactionary forces, which in turn are driven by inflation, that prevail when attempting to increase customer rates.

Another model input is the population shift the United States has witnessed and will continue to experience in the future. For over half a century the population shift has been from a rural environment to a metropolitan area and if another energy crisis occurs again, similar to what occurred in the last decade, the population will shift from the suburb to the urban area.

Technology is another important driver for future planning of distribution systems. Power systems experiencing a reasonably large peak power demand will have to consider solar and wind-driven generators and fuel cells in order to supplement the power generating capabilities during peak demand periods. The advantage of these secondary sources is that they have essentially no waste by-products that could be harmful to mankind. The disadvantage of the solar/wind type generators is the fact that the energy source is variable and the level of the energy source is dependent on the location of these generators. Fuel cells, on the other hand, can store energy during low demand periods and return the energy during high power demand and can be located just about anywhere.

VI. Load Management

In the past, distribution power system design was based on the philosophy of meeting the user demand through the expansion of the utility system. Today this philosophy is changing because power utilities are realizing the cost of labor, materials, and fuel.

An alternative to expansion is to utilize an existing system more efficiently by load management. Large blocks of power can be transmitted across the United States as the peak power demand locations move across our continent. Careful management of power flow may reduce the burden placed on distribution systems and even extend the usefulness of the system components.

Delgado [2.2] has specified a set of requirements for a successful load management program. They are as follows:

Acceptable reliability level

Provide acceptable user convenience

Acceptable cost/benefit ratio

Functionally compatible with system operation

Provide a more economical system

Controlling demand during critical load demand periods

Reduce customer rates

By designing distribution systems with the above requirements as objects, load management allows better use of power systems.

VII. Optimum Rectangular Load Area with a Uniform Load Density

Many factors impact the final electrical terrestrial system geometrical configuration. In order to gain an insight into distribution system planning, the load area is assumed to have a uniform density D (kva per unit area) and a rectangular shape as shown in Figure 2.3. The system has one feed point or substation supplying power to the lateral transmission lines via a main transmission line. Van Wormer [2.3] has investigated this problem and developed an expression relating the allowable normalized voltage drop V_d between the feed point and the end of the last lateral. The equation for V_d can be written

$$V_d = k_1 \frac{DZ_1}{E^2} a^2 c + k_2 \frac{DZ_2}{E^2} c^2 d \qquad (2.1)$$

where k_1 and k_2 are proportionality constants, D is the kva density, Z_1 and Z_2 are the magnitudes of the per unit impedance of the main and laterals respectively, and E is the line voltage. The first term in Equation (2.1) accounts for the normalized voltage drop in the main and the latter term the normalized voltage drop in the last lateral.

For a given V_d, Equation (2.1) may result in a long main and short laterals ("a" large and "c" small) or a short main and long laterals ("a" small and "c" large). In both cases the service area (A = 2ac) is small. Between these two extreme conditions, there is a condition where the value of A is maximum. Reference [2.3] indicates that this occurs when 1/3 of the total normalized voltage drop occurs in the last lateral ($k_2 DZ_2/E^2 c^2 d = V_d/3$). The remaining 2/3 of V_d occurs in the main transmission line. This result also indicates that large transmission line voltage E produces a large maximum service area for a given V_d, D, Z_2, d, and k_2. Decreasing the value of Z_2 will cause the mass of the laterals to increase which is counter-productive from a space power system viewpoint.

The geometry of the maximum rectangular service area can be studied as a function of the voltage E for a constant D, conductor size, V_d by expressing the ratio of two transmission line voltages by E_2/E_1. For maximum service area the results are shown in Table 2.3. Doubling the transmission line voltage increases the length of the main by $\sqrt{2}$, laterals by 2, ratio of main to lateral by $1/\sqrt{2}$, and the service area by $2^{3/2}$. Increasing the system operating voltage causes the geometry of the service area to become more rectangular because the lateral dimension "a" is increasing faster than the main transmission line dimension "b".

VIII. Optimum V_d for a Thermally Limited Feeder Servicing a Rectangular Area

As the load density D increases, the kva feeder load increases. At some value of D, a thermal limitation is reached and the service area is determined by the maximum kva load $(kva)_m$ which can be expressed by the following relationship

$$(kva)_m = 2acD. \qquad (2.2)$$

Equation (2.1) can be expressed with the constraint imposed by Equation (2.2) as follows

$$V_d = \frac{k_1 Z_1 (kva)_m^2}{E^2\, 4cd} + \frac{k_2 D Z_2}{E^2} c^2 d. \qquad (2.3)$$

The length of the main transmission line is also constrained (a = (kva)m/2cd). As the length of the laterals increase, the majority of the normalized voltage drop shifts from the main to the laterals and the length of the laterals decreases.

Assuming a thermally limited condition for the distribution system, increasing the system operating voltage will increase the service area, but the functional behavior will be different from the voltage limited condition. For the thermally limited case the service area is proportional to the system operating voltage E(A = (kva)m/D E/D) since $(kva)_m$ depends directly on E. Optimizing Equation (2.3) with respect to the lateral dimension c, while maintaining a constant cable size and load density, the functional behavior of the distribution parameters with respect to E can be investigated. Table 2.4 lists the results. Comparing the results of Table 2.3 and 2.4 the service area increases faster for the voltage limited system (V_d held constant) when compared to a thermally limited system. It is also advantageous to increase the voltage E since V_{dmin} is inversely proportional to the three-halves power of E. Hence, a larger operating voltage reduces the corresponding V_{dmin} for the thermally limited case.

IX. Conclusions on Terrestrial Power Distribution Systems

The investigation of economic, economic, demographic, and technical factors that influence the structure of a terrestrial power distribution system, has been conducted. At very large power levels both terrestrial and non-terrestrial electrical power systems will have similar characteristics. Both systems must accommodate faults that may occur by isolating the faulted segment before there is a catastrophic collapse of the power system causing serious outage.

One of the major differences between terrestrial and space power systems is the fact that man can survive a major terrestrial power outage because his bodily needs are provided by natural processes that existed long before the use of electrical energy. In space practically all systems depend on electrical energy to support man's biological needs.

Another difference between the two systems is that the space power system must be transported at a very large cost per kilogram to its final destination. The actual assembling process of a space power system in space takes very careful planning because any system modification in space is almost prohibitive. Optimization of system mass is very important in order to launch large power systems at a reasonable cost.

From a technical viewpoint, distribution systems are very complex and become more complex as power levels increase. A rectangular distribution system was chosen with uniform kva density in this chapter in order to be able to describe the developmental model of a non-terresterial electrical power system.

For a given voltage regulation it was shown that the maximum service area grew in size with increasing system voltage, with the lateral transmission lines growing faster than the main feeder line creating a more rectangular service area.

If the power system is operated such that it is thermally limited, the service area increases with operating voltage, but not as rapidly as for the constant voltage regulation case.

TABLE 2.1 Factors Affecting Load Forecasting

Alternative Energy Sources

Load Density

Population Growth

Historical Data

Geographical

Land Use

City Plans

Industrial Plans

Community Development Plans

TABLE 2.2 Operations Research Techniques Used for System Planning Models

Alternative - policy method

Decomposition of large problem method

Linear - programing method

Dynamic - programing method

TABLE 2.3 Maximum Service Area Dimensions for Different Transmission Line Voltages (E_2/E_1)

Main	$a_2/a_1 = (E_2/E_1)^{1/2}$
Laterals	$c_2/c_1 = E_2/E_1$
Ratio main to lateral	$\frac{a_2/c_2}{a_1/c_1} = (E_1/E_2)^{1/2}$
Service Area	$A_2/A_1 = (E_2/E_1)^{3/2}$

TABLE 2.4 Effect of Increasing Operating Voltage for a Thermally Limited Distribution System

Main	$a_2/a_1 = (E_2/E_1)^{1/3}$
Laterals	$c_2/c_1 = (E_2/E_1)^{2/3}$
Ratio main to lateral	$\frac{a_2/c_2}{a_1/c_1} = (E_1/E_2)^{1/3}$
Service Area	$A_2/A_1 = E_2/E_1$
Minimum normalized voltage drop	$\frac{Vd_{min2}}{Vd_{min1}} = \left(\frac{E_1}{E_2}\right)^{2/3}$

REFERENCES

[2.1] Gönen, T., "Electric Power Distribution System Engineering, McGraw-Hill Book Company, 1986.

[2.2] Delgado, R., "Load Management - A Planner's View," IEEE Trans. Power Appar. Syst., Vol. PAS-102, No. 6, 1983.

[2.3] Van Wormer, F. C., "Some Aspects of Distribution Load Area Geometry," AIEE Transactions, December 1954.

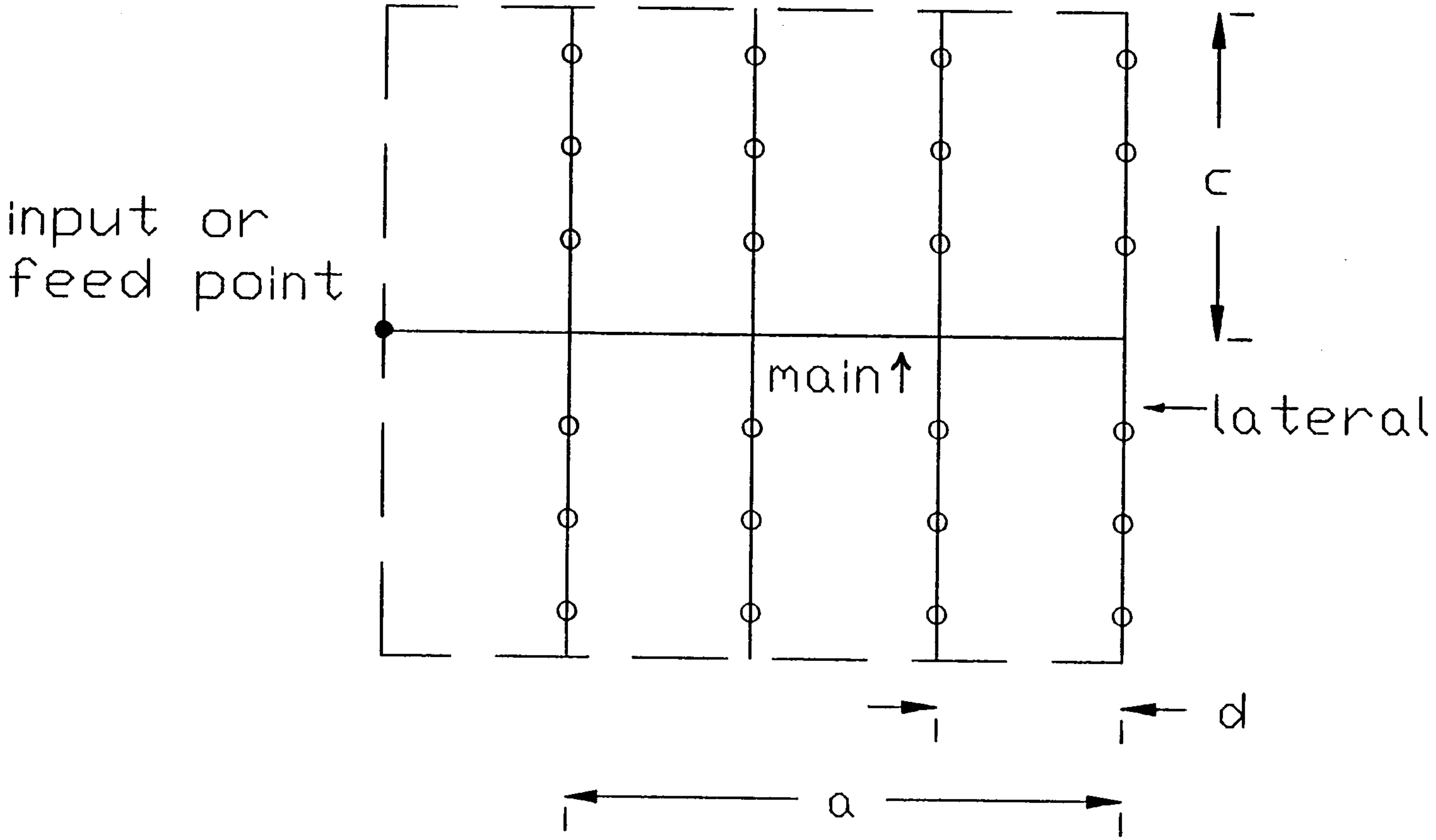

Figure 2.1 Rectangular distribution load area

Chapter 3

RADIATOR MASS TRADE-OFF WITH SYSTEM TEMPERATURE

I. Introduction

All physical systems experience a rise in temperature due to their inefficiency. Either the system itself will fix the temperature bounds because of such constraints as reliability, life span, and etc., or the temperature bounds may be specified by exterior systems such as man. If systems are not compatible temperature-wise, they must be insulated from each other. One method of increasing thermal resistance among subsystems is to separate them by space.

If the systems are mechanically or electrically coupled, total system mass increases because coupling (such as mechanical shafts, pipes, or electrical transmission lines) is required to transport energy from one system to another system. Terrestrially, this approach of using space as a thermal barrier is used everyday. However, in space this scenario would be very expensive because of the transport mass cost.

Unlike terrestrial systems, a spacecraft is in essence an autonomous system that is located in vacuum; the only mechanism for heat rejection is through radiation. There is no local infinite heat sink available in space such as found on the earth's surface. Radiators must be designed to radiate all input power to the spacecraft (including the heat radiated by man) via radiators. If the spacecraft is not in thermal equilibrium, the spacecraft's temperature will either increase or decrease until equilibrium is achieved.

Watts dissipated as heat due to system inefficiency and watts available to do useful work eventually become an equivalent heat load that must be radiated back into space. Because of the inverse relationship between radiator mass and the fourth power of radiator temperature, it is advantageous to operate the spacecraft at the highest temperature possible. However, man and equipment place an upper bound on spacecraft temperature, thus limiting the minimum radiator size. Separating systems into spatial regions of high and low temperature (thermal isolation) may improve the situation.

II. Mass Trade-off for System Operation at Two Different Temperatures

A system operating at temperature T_3 requires only one radiator as shown in Figure 3.1.a. The higher the temperature, the smaller the radiator mass for a given input power and generally lower system reliability and life span. Figure 3.1.b represents a system that has been separated into two subsystems operating at temperatures T_1 and T_2 where $T_1 > T_2$. Two radiators and an energy transport coupler between the systems are required . This coupler could represent an electrical or mechanical transmission line, a pipe that passes a fluid back and forth, or a combination of transport systems between the subsystems.

Generalized quantities Q_1, Q_2 and ΔQ_1 are used in the model. If the coupling system is an electrical transmission line, Q_1, Q_2, and ΔQ_1 represent respectively output voltage, current, and the voltage drop across the coupler. If the coupler is an a.c. transmission line, the power output is $E_1 I_2 \cos\theta$ where $Q_1 = E_1$, $Q_2 = I_2 \cos\theta$, and θ is the phase difference between E_1 and I_2. It is assumed that the total subsystem mass ($M_1 + M_2$) is equal to the mass M_3. Let Q_2 be equal to $\eta_1 P_i / Q_1$ where η_1 represents the system #1 efficiency.

A ratio mass comparison will be conducted between Figure 3.1.b and 3.1.a. If the ratio is greater than unity, the 3.1.b system is more massive than 3.1.a system.

The separation distance ℓ is determined by the hazard level H that system #2 can tolerate from system #1. Typically, H is directly proportional to the power level P_i and inversely proportional to ℓ^2. The mass ratio Γ $\left(\Gamma = \left(M_{R1} + M_{R2} + M_c\right)/M_{R3}\right)$ according to Appendix 3.A is

$$\Gamma = (1-\eta_1) + \eta_1(T_1/T_2)^4 + \left(\frac{\rho_c \rho_{mc} \; k_1 \; K_1}{\rho_{R1}}\right)\left(\frac{\eta_1 \; P_i T_1^4}{H \; \Delta Q_1 \; Q_1}\right). \qquad (3.1)$$

See appendix for definitions of terms and assumptions. If $\eta_1 = 0$, Γ is unity which indicates that topologically both systems are identical.

According to Equation (3.1), the coupler mass depends on the ratio P_i/Q_i. As the power level increases, this ratio should remain relatively constant, otherwise the mass ratio will increase. In the case of an electrical system, this indicates that system operating voltage should track with increasing power level. Reducing either H or ΔQ_1 increases the mass ratio.

III. Conclusion

The above analysis indicates that a single system operating at temperature $T_1 = T_3$ is less massive when compared to a dual temperature system operating at two temperatures T_1 and T_2 where $T_2 < T_1$. The increase in mass is due to the addition of the second radiator at temperature T_2 and the energy transport mechanism between the two systems. Generally, a multi-temperature system is necessary in order to accommodate the external temperature specifications determined by electronic equipment and man.

Results also point out that the ratio of the input power to the generalized parameter Q_1 should remain essentially constant as the power rating of the system increases. For an electrical system where Q_1 represents voltage, this means the system voltage should increase with increasing power.

In the case of a power source that depends on a thermodynamic heat cycle, the system efficiency η_1 depends on the ratio of input to output temperature. For high efficiency $T_{1_{OUTPUT}}/T_{1_{INPUT}}$ must be as large as possible. Since $T_{1_{OUTPUT}} = T_1$ and T_2 is specified by the system electronic component thermal characteristics and/or man, T_1 should be as low as possible with the constraint that $T_1 > T_2$. Thus, the input temperature $T_{1_{INPUT}}$ must increase with system output power rating, otherwise there is a mass penalty.

Appendix 3.A

With reference to Figure 1-B-1, the mass ratio Γ is

$$\Gamma = \frac{\dfrac{(1-\eta_1)\,P_i\,\rho_{R1}}{k_1\left(T_1^4 - T_0^4\right)} + \dfrac{\eta_1\,P_i\,\rho_{R2}}{k_2\left(T_2^4 - T_0^4\right)\left(1+\frac{\Delta Q}{Q1}\right)} + \dfrac{\rho_c\,\rho_{mc}\,\ell^2\,\eta_i\,P_i}{\Delta Q_1\,Q_1\left(1+\frac{\Delta Q}{Q1}\right)}}{\dfrac{P_i\,\rho_{R3}}{k_3\left(T_3^4 - T_0^4\right)}} \qquad (A.1)$$

where η_1 = system #1 efficiency

P_i = power input

ρ_{R1}, ρ_{R2}, ρ_{R3} are radiator mass densities

k_1, k_2, k_3 are radiator constants

T_1, T_2, T_3 are radiator temperatures

T_0 = sink or background temperature

ρ_c = generalize coupler resistivity

ρ_{mc} = coupler mass density

ℓ = spatial system separation

Q_1 = generalize coupler operating potential

ΔQ_1 = generalize coupler potential drop

In order to simplify Equation (A.1) the following assumptions are imposed

$\rho_{R1} = \rho_{R2} = \rho_{R3}$

$k_1 = k_2 = k_3$

$T_1 = T_3$

Operating temperatures T_1, T_2, and T_3 are much greater than T_0

Hazard level $H = K_1 P_i / \ell^2$

The mass ratio can be expressed as follows

$$\Gamma = (1-\eta_1) + \eta_1 (T_1/T_2)^4 + \left(\frac{\rho_c \; \rho_{mc} \; k_1 \; K_1}{\rho_{R1}}\right) \left(\frac{\eta_1 \; P_i \; T_1^4}{H \Delta Q_1 \; Q_1}\right) \tag{A.2}$$

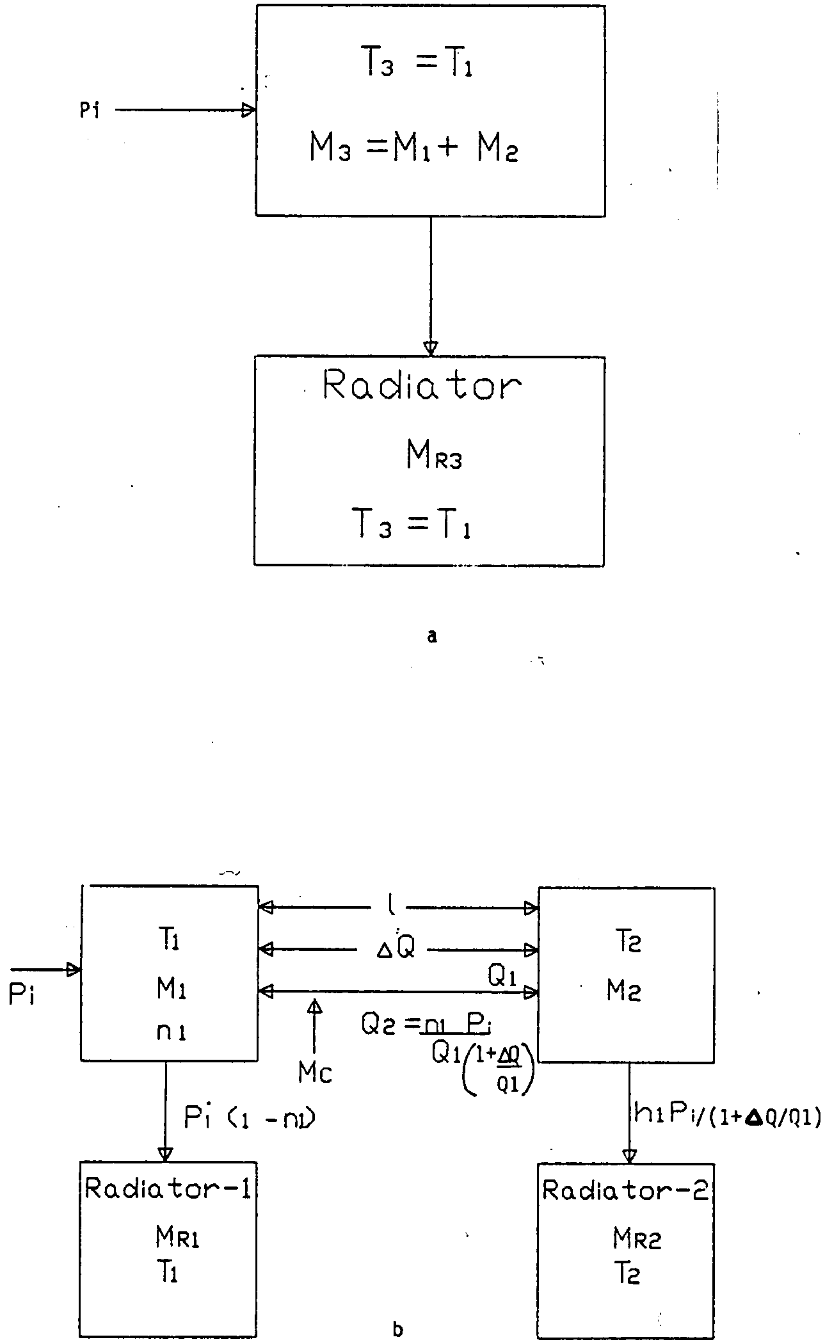

Figure 3.1 System configurations operating at one temperature and two different temperatures

Chapter 4

GENERAL ELECTRICAL CHARACTERISTICS OF TERRESTRIAL/SPACE POWER SYSTEMS

I. Introduction

The function of an ac electrical transmission system is to provide bulk power to load centers in an economical manner. The system also must have both steady-state and transient stability to accommodate load changes and aperiodic disturbances.

Besides the normal variation in power demand, the system will experience aperiodic system disturbances due to faults that occur within the system itself. Line faults have the greatest effect on the system causing the system to experience a transient. A power system has transient stability if the system will regain equilibrium following a system fault. Maintaining transient stability requires that the system be able to isolate the fault from the rest of the system in the shortest possible time. In a terrestrial three phase power system, there are four types of faults that the system can experience. In order of increasing effect on transient stability, they are:

1. Line to ground fault
2. Line to line fault
3. Two lines to ground
4. Three phase fault

Except for extremely large power systems, spacecraft will probably employ single phase for power distribution which eliminates the more severe faults and retains only the line to ground fault.

II. Power Limits of Transmission Lines

The complex power, $P_r + j\,Q_r$, delivered to a load is dependent on the sending-end line voltage E_s, receiving-end voltage E_r, the phase angle δ between E_s and E_r, and the transmission line characteristics. If the ratio of transmission line inductive reactance to resistance X/R and the shunting capacitive reactance are large, the expression for real power flow at angle δ can be simplified considerably [4.1] and is given by the following equation

$$P_r = \frac{E_s E_r}{X} \sin\delta \qquad (4.1)$$

For a given E_s, E_r, and X, the load power is a function of the phase angle between E_s and E_r and is maximum when δ is 90°. Power systems use voltage regulators at the sending and receiving-end to maintain a constant value for E_s and E_r. The transmission line reactance X is directly proportional to the product of line frequency and its length. When either the frequency or line length increases, the sending and receiving-end voltage must increase accordingly in order to maintain P_r (max). Paralleling transmission lines reduces X, but the total transmission line mass will increase directly with the number of parallel transmission lines. This point is very important when high frequency spatial electrical power systems are considered.

Terrestrial power systems never operate at P_r (max), but at approximately 70 to 75 percent of P_r (max). The corresponding limit for δ is approximately $1/2 \tan^{-1}(X/R)$ or 45° for a transmission line that has a large X/R ratio. In order to appreciate the operation of a power system, a typical receiver-end power circle diagram [4.1] is shown in Figure 4.1. This diagram is based on E_s remaining constant. The complex power $P_r + jQ_r$ depends on the position of a geometrical line from the center of circles to the corresponding circle which is determined by Er/Es. Highly inductive loads (small power factor lagging) create a condition of low P_r. By adding an equivalent bank of capacitors (zero power factor leading) at the receiving-end, the net power factor at the receiving-end will increase toward unity, and if the leading capacitor current is large enough, the receiving-end power factor can be leading. Accordingly, the receiver-end power will increase. This is equivalent to creating a partial resonant circuit at the receiving-end. A sending-end power circle diagram can be constructed in a similar manner and the corresponding power factor correction can be implemented at the sending-end using an equivalent bank of capacitors. With proper capacitor switching it is possible to increase the normal circuit transmission line capacity without excessive transmission line losses according to Brewer et al. [4.2]. This technique does add capacitor and switching mass to the power system. From a space power system viewpoint, capacitors switching is a mass penalty, but there may be transmission line mass savings to counter balance this mass penalty.

Power system transient stability is a measure of the electrical sources regaining equilibrium after an aperiodic system disturbance. Line faults, which have the greatest effect, can result in an isolation of a major transmission line causing a load loss. This requires an adjustment of phase angles in the system. Instability results when one or more smaller electrical generators lose synchronism with the larger generators causing the smaller sources to act as a load for the larger source. This domino-effect can cause a complete power system collapse. If the system can accommodate the aperiodic fault, the loss of power demand through circuit isolation, and maintain synchronism at the new power level, the system has transient stability.

III. Parametric Study of a Coaxial Transmission Line

The maximum power at the receiving-end of a transmission line is

$$P_r\ (\max) = \frac{E_s E_r}{2\pi f L \ell} \tag{4.2}$$

where f is the system's operating frequency, L is the per unit transmission line inductance, and ℓ is the transmission line length. As P_r (max) increases, the transmission line mass will increase. The exact relationship between P_r (max) and the total transmission line mass will depend on the geometrical cross-section of the transmission line.

For illustrative purposes consider a coaxial transmission line shown in Figure 4.2. According to the results in Appendix 4.A, the total transmission line mass is

$$M_T = 2\pi\rho_m\ (b(\Delta b) + a(\Delta a)). \tag{4.3}$$

The dimension b can be expressed in terms of the other system parameters as

$$b = a\ e^{(K/a^2)} \tag{4.4}$$

where $K = \left(P_r\ (\max)\ f\ \mu_0 \ell\right)/\varepsilon_{max}{}^2$. See Appendix 4.A for definition of various terms and approximations.

The dimension b will reach an optimum point when db/da = 0 or when $a = \sqrt{2K}$ and $b = \sqrt{2Ke}$. The corresponding transmission line mass M_T is

$$M_T' = M_T \Big|_{a = \sqrt{2K},\ b = \sqrt{2Ke}} = 2\pi\rho_m \ell \quad \sqrt{2K}\ \left\{ \sqrt{e}\ (\Delta b) + (\Delta a) \right\} \tag{4.5}$$

For a given Δa, Δb, and ε_{max}, M_T' is proportional to the various system parameters as shown by the following equation

$$M_T' \quad (P_r(max)\, f)^{1/2} \ell^{3/2} \{\sqrt{\bar{e}}\, \Delta b + \Delta a\}. \qquad (4.6)$$

According to Equation (4.6), for high power electrical systems operating at high frequency and over long distances, the wall thicknesses Δb and Δa will have to decrease in order to maintain an acceptable value for M_T'. There is a limit to this approach because the transmission line must maintain rigidity in order to preserve its dimensional integrity and also maintain an acceptable per unit line resistance. Note the above equations are based on a high X/R ratio.

IV. Conclusions

A rudimentary analysis on power system stability has been conducted in this chapter. Using the same approach as employed in terrestrial power system design, the spatial electrical power system receiving-end power depends on the product of the magnitude of the sending and receiving-end voltage and the sine of the phase angle (transmission line angle) between these two voltages. The analysis was based on a transmission line that has a large inductive to resistance ratio. Results indicate that receiving-end power will reach a maximum when the transmission line angle is 90°. In practice a transmission line is operated at approximately 70% of the maximum receiving-end power which corresponds to a 45° transmission angle.

As the power level increases, the sending and receiving-end voltage must increase or the transmission line inductance must decrease in order to maintain power system stability. For long-length transmission lines operating at high frequencies, the per unit line inductance must be decreased in order to reduce the transmission line inductance. Reducing the transmission line-to-line separation reduces the inductance, but this action limits the maximum transmission line operating voltage.

Increasing the relative dielectric constant of the medium between the transmission line conductors permits the line to operate at a higher voltage without changing the transmission line per unit inductance. For a coaxial transmission line configuration it was shown that there is an optimum value for the outer coaxial dimension with respect to inner coaxial dimension.

A robust or stiff power system is a system that can tolerate load and fault disturbances and still maintain stability. For a given receiving-end power, the phase angle between sending and receiving-end voltage must be as small as possible in order to create a stiff power system. This implies that both the sending and receiving-end voltages must be large and the transmission line reactance small. From a space power system viewpoint this creates a transmission line mass savings at the expense of increasing the support mass required, such as insulation and transmission line structural support. Also, the personnel safety on a manned mission must be considered if they are in the vicinity of the transmission line voltages that are large in value.

References

[4.1] Fink, D. G. and Beaty, H. W.: Standard Handbook for Electrical Engineers, Eleventh Edition, McGraw-Hill Book Co., New York.

[4.2] Breuer, G. D., Rustebakke, H. M., Gibley, R. A., and Simmons, H. O.: The Use of Series Capacitors to Obtain Maximum EHV Capability, Transaction IEEE Power Group, November, 1964.

Appendix 4.A

With reference to Figure 4.2, the total transmission line mass M_T, the maximum transmission line voltage, the per unit transmission line inductance, maximum receiving-end power P_r (max) are respectively

$$M_T = 2\pi\rho_m \ell \, [(b(\Delta b) + a(\Delta a)] \qquad (A.1)$$

$$E_{max} = \varepsilon_{max} \, a \, \ell n \left(^b/_a\right) \qquad (A.2)$$

$$L = \frac{\mu_o}{2\pi} \ell n \left(^b/_a\right) \qquad (A.3)$$

$$P_r \, (max) = E_s E_r \, /X \qquad (A.4)$$

where P_m = the conductor mass density

ℓ = transmission line length

b = inside dimension of the outer coaxial conductor

a = outside dimension of the inner coaxial conductor

Δb = outer coaxial conductor thickness ($\Delta b << b$)

Δa = inner coaxial conductor thickness ($\Delta a << a$)

E_{max} = maximum coaxial voltage

ε_{max} = maximum electric field intensity

L = transmission line per unit inductance

μ_o = free space permeability = $4\pi\times10^{-7}$ H/m

P_r(max) = maximum receiving-end power

E_s = sending-end voltage

E_r = receiving-end voltage

X = total transmission line inductance = $2\pi f L \ell$.

Combining Equations A.1, A.3, and A.4, the dimension b can be expressed as follows

$$b = a\ e^{(K/a^2)} \tag{A.5}$$

where $K = (P_r\ (max)\ f\ \mu_0\ \ell)/\varepsilon_{max}^2$. The dimension $b \to \infty$ as $a \to 0$ or $a \to \infty$. The optimum value of b is determined by setting the first derivative of b with respect to a to zero. The minimum value of b is $\sqrt{2Ke}$ and occurs when $a = \sqrt{2K}$ and the corresponding transmission line mass is

$$M_T' = M_T \Big|_{a = \sqrt{2K},\ b = \sqrt{2Ke}} = 2\pi\rho_m \ell\ \sqrt{2K}\ \{\sqrt{e}\ \Delta b + \Delta a\} \tag{A.6}$$

ORIGINAL PAGE IS
OF POOR QUALITY

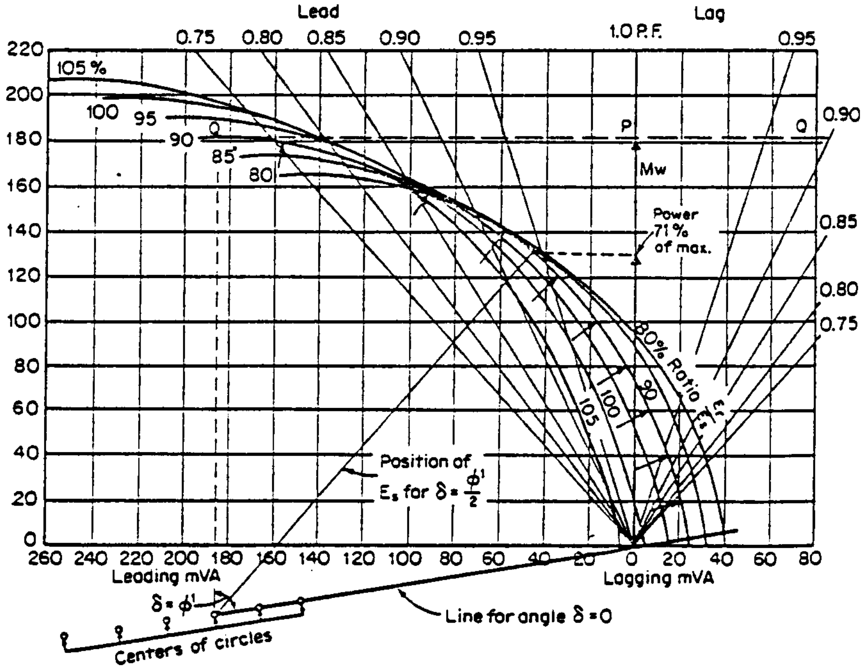

FIGURE 4.1 Receiver-end power-circle diagram showing maximum power conditions.

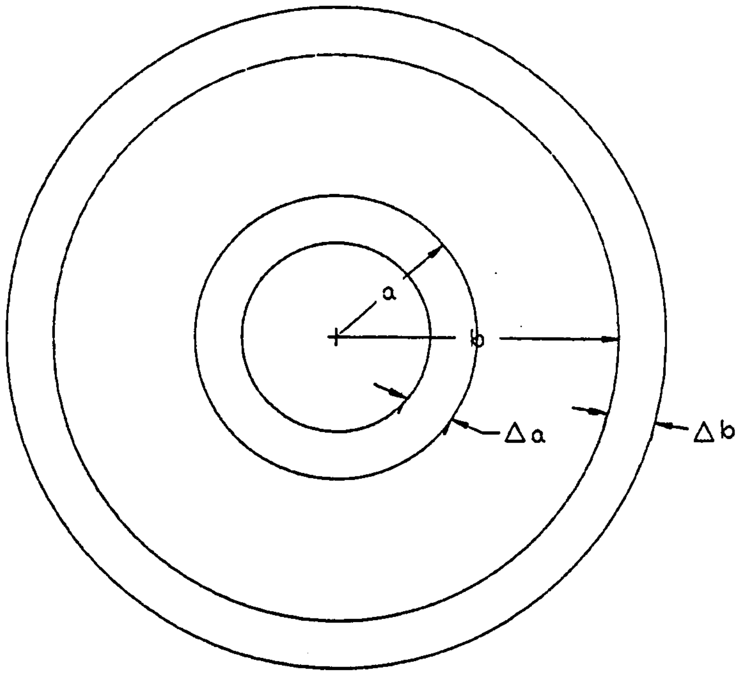

Figure 4.2 Cross sectional view of a coaxial transmission line.

Chapter 5

ADAPTIVE/EXPERT POWER SYSTEMS

I. Introduction

In general, any system must match the demands placed on it while maintaining a specified level of performance. For a time invariant load profile and a given performance level, a system could be designed, in principle, in a very deterministic manner. Unfortunately, complex systems, such as power systems, do not enjoy a load-time invariance because the needs of the user continually change. In other words, the power system must be able to adapt to the changing power demands.

All systems are not perfect. They will experience faults or disturbances during their lifetime. As an example, a power system experiencing a fault can become unstable and collapse, leaving the unfaulted portion inoperative.

Also, a system must be maintained in order to meet its performance objective. Components fail according to the laws of probability and should be replaced as they approach a time when the probability of failure is unacceptable. In space it is not practical to use personnel to perform the entire task of meeting performance objects and system maintenance because the power system is the life line for survival and would accordingly require a large component of personnel to just keep the power system operative.

An adaptive control system coupled with an expert system would remove the tedious power system tasks and allow the personnel to perform other more meaningful duties.

II. Adaptive Control System

Because technological systems are becoming very complex, as well as their controls, adaptive control is experiencing a very rapid growth. Adaptive control drives a given process to an optimum performance according to some strategy.

Ideally an adaptive control system should have the following features [5.1]:

- Adapt in a continuous manner to bounded environmental perturbations and/or variational system demands.
- Adaptive control systems should have learning abilities.
- For a changing situation the process controller must be able to be parametrically modified and develop a new set of strategies in real time.
- It should be "self-healing" if internal parameters fail.
- It should be insensitive to environmental and/or system parameter and modeling errors.

In the real-world of complex dynamic systems, neither the system to be controlled nor its environment can be completely described and in many cases their characteristics cannot be measured in advance. With little or no a priori knowledge of the controlled system and environmental disturbances, not enough information is available to construct an adaptable controller. However, a learning process during the system operation can be used to gain information, which, in turn, can be used to formulate a control strategy.

III. Structure of an Adaptive Control Problem

The following set of equations describe a nonlinear/time-varying vector differential equation of a controlled process or plant:

$$\frac{dx}{dt} = f[x(t), u(t), w(t), t] \qquad t \geq to \qquad (5.1)$$

where $x(t)$ is an n-dimensional state vector of the plant.

$u(t) = u(x,t)$ is a m-dimensional state feedback control input.

$w(t)$ is a p-dimensional disturbance vector on the plant states and its parameters.

$f[\,]$ describes an n-dimensional nonlinear/time varying plant to be controlled.

The measured plant output that generally contains noise can be described as follows:

$$y(t) = g[x(t), u(t), v(t), t] \qquad (5.2)$$

where $y(t)$ is a q-dimensional state vector of the plant measurements.

$v(t)$ is a r-dimensional state vector of measured noise.

$g[\,]$ describes a nonlinear/time varying function that relates plant measurements to measured noise, plant state vector, and feedback control inputs.

Finally, a performance criterion J that describes operating performance of the system can be stated as

$$J = \int_{to}^{t} L[y(t), u(t), w(t), t]dt \qquad (5.3)$$

where L [ ] is a nonlinear scalar function of measurement $y(t)$ and control $u(t)$. In many cases this nonlinear scalar function is modeled as a quadratic function of $x(t)$ and $u(t)$. See Figure 5.1 for a conceptual realization of the control process.

Consider the elementary control problem shown in Figure 5.2. The objective of the system is to have the output $c(t)$ as close to $r(t)$ as possible. Ideally, the tracking error between c(t) and r(t) should be zero ($e(t) = r(t) - c(t) \to o$). The dynamic process is controlled by varying the physical quantity m(t) which is sometimes referred to as the control effort. If the dynamic process can be described with sufficient accuracy, then a controller can be designed to match the dynamic characteristics of the process. In essence, the design procedure involves: measuring the dynamic characteristics of the process, determining the controller's characteristics, and constructing a controller with the required dynamic characteristics. An adaptive controller will automatically perform the above three design steps in an optimum manner.

If the dynamic process (which is sometimes referred to as the plant) changes for some reason, a new controller is configured with a set of new dynamic characteristics that will match the new plant's dynamic characteristics. This eliminates attempting to design a controller that would cover all the variational dynamics of the plant.

Kalman [5.2] has suggested the following requirements for an adaptive controller

- It must be a digital computer. Measure the dynamics characteristics of the process. Construct an optimum controller. Provide the required control action m(t).
- The process of control design must not interact with the control action.
- Process dynamic characterization requires a large number of measurements in order to reduce the noise contamination.
- The most recent output c(t) has the highest impact on the determination of the controller's structure.
- Numerical computation should be very efficient.

The system performance J can be modeled using the mean square error technique that compares the squared error between past values of the actual output and the predicted output values. By adjusting the process parameters continuously via the controller, the system performance can be optimized.

IV. Adaptive Control Power System

Power systems are nonlinear and exhibit time varying parameters and are well suited for adaptive control strategies. Electrical systems, whether operating in a terrestrial or space mode, have essentially three time profiles. These are aging, load cycles, transient response. Components failure or external disturbance is another system response, but this response is non-determinisic and therefore cannot be defined with any degree of certainty.

Aging is the slowest time response that the power system experiences. For space power systems this is reflected by such items as the photovoltaic or nuclear degradation with time. Adaptive control could be useful, but system aging probably does not have a very high priority.

Load cycles, which exhibit a shorter time response than aging, have a greater impact on the power system performance. Parametric system variations are more sensitive to these types of cycles. For example, input turbine temperature or pressure variations would reduce the total system efficiency. An adaptive control would adjust the process parameters so as to maintain a specified system efficiency if this is its only objective, which is usually not the case.

Plant transient response, which is faster, can be more serious in terms of maintaining system stability. Adaptive control design would remove some of the responsibility from the space personnel. This in turn would reduce the number of control engineers and allow the personnel to perform higher priority functions.

Because of the unpredictability of components failure or external disturbances, there would be periods where control operators would be exposed to stressful burdens where critical decisions could have a lasting effect on the power system. Adaptive control with automatic fault detection, identification and compensation as part of its design would reduce the impact of sudden component failure and external disturbances.

Quiescent power system failures are probably the most insidious types which are apparent when it is too late to perform the appropriate correction. For example, an undetected device failure that becomes known to the system when the device is activated. An adaptive system with a periodic testing research routine that could detect and identify the faulty device prior to its use would produce a more reliable system. Advanced detection algorithms in the adaptive control system should be structured such that when testing for faulty devices, the power system does not experience disruptive plant operations.

V. Autonomous Power Systems

Autonomy or expert systems are one level higher than adaptive systems. It has the rudimentary features of artificial intelligence which significantly enhances the performance of the power system. This frees the space personnel for performing other tasks that have a higher priority.

According to reference [5.3] the expert system has the facility to provide load management and autonomous control and determines or predicts overall power system performance. The autonomous control system should include the following features.

- Performance Monitoring

- Fault Detection/Diagnosis
- Fault Recovery

After the fault has been detected and isolated, an expert system, according to a strategy plan, must account for the faulted power segment by reconfiguring the non-faulted portion of the power system for safe operation and report to the space personnel a new mission load profile plan.

In a normal operation mode the expert system must be capable of digesting large amounts of information. With appropriate algorithms it must predict a potential fault by detecting any signature changes in the system performance parameters. With mean time to failure information, plus other statistical parametric data, it must replace equipment that is approaching a predetermined probability of failure. Scheduling equipment maintenance and/or replacement prior to a time when potential failure is eminent would significantly reduce the occurrence of multiple failures during a major fault.

Signature analyses of high priority equipment that could have high impact on the power system during a fault would have to be evaluated using long-term data trends. Once the trend exceeds a prescribed limit, the expert system must identify the questionable equipment and take appropriate action to isolate the potential failure from the rest of the system.

If the primary source, such as a photovoltaic array, has a power duty cycle less than 100%, some means of electrical energy storage is required to maintain power system operation during an eclipse. The expert system must devise a mission plan that provides sufficient energy storage plus an energy margin for any unexpected energy demand during the eclipse period. If the state of energy storage cannot be met during one power duty cycle, succeeding cycles will have to take into account the energy imbalance via the expert system. During this period corrective modifications to the load profile may be necessary. All loads would be prioritized from critical to noncritical with the noncritical loads placed in a standby mode. As the power system reaches steady-state, the expert system would return the low priority disconnected loads to an operational mode.

Information about the status of the power system would provide information to the space personnel on a display board. System configuration and fault status would be reported continuously. For a serious fault situation, the expert system must provide a list of strategies and the consequences of choosing a particular one to the personnel and allow the system operator to select the optimum strategy.

Some form of circuit breakers, current limiters, or fuses would be the first line of defense against a fault because of their fast response. After the expert system has been notified of the disruption, the expert system can then proceed through a series of rules to determine the level of the fault and its impact on the rest of the system without being confronted with system safety.

IV. Conclusions

In order to have a highly reliable electrical power system that involves a minimum number of space personnel, the system must be structured in such a manner that an expert system will be the overseer of the entire system with an adaptive system as its servant.

An expert system will have the following architecture

- Its source of energy must be uninterruptable
- It must be able to make logical decisions with a minimum number of power system constraints, rules, or boundaries for adequate system description.

- Power system models that are used by the expert system for purposes of operation and fault nodes must be designed to enhance the speed of analysis.
- Immediate fault isolation will be required so that the expert system can step through various scenarios, develop a strategy according to a set of rules before econfiguring the power system.
- The expert system must be compatible with all other expert systems having the same mission.
- The expert system should operate in such a manner as to observe the power system and take appropriate action according to a set of rules and not to be intimately coupled to the power system.

The adaptive control system which is subservient to the expert system must have the following structure:

- It must adapt continually within a set of bounds.
- It must continuously change its controller characteristics through parametric/strategy evolution.
- It must be able to maintain its internal structure.
- It must control the dynamic system in a robust manner such that the dynamic system is insensitive to random environmental disturbances.
- It should have some rudimentary learning abilities so as not to burden the expert system.

REFERENCES

[5.1] Gupta, Madan M., "Adaptive Methods for Control Design: An Overview," Adaptive Methods for Control System Design, IEEE Press, New York, 1986.

[5.2] Kalman, R. E., "Design of a Self-Optimizing Control System," Trans. ASME, Vol, 80, 1958.

[5.3] Barton, J. R. and Liffring, M. E., "Autonomous Power System Test Bed Development (A Status Update)," Proceedings of the 20th IECEC, Vol. 1, 1985.

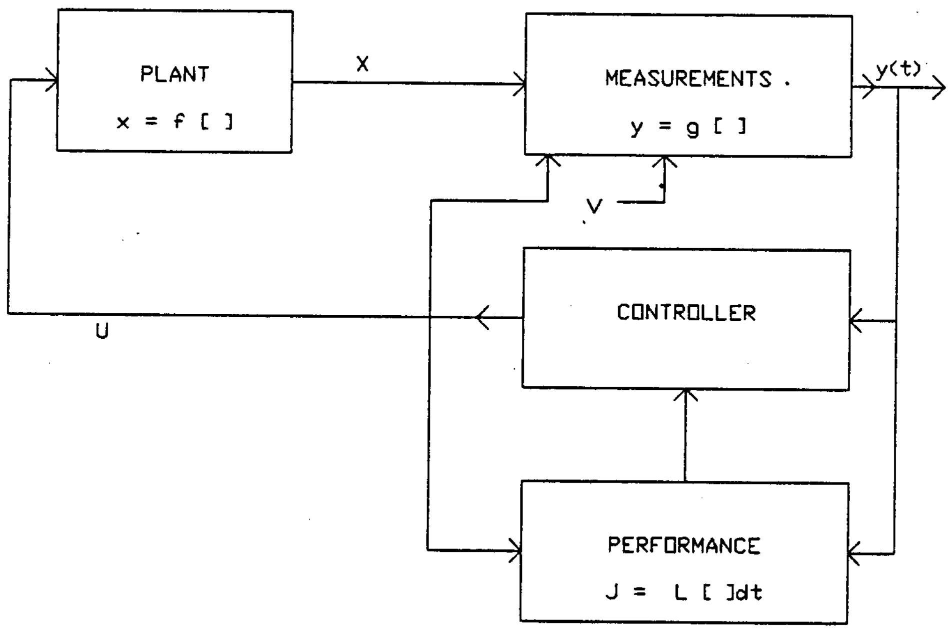

Figure 5.1 Feedback conceptual control system

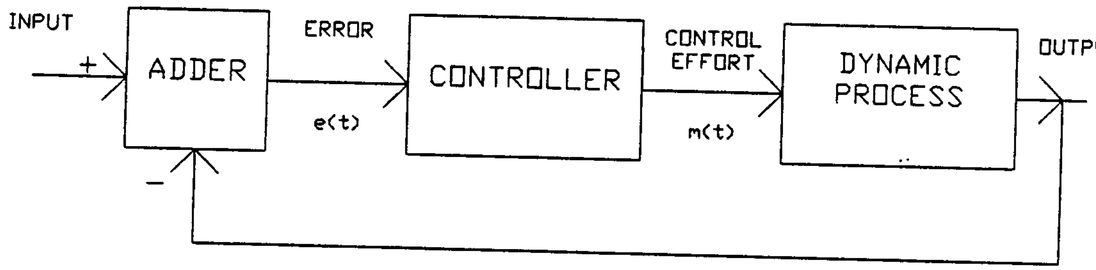

Figure 5.2 Simplified block diagram of a control problem.

Chapter 6

RADIATOR SURFACE AREA REDUCTION BY INCREASING SYSTEM EFFICIENCY OR OPERATING TEMPERATURE

I. Introduction

This chapter will investigate the reduction of radiator surface area by increasing the system efficiency or system's operating temperature. In order to compare the effect that each variable has on radiator surface area, the surface area reduction due to changing the efficiency or temperature will be equated. Thus, either effort will produce the same area reduction.

In order to make comparisons, the change in system efficiency and temperature will be normalized respectively to a base efficiency and temperature. They will be designated as normalized efficiency and temperature and be considered as drivers or efforts to reduce the radiator surface area. For equal area reduction, the efforts are equivalent when the normalized efficiency and temperature are equal.

It should be remembered that the normalized efficiency and temperature are a mathematical concept and do not necessarily reflect the physical effort (dollars, time, etc.) that must be applied to improve either the system efficiency or temperature. For example, an improvement of 1 percent in efficiency is more difficult to accomplish, in general, at a base efficiency of 98 percent than at 60 percent. This is due to the fact that efficiency has an upper bound of unity. Increasing the system temperature presents other physical barriers that may be difficult to cross because of lack of technology. Since we will be dealing with mathematical rather than physical quantities, efficiency will always be less than 100 percent, while the upper radiator temperature will not be bounded mathematically. Physically, increasing the operating temperature by a factor of two or three is, in general, a formal technological task.

II. Analysis

The general expression relating the power input, surface area, and temperature of a radiator is given by the following expression.

$$P_o\left(\frac{1}{n_o} - 1\right) = \sigma\varepsilon(1-F)\, A_{so}\left(T_o^4 - T_s^4\right) \qquad (6\text{-}1)$$

where P_o, n_o, σ, ε, $(1-F)$, A_{so}, T_o, and T_s represent respectively the nominal value of the system's power output, efficiency, Stefan-Boltzmann constant, view factor, radiator surface area, radiator temperature, and the background or sink temperature. Figure 6.1 illustrates the system and radiator. Changing either the efficiency or temperature T_o will change the value of the surface area A_{so}. All the other quantities will be treated as parameters. Letting Δn and ΔT represent the change in efficiency and temperature respectively, the change in radiator area can be expressed by the following set of equations

$$\Delta A_{s_1} = \frac{P_o\left(\frac{1}{n_o} - 1\right) - \sigma\varepsilon(1-F)\left((T_o + \Delta T)^4 - T_s{}^4\right)A_{so}}{\sigma\varepsilon(1-F)\left[(T_o + \Delta T)^4 - T_s^4\right]} \qquad (6\text{-}2\text{-}a)$$

$$\Delta A_{s_2} = \frac{P_o\left(\frac{1}{n_o + \Delta_n} - 1\right) - \sigma\varepsilon(1-F)\,(T_o^4 + \Delta T_s^4)A_{so}}{\sigma\varepsilon(1 - F)\,(T_o^4 - T_s^4)} \qquad (6\text{-}2\text{-}b)$$

where ΔA_{s_1} and ΔA_{s_2} represent the change due to a change in temperature and efficiency respectively. Equating the two differential areas ($\Delta A_{s_1} = \Delta A_{s_2}$), relates the effort of increasing the efficiency or temperature.

Normalizing the efficiency ($\Delta n/n_o$) and temperature ($\Delta T/T_o$), Equation 6-2 can be expressed as

$$\frac{(\Delta n/n_o)}{1 + (\Delta n/n_o)} = (1 - n_o) \left\{1 - \frac{(T_o/T_s)^4 - 1}{(T_o/T_s)^4(1 + \Delta T/T_o)^4 - 1}\right\} . \qquad (6\text{-}3)$$

According to Equation (6-3) the normalized efficiency and temperature depend on the parametric values of n_o, T_o, and T_s and is independent P_o, σ, ε, $(1-F)$, and A_{so}.

Since the efficiency cannot exceed unity, $(\Delta n/n_o)_{max}$ is equal to $(1-n_o)/n_o$. Except for physical limitations on the radiator operating temperature it will be assumed that there is no upper bound on $\Delta T/T_o$.

Results of normalized efficiency versus normalized temperature is illustrated in Figure 6.2 for several different base efficiencies, a T_o = 350°K, and T_s = 250°K sink temperature. All three curves exhibit a saturation characteristic because of the upper bound on the normalized efficiency.

The slope of a straight line connecting any point $(\frac{\Delta T}{T_o} \; \frac{\Delta n}{n_o})$ to the origin as shown in Figure 6.2 indicate whether it would be more beneficial to improve the system efficiency or raise the operating system temperature for $\Delta A_{s_1} = \Delta A_{s_2}$. For a slope of unity at the origin, efforts to improve efficiency or increase temperature are equal mathematically. Technologically, that may not be the case because of barriers that must be overcome to achieve an improvement in efficiency or an increase in system operating temperature.

Consider the case for n_o = 0.7 in Figure 6.2. Initially, the slope is approximately unity indicating that $\Delta T/T_o \approx \Delta n/n_o$. This implies that it will mathematically require the same normalized effort to increase the system temperature and efficiency. Again, it should be noted that from a technological viewpoint it may be more difficult to raise temperature than increase the efficiency or visa versa. As the value of $\Delta T/T_o$ increases, the slope of the straight line decreases below unity indicating that $\Delta T/T_o > \Delta n/n_o$ which implies that it will mathematically require more normalized temperature effort than normalized efficiency effort. For the cases of initially higher system efficiencies ($n_o = 0.8, 0.9$), $\Delta T/T_o$ will always be greater than $\Delta n/n_o$ which suggest that improving the system efficiency would be a better mathematical strategy. However, it should be noted that there is a $\Delta n/n_o|_{max}$ boundary. As n_o is increased, it takes more technological effort to improve on the system efficiency.

Differentiating Equation (6-3) $\left(d(\Delta n/n_o)/d(\Delta T/T_o)\right)$ will determine the slope at any point ($\Delta T/T_o$, $\Delta n/n_o$) and is given by

$$\frac{d(\Delta n/n_o)}{d(\Delta T/T_o)} = \left(1 + \frac{\Delta n}{n_o}\right)^2 (1 - n_o) \left\{ \frac{4\left(\left(\frac{T_o}{T_s}\right)^4 - 1\right) \left(1 + \frac{\Delta T}{T_o}\right)^3 \left(\frac{T_o}{T_s}\right)^4}{\left(\left(\frac{T_o}{T_s}\right)^4 \left(1 + \frac{\Delta T}{T_o}\right)^4 - 1\right)^2} \right\} . \qquad (6\text{-}4)$$

At the origin $\left(\Delta T/T_o = 0,\ \Delta n/n_o = 0\right)$, Equation (6-4) becomes

$$\frac{d(\Delta n/n_o)}{d(\Delta T/T_o)} = \frac{4\left(\frac{T_o}{T_s}\right)^4 (1 - n_o)}{\left(\frac{T_o}{T_s}\right)^4 - 1} . \qquad (6\text{-}5)$$

From a strategy viewpoint the two efforts $\Delta T/T_o$ and $\Delta n/n_o$ are equal when the slope is unity. Setting the derivative equal to unity in Equation (6-5) results in the following relationship between n_o and T_o at the origin

$$\eta_{oc} = \frac{1 + 3\left(\frac{T_o}{T_s}\right)^4}{4\left(\frac{T_o}{T_s}\right)^4} . \qquad (6.6)$$

where η_{oc} represents the critical efficiency that causes the slope of $\Delta\eta/\eta_o$ versus $\Delta T/T_o$ at the origin to be equal to unity. According to Equation (6-5) if $\eta_o > \eta_{oc}$, the slope is less than unity and if $\eta_o < \eta_{oc}$, the slope is greater than unity. Assuming $1 \leq (T_o / T_s) \leq \infty$, the maximum and minimum upper bound for η_{oc} is 1 and 0.75 respectively.

For the case when $\eta_o < \eta_{oc}$ (slope > unity at the origin), there is a point where the normalized temperature $\Delta T/T_o$ is equal to the normalized efficiency $\Delta\eta/\eta_o$. That condition exists when the constraint $\Delta\eta/\eta_o = \Delta T/T_o$ is placed on Equation (6-3). Figure 6.3 illustrates the functional behavior of $\Delta\eta/\eta_o$ or $\Delta T/T_o$ as a function of efficiency η_o treating (T_o / T_s) as a parameter. The range of η_o is from 0 to η_{oc} where η_{oc} is determined by Equation (6.6). As the efficiency η_o increases, the point where the two variables $\Delta T/T_o$ and $\Delta\eta/\eta_o$ are equal occur sooner and at $\eta_o = \eta_{oc}$ the equality occurs at the origin in Figure 6.2. For $\eta_{oc} < \eta_o \leq 1$, $\Delta T/T_o > \Delta\eta/\eta_o$. Hence, as $\Delta T/T_o$ increases, there is no point where $\Delta\eta/\eta_o = \Delta T/T_o$.

III. Results

The above analysis illustrates that for equal radiator area reduction there is a relationship between normalized efficiency and temperature. When these two normalized quantities are equal, increasing the per unit efficiency or temperature is equivalent. Because the normalized efficiency is physically bounded and the normalized temperature has no mathematical bound, initially, it appears improving the system efficiency is a better strategy than increasing the system's operating temperature provided that the actual efficiency is above a critical efficiency.

It was demonstrated that the critical efficiency depends on the ratio of the initial system's operating temperature to the background or sink temperature. Results show that the critical efficiency can vary from 0.75 to 1 depending on whether the initial system temperature is at infinity or background temperature.

Although results do indicate the best mathematical strategy for reducing radiator surface area, it does not take into account the human efforts to accomplish these improvements. As efficiency approaches unity or system operator temperature increases, a point is reached where a tremendous effort is required for a small change in either variable. If $n_o > n_{oc}$, the slope will be less than unity indicating that $\Delta T/T_o > \Delta n/n_o$. Assuming the lower and upper bound on T_o/T_s is 1 and ∞, $n_{ocmax} = 1$ and $n_{ocmin} = 0.75$. The actual efficiency must be less than n_{oc} in order to achieve a slope greater than unity at the origin.

Figure 6.3 illustrates the functional behavior of $\Delta n/n_o$ versus $\Delta T/T_o$ under constraint that the slope is unity and $n_o < n_c$.

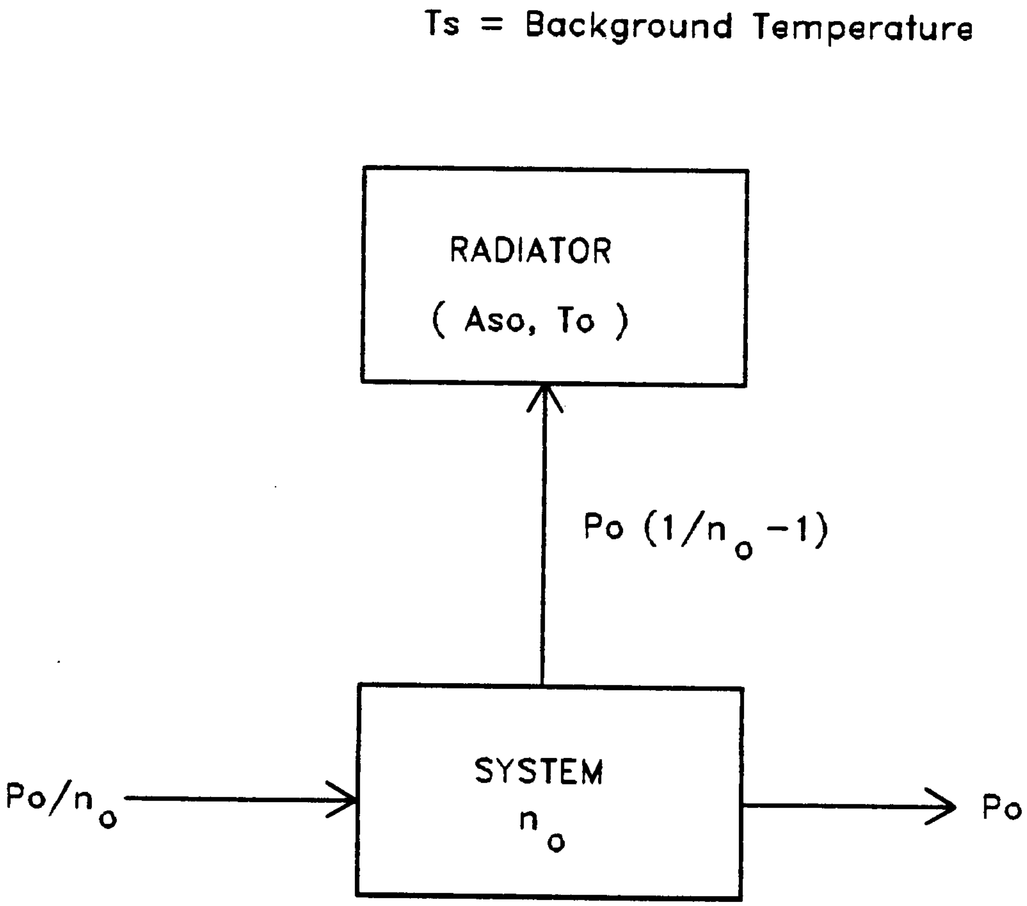

Figure 6.1 General System connected to a radiator

Figure 6.2 Normalized Efficiency vs Normalized Temperature

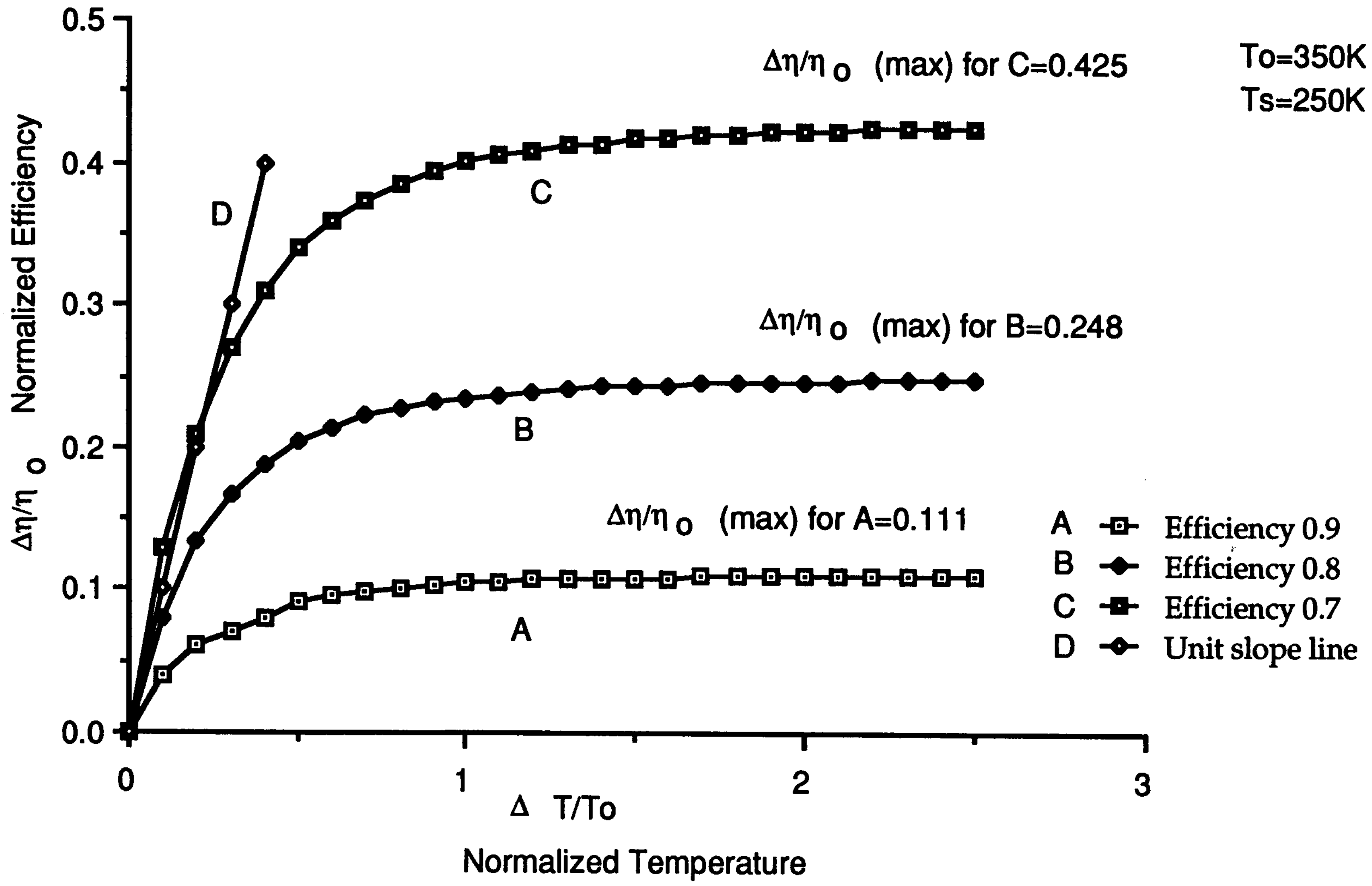

Figure 6.3 Norm. Efficiency or Norm. Temp. vs Base Efficiency

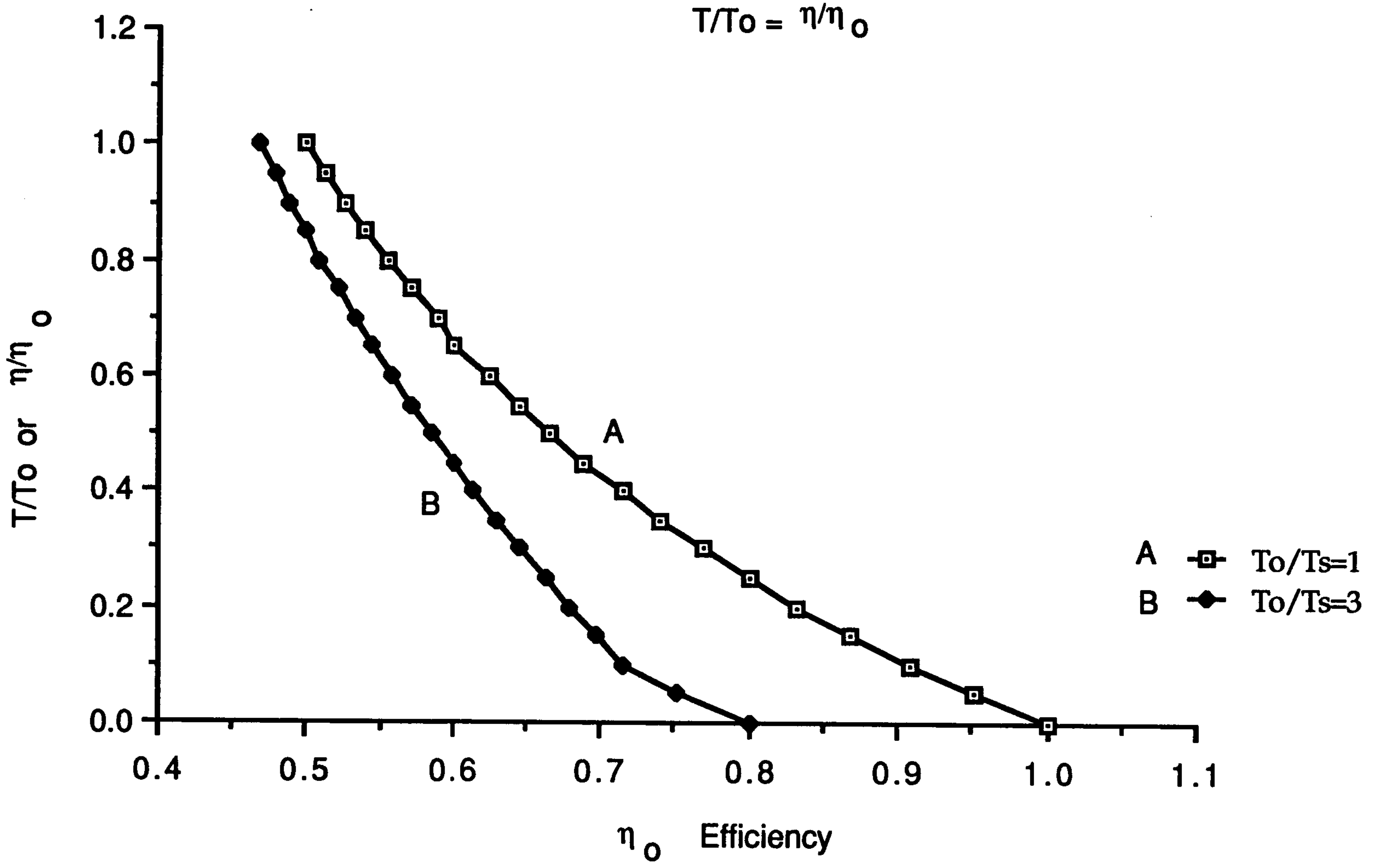

Chapter 7

THE BEHAVIOR OF TRANSMISSION LINE MASS AND TEMPERATURE AS A FUNCTION OF TRANSMISSION LINE EFFICIENCY

I. Introduction

A substantial portion of an electric power system mass is the transmission lines, especially as the power level becomes significant ($P_{out} \geq 100$ KW). This chapter will investigate the functional behavior of the transmission line mass and operating temperature versus transmission line efficiency.

It will be shown that as the spatial size of the power system increases, the corresponding operating system voltage must also increase; otherwise, the transmission line becomes very massive if high efficiency is to be maintained.

Like any space system that has losses, transmission line power loss must be radiated into the surrounding space in order to maintain an equilibrium or quiescent operating temperature. For a given efficiency the amount of power that must be radiated is directly proportional to the load power.

II. Analysis

In the following model it will be assumed that heat transfer between the transmission lines and the lunar surface is zero. The radiated heat exchange between the two conductors will be accounted for by introducing a configuration factor for two parallel cylindrical conductors. The percentage of radiated energy to the background or sink environment will be taken into account by introducing a view factor which is one minus the configuration factor. The transmission line model is shown in Figure 7.1.

Assume copper conductors having a resistivity $\rho_1 = 1.724 \times 10^{-8}/°C$ at 293°K and a mass density $\rho_2 = 8.89\ 10^3\ kg/m^3$.

In Figure 7.2 a simplified model of a transmission line connected to a load $Z_L = R_L \pm JX_L$. The plus-minus sign denotes inductive or capacitive load.

The system efficiency is given by the following expression

$$n = \frac{1}{1 + \frac{R_T \ell}{R_L}} \qquad (7\text{-}1)$$

where quantities are defined in either Figure 7.1 or 7.2. For a highly efficient transmission line, $R_T\ell/R_L$ must be much less than unity. For a given power output and length ℓ, the load resistance R_L varies directly and the per unit transmission line resistance R_T varies inversely with transmission line operating voltage. In other words, for a given load power a low voltage power system is much more massive when compared to a high voltage power system. This is consistent with the design philosophy that is used in terrestial power systems. It should be pointed out that if the operating voltage is extremely high, the support material such as insulation, structural support towers, etc tend to increase the total system mass. As can be seen from Equation (7-1), the transmission line of efficiency decreases as the line length increases. For large spatial power systems (large ℓ) the ratio R_T/R_L must be reduced in order to maintain a high efficient transmission line.

The total transmission line mass is given by the following expression

$$M = \frac{4\rho_2\rho_2\ell^2}{R_L(\frac{1}{n} - 1)} \quad . \tag{7-2}$$

In order to maintain a reasonable high efficient transmission line, the load resistance must track with the transmission line length squared which in turn demands that the system operating voltage increase as the value of ℓ increases; otherwise, the transmission line mass will increase as the efficiency increases.

As the transmission line operating temperature increases, the resistivity ρ_1 increases in the following manner

$$\rho_1 = 1.724 \times 10^{-8}(1 + 3.9 \times 10^{-3}(T-293)) \quad . \tag{7-3}$$

where temperature is degrees Kelvin.

The configuration factor F for a pair of parallel cylindrical conductors can be expressed as

$$F = \frac{1}{\pi} (\sqrt{x^2 - 1} - x + \pi/2 - \cos^{-1}(\frac{1}{x})) \tag{7-4}$$

where $x = 1 + t/d$ and $d = \sqrt{2M/(\pi\rho_2\ell)}$ (see Figure 7.1 for definition of parameters.) For a given conductor separation t, increasing the transmission line mass increases the conductor diameter causing the value of x to decrease until it approaches its lower bound of unity. The maximum value of the configuration factor occurs when x = 1 and is equal to

$$F_{max} = \frac{1}{\pi} (\pi/2 - 1) = 0.182 \tag{7-5}$$

and the corresponding view factor $(1 - F_{max})$ is 0.818. For a worse-case-scenario $(M \to \infty)$ the transmission line will radiate 82% of its power dissipation to the background. As $m \to 0$, d,x,F, (1-F) approach respectively zero, infinity, zero, and unity.

The surface area of the conductor is related to the total transmission line mass according to the following expression

$$A_s = \left[\frac{2\pi M \ell}{\rho_2} \right]^{1/2} . \tag{7-6}$$

The transmission line operating temperature is given by

$$T = \left\{ \frac{P_o(\frac{1}{\eta} - 1)}{2\sigma\varepsilon A_s(1 - F)} + T_s^4 \right\}^{1/4} \tag{7-7}$$

where P_o equals the power delivered to the load, T_s is background temperature, σ and ε represent Stephan-Boltzmann constant and the emissivity of the conductors respectively. The factor 2 was introduced in Equation (7-7) to account for the fact that the power dissipation is divided equally between the two conductors.

As stated earlier, increasing the transmission line efficiency increases the total line mass and decreases the operating transmission line temperature. Results are shown in Figures 7.3, 4, 5, and 6 for an output power of 100 KW, a 250°K background temperature, and a 2-ohm load resistance. Line length and conductor separation are treated as parameters. All curves depict the same trends for temperature and mass versus efficiency. As the efficiency approaches unity, the operating temperature and transmission line mass approach respectively the background temperature and infinity.

Figures 7.3, 4, and 6, illustrates the relationship between temperature and mass versus efficiency for t = 0.01 meter. For a given efficiency the total transmission line mass and its derivative increase as the length of the transmission line increases and the operating temperature decreases approaching the lower bound of 250°K or background temperature.

Figures 7.4 and 5 illustrates the behavior of temperature and mass versus efficiency for ℓ = 200 meters and t = 0.001 and 0.02 meter. As can be seen, the corresponding curves of temperature or mass are essentially identical when the conductor separation is doubled. It appears that the conductor's separation has secondary effect on the mass and temperature of a transmission line.

III. Results

From the above analysis it is apparent that a high efficient transmission line would become very massive if the load resistance R_L(see Equation (7-2)) does not track with the square of the transmission line length. For a given power output, the value of R_L is inversely related to the load or system voltage.

At a higher operating voltage the size and corresponding conductor mass is also reduced. However, the mass required to support the transmission lines, such as towers and insulation, becomes an important part of the total mass when the operating voltage becomes very large.

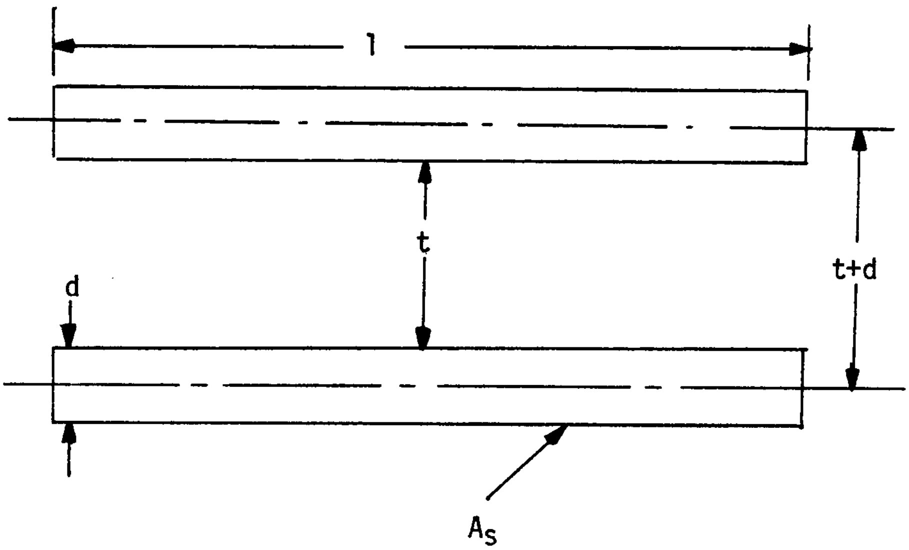

P_1 = conductor resistivity

P_2 = conductor mass density

l = transmission line length

d = conductor diameter

t = conductor separation

R_t = resistive ohms per unit length (both conductors)

X_t = inductive ohms per unit length

M = total transmission line mass

A_s = conductor surface area

Figure 7.1 Transmission Line Model

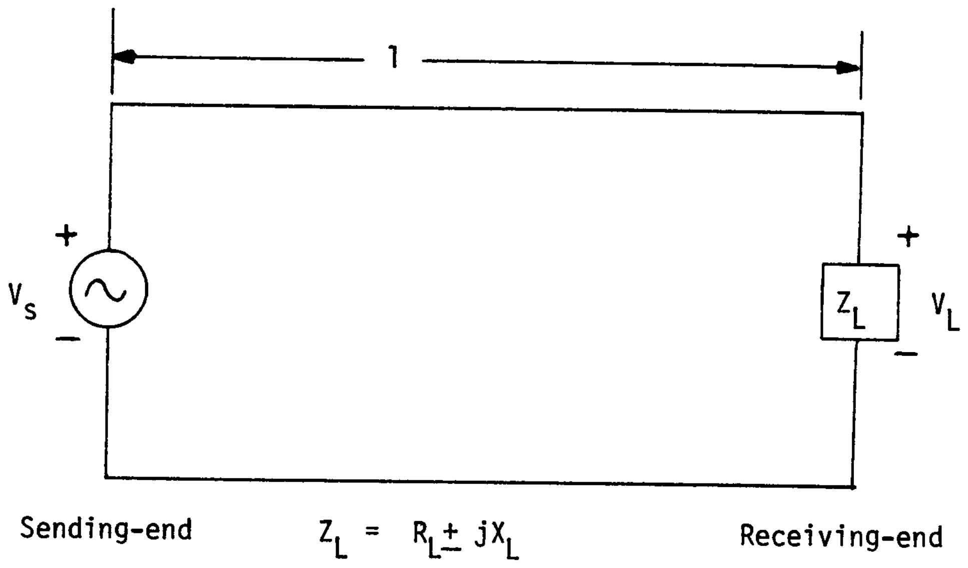

Figure 7.2 General Power System Model

Figure 7.3 Temperature or Mass vs Efficiency

$L=100(m)$, $t=0.01(m)$, $P_o=10^5(W)$, $T_S=250(K)$, $R_L=2(\Omega)$
$\rho_2=8890(KG/m^2)$

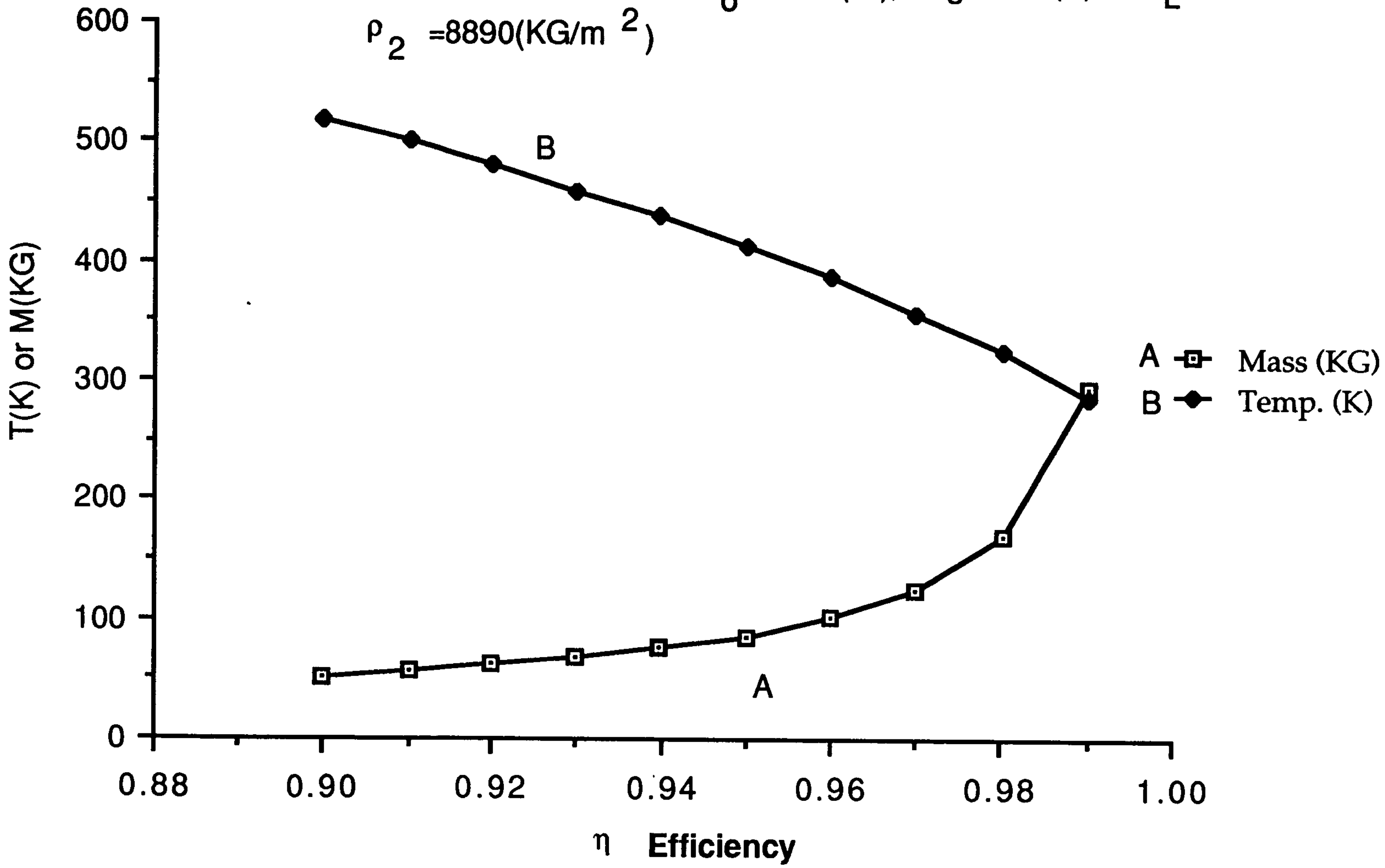

Figure 7.4 Temperature or Mass vs Efficiency

$L=200(m)$, $t=0.01(m)$, $P_o=10^5$ (W), $T_s=250(K)$, $R_L=2\ (\Omega)$

$\rho_2=8890(KG/m^2)$

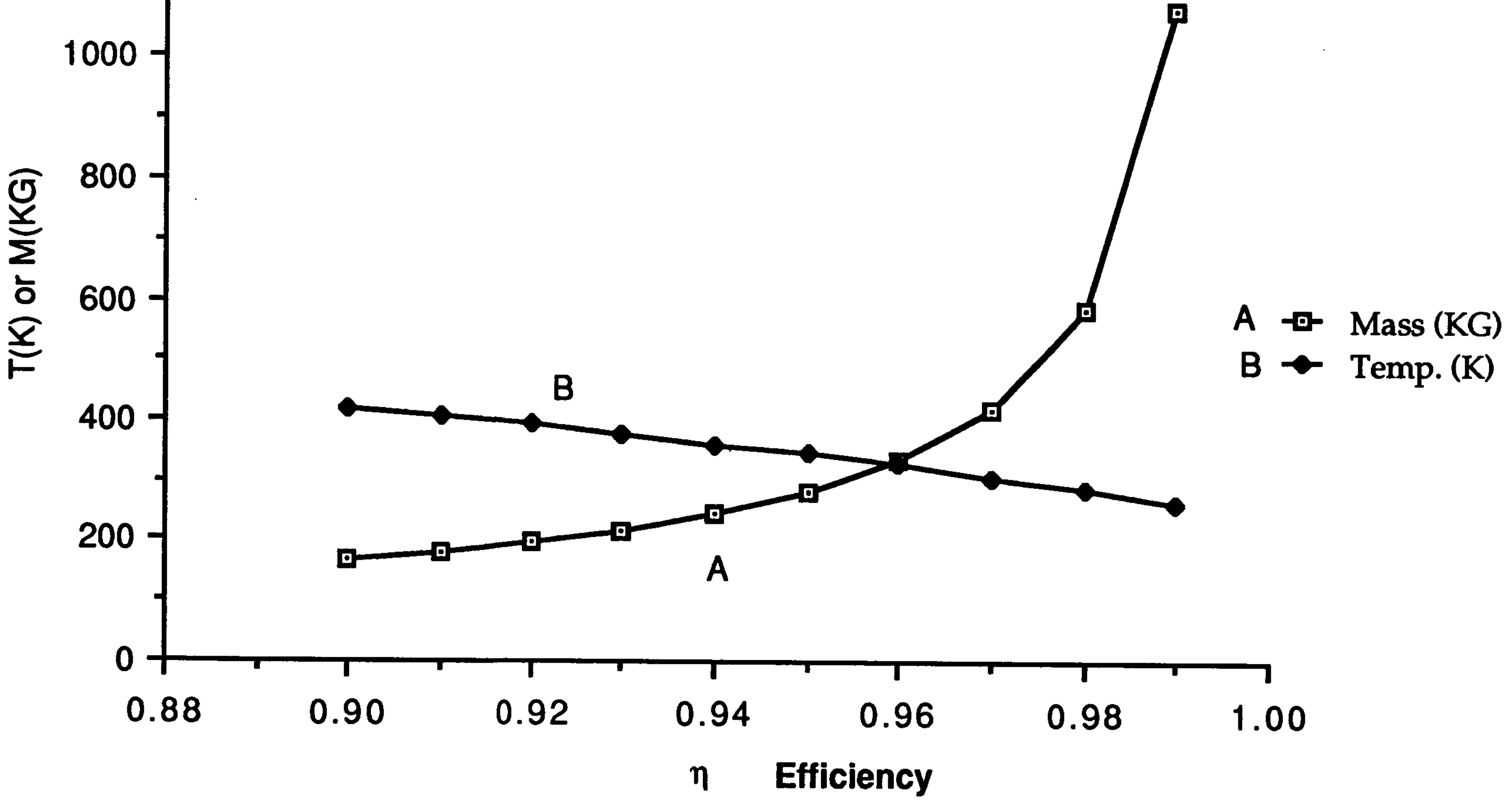

Figure 7.5 Temperature or Mass vs Efficiency

L=200(m), t=0.02(m), $P_o = 10^5$ (W), R_L=2 (Ω), T_S =250(K)

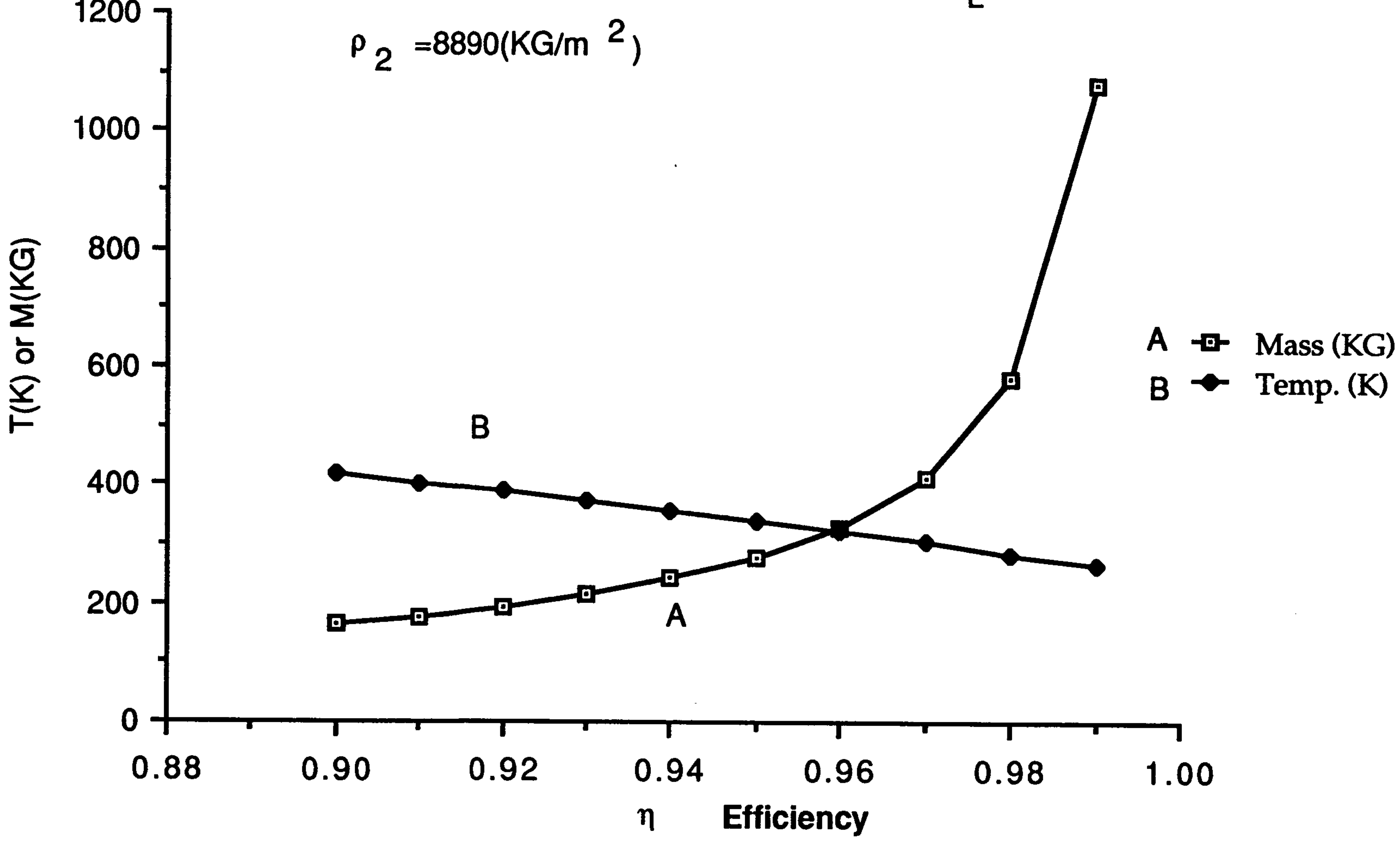

Figure 7.6 Temperature or Mass vs Efficiency

L=400(m), t=0.01(m), $P_o = 10^5$ (W), T_s =250(K), R_L=2 (Ω)
ρ_2 =8890(KG/m^2)

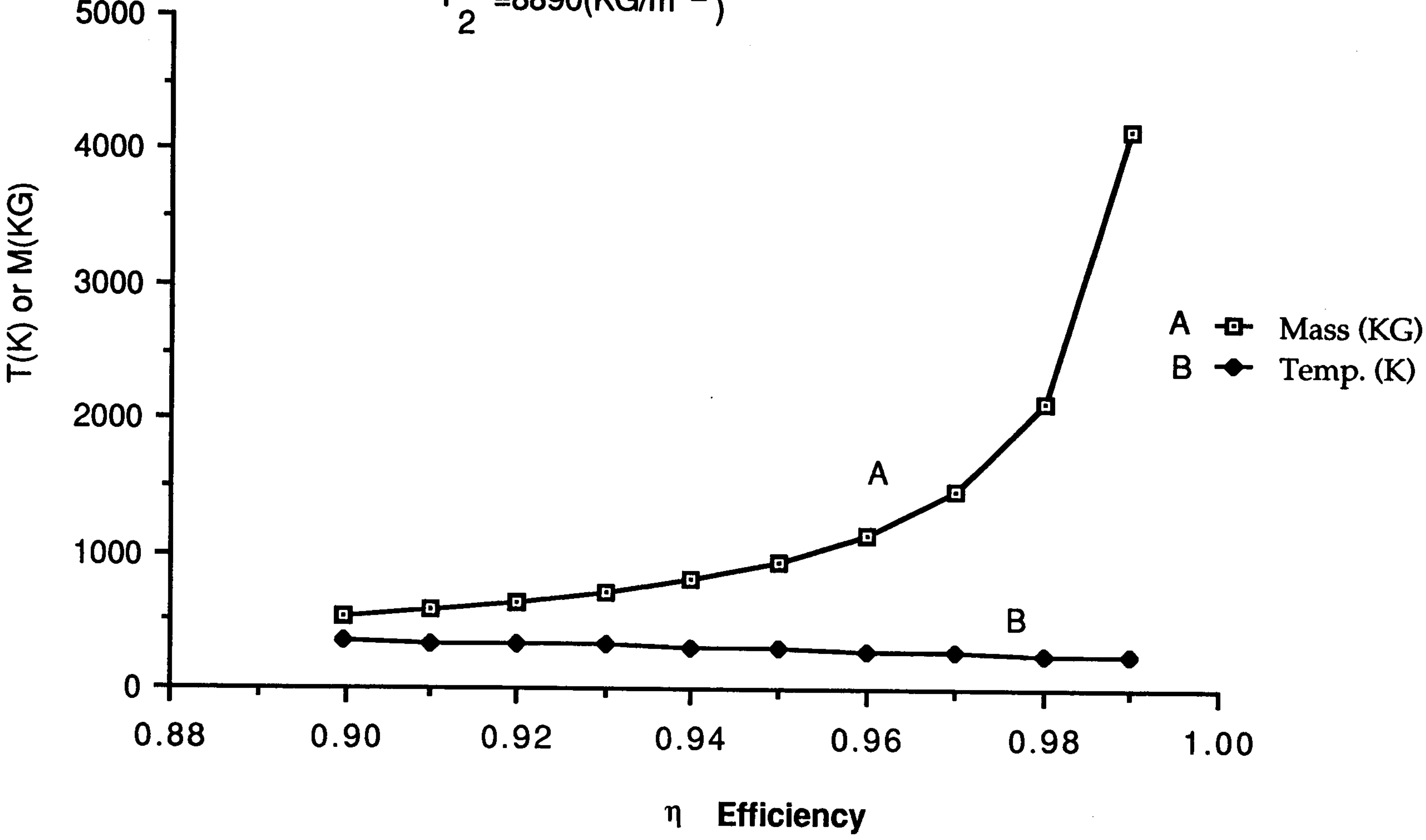

Chapter 8

VOLTAGE REGULATION AND ITS EFFECT ON TRANSMISSION LINE PARAMETERS

I. Introduction

All power systems must provide some means of voltage regulation in order to isolate the effect that a load change has on the other loads in the system. Ideally, when a load is connected to a power system, the load voltage should remain constant. Load voltage fluctuations, if severe, can cause the loads to operate improperly. In this chapter, voltage regulation will be investigated to determine what parameters contribute to "good" voltage regulation.

II. Analysis

Since a multiport power system is very complicated to analyze mathematically, a simple model consisting of a power source, transmission line, and a load, as shown in Figure 8.1, will be employed. It will be assumed that the power system is AC and operating at a frequency such that the line length is a fraction of a wavelength. Even if the operating frequency is in the range of 20 to 50 kHz, the line length in wavelengths is still small provided that the physical transmission line length does not exceed a few hundred meters. This condition will be met quite easily for space power systems.

According to Figure 8.1, the load voltage can be expressed as a function of the sending-end voltage V_S. Assuming the transmission line is a fraction of a wavelength, the load voltage is

$$\dot{V}_L = \dot{V}_S - (\dot{Z}_T \ell)\dot{I}_L \qquad (8.1)$$

where the dot denotes a phasor quantity. The voltage regulation can be defined as

$$\alpha = \frac{|\dot{V}_{L,NL}| - |\dot{V}_{L,FL}|}{|\dot{V}_{L,FL}|} \tag{8.2}$$

where $|\dot{V}_{L,NL}|$ is the magnitude of the load voltage at no load and $|\dot{V}_{L,FL}|$ is the magnitude of the load voltage at full load with $|\dot{V}_S|$ constant. Substituting (8.1) into (8.2) results in the following expression

$$\alpha = \left|1 + \frac{\dot{Z}_T \ell}{\dot{Z}_L}\right| - 1 \tag{8.3}$$

where $\dot{Z}_T$, ℓ, and $\dot{Z}_L$ represent the per unit transmission line impedance, line length, and load impedance, respectively. From the above expression $(\dot{Z}_T \ell)/(\dot{Z}_L)$ should be small in order to have good voltage regulation. As the line length increases, the ratio $(\dot{Z}_T/\dot{Z}_L)$ must decrease; otherwise, the voltage regulation will be increase.

Let $(\dot{Z}_T \ell)\dot{Z}_L$ be expressed in terms of a magnitude and a corresponding phase as follows

$$\frac{\dot{Z}_T \ell}{\dot{Z}_L} = A_1 \, e^{j(\Theta_T + \Theta_L)} \tag{8.4}$$

where $A_1 = (|\dot{Z}_T| \ell)/|\dot{Z}_L|$.

Substituting (8.4) into (8.3) and rearranging the expression results in the following equation

$$\frac{|\dot{V}_{L,NL}|}{|\dot{V}_{L,FL}|} = \left|1 + A_1 \, e^{j(\Theta_T + \Theta_L)}\right| = 1 + \alpha \, , \tag{8.5}$$

For a given voltage regulation (α = constant) there is a relationship between A_1 and $(\Theta_T+\Theta_L)$ such that (8.5) is satisfied. Figure 8.2 illustrates this functional behavior for voltage regulation from + 0.02 to - 0.02 in .01 increments. The variable A_1 represents the ratio of magnitude voltage line drop to the magnitude of the load voltage $(A_1 = (|\dot{Z}_T|\ell|\dot{I}_L|)/(|\dot{Z}_L||\dot{I}_L|)$. Negative voltage regulation indicates the $|\dot{V}_{L,FL}| > |\dot{V}_{L,NL}|$ which exists for $(\Theta_T+\Theta_L) > 90°$. This occurs for the case when the power factor of the load is leading or capacitive. As $(\Theta_T+\Theta_L)$ increases for a given positive voltage regulation, the value of A_1 increases. However, for negative voltage regulation, $(\Theta_T+\Theta_L)$ must decrease and then increase as depicted in Figure 8.2.

The parameter A_1 can also be expressed in terms of volt-amperes or power at the load and is given by

$$A_1 = |\dot{Z}_T|\ell \quad \frac{(VA)_L}{|\dot{V}_L|^2} \tag{8.6.a}$$

or

$$A_1 = |\dot{Z}_T|\ell \quad \frac{P_L}{|\dot{V}_L|^2 \cos\Theta_L} \tag{8.6.b}$$

The bracketed terms emphasize the parameters that are associated with the transmission line and the load respectively. For a transmission line approaching 100% efficiency, $|\dot{Z}_T| \rightarrow |\dot{X}_T|$ since there cannot be any transmission power loss and Θ_T must approach 90°. Accordingly, the sign of the voltage regulation depends on whether the power factor of the load is positive or negative (capacitive or inductive).

Although not shown in Figure 8.2, there is an upper and lower bound for A_1 and the results are indicated in Table 8.1. Also, it can be shown for α

< 0, the minimum value of $(\Theta_T+\Theta_L)$ occurs when $A_1 = \left(1 - (1+\alpha)^2\right)^{1/2}$ and $(\Theta_T+\Theta_L) = 180° - \sin^{-1}(1+\alpha)$.

Since the transmission line efficiency is an important parameter, it must be introduced to determine how transmission line efficiency and voltage regulation are mathematically related. Ideally, the value of α should be zero when $n = 1$.

The variable A_1 can be expressed in terms of the R_T and R_L as follows

$$A_1 = (|\dot{Z}_T|\ell)/|\dot{Z}_L| = \frac{(R_T\ell)\cos\Theta_L}{R_L\ \cos\Theta_T} \tag{8.7}$$

From a previous chapter it was shown that $(R_T\ell)/R_L = (1-n)/n$, thus $A_1 = (1-n)\cos\Theta_L/(n\cos\Theta_T)$. It is to be noted that as $n \to 1$, $A_1 \to (|\dot{X}_T|\ell)/|\dot{Z}_L|$, $(\Theta_T+\Theta_L) \to (90° + \Theta_L)$ and A_1 is at its lower bound. For a given efficiency and voltage regulation, Figure 8.2 and $A_1 = (1-n)\cos\Theta_L/(n\cos\Theta_T)$ are equivalent to two nonlinear equations with unknowns Θ_L and Θ_T. Using commercial software PC the value of Θ_L and Θ_T can be determined uniquely for a given efficiency and voltage regulation.

Equation (8.6.b) and the value of Θ_L permits one to study the trade off between the transmission line, load power, and load voltage for a given efficiency and regulation. Since A_1 and Θ_L are known for a given n and α, Equation (8.6.b) can be expressed in the following manner

$$[|\dot{Z}_T|\ell]\ [P_L/|\dot{V}_L|^2] = A_1\ \cos\Theta_L \tag{8.8}$$

Accordingly, the transmission line parameters $[|\dot{Z}_T|\ell]$ must decrease as the load parameters $[P_L/|\dot{V}_L|^2]$ increase for a given α and n. Table 8.2 lists the values of $A_1\ \cos\Theta_L$ for a selected set of α and n.

Since (8.8) represents a hyperbola for a given $A_1 \cos\Theta_L$, it is obvious that as $P_L/|\dot{V}_L|^2$ increases, the value of $|\dot{Z}_T|\ell]$ must decrease in order to maintain a specified efficiency and voltage regulation. Generally, power levels and transmission line lengths increase with system growth and if $|\dot{V}_L|^2$ does not track with P_L, the per unit transmission line impedance $|\dot{Z}_L|$ must decrease causing the mass of the transmission line to become excessive.

III. Conclusions

A relationship between the transmission line parameters, $|\dot{Z}_T|\ell$, and the ratio of load power to the square of the load voltage, $P_T/|\dot{V}_L|^2$ has been established for a specified transmission line efficiency and voltage regulation. Based on the increasing power level and physical size of an electric power system, the transmission line voltage must track with power; otherwise, the transmission line mass will increase.

Table 8.1 Upper and Lower Bounds for A_1

α	$A_{1,LB}$	$(\theta_T+\theta_L)$	$A_{1,UB}$	$(\theta_T+\theta)$
Greater than zero	α	0	$2+\alpha$	180°
Equal to zero	0	0	2	180°
Less than zero	$-\alpha$	180°	$2-\alpha$	180°

Table 8.2 Behavior of $A_1 \cos\Theta_L$ as a Function of Efficiency and Voltage Regulation

	A_1	$\Theta_T+\Theta_L$ degrees	Θ_T degrees	Θ_L degrees	$A_1 \cos\Theta_L$
n = 0.98	α = 0.01				
	.051	80	66.90	13.09	$4.97 \cdot 10^{-2}$
	.254	95	85.45	9.55	$25.0 \cdot 10^{-2}$
	.398	100	87.14	12.87	$38.8 \cdot 10^{-2}$
n = 0.98	α = 0.00				
	0.1	92.86	78.58	14.28	$9.69 \cdot 10^{-2}$
	0.3	98.63	86.19	12.44	$29.3 \cdot 10^{-2}$
	0.4	101.54	87.16	14.38	$38.7 \cdot 10^{-2}$
n = 0.98	α = -0.01				
	0.1	98.57	78.92	19.64	$9.42 \cdot 10^{-2}$
	0.3	100.55	86.22	14.33	$29.1 \cdot 10^{-2}$
	0.4	102.99	87.19	15.80	$38.5 \cdot 10^{-2}$
n = 0.96	α = 0.00				
	0.1	92.86	67.84	25.02	$9.06 \cdot 10^{-2}$
	0.3	98.63	82.34	16.29	$28.8 \cdot 10^{-2}$
	0.4	101.54	84.29	17.25	$38.2 \cdot 10^{-2}$

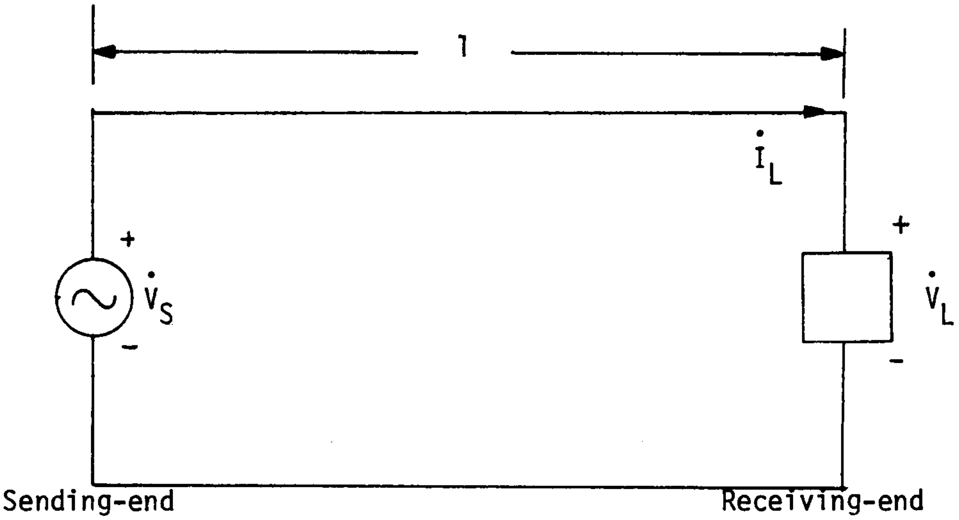

$\dot{Z}_T$ = per unit transmission line impedance

Figure 8.1 Two port electrical power system

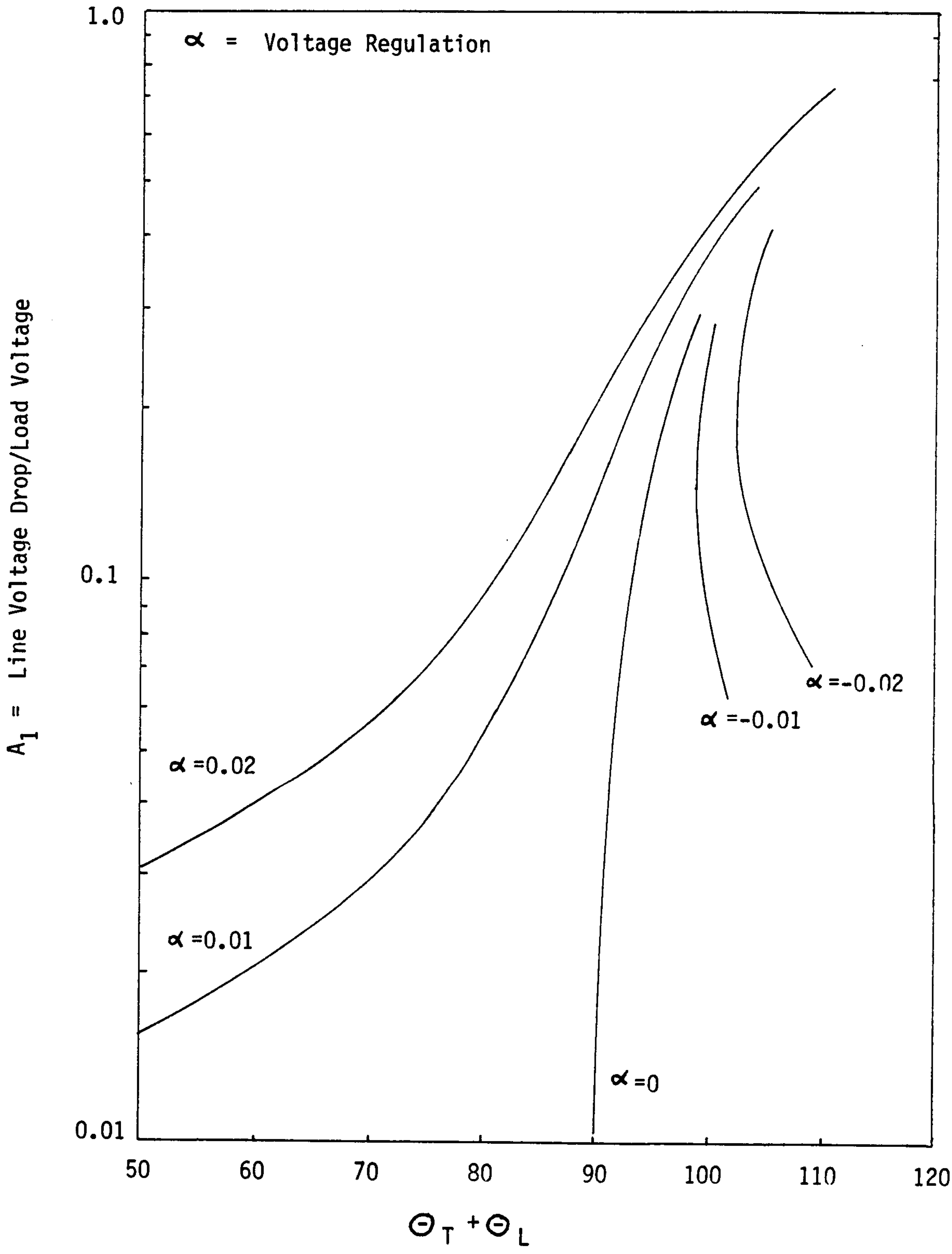

Figure 8.2 Normalized Line Voltage Vs. Transmission Line Plus Power Factor Angle

Chapter 9

HIGH TEMPERATURE ELECTRONIC MATERIALS

I. Introduction

From previous chapters, operating a system at high temperature reduces significantly the size and corresponding mass of radiators that are required to dissipate the system's internal generated heat. This drive toward higher temperature takes on the forms of a nemesis when the system contains electronic components. Using silicon technology the maximum operating temperature is approximately 573°K (300°) based on a bandgap of 1.1 ev.

II. Comparison of Semiconductor Materials

Electronic semiconductor materials must have certain salient features if they are to be used in a broad-based-sense. These characteristics are carrier mobility, thermal conductivity and physical stability at high temperature according to Powell [9.1]. Other difficulties which determine the semiconductor device lifetime at high temperature are inter-diffusion of metal (from contacts) into the semiconductor material and embrittlement due to grain growth at high temperature [9.2].

Carrier mobility measures essentially the drift velocity of a carrier to an applied electric field. At high frequencies the inherent shunting capacitance tends to reduce the electric field causing the semiconductor to become ineffective. The shunting capacitance is a combination of contact and internal material capacitance. Also, carrier mobility decreases as temperature increases causing the high frequency characteristics to deteriorate at high temperature.

Since there is always an electrical power loss associated with a semiconductor device when it is electrically active, the internal generated heat must be conducted through the semiconductor bulk material before it can be heat sinked. For devices that control a substantial amount of power such as in the case of 20 KHZ converter, the semiconducting material must exhibit good thermal conductivity; otherwise the mean time to failure will decrease as the power demand increases.

At high temperature the physical stability is very important, because if there are any changes in the crystalline patterns of the semiconductor material, the electrical characteristics will be altered causing the device to have an early failure.

Diffusive metallic transport from the metallic contact must be considered at elevated temperatures. A mechanism that impedes this diffusion within the metal-semiconductor system has to be developed. A very common approach of reducing the transport between dissimilar materials is to introduce diffusion barriers of intervening metallization layers.

Table 9.1 indicates in a qualitative manner the basic characteristics that semiconducting materials should possess in order to be a successful candidate at high temperature. Starting with silicon, the three characteristics, as shown in Table I, are qualitatively good, but the maximum operating temperature is only 573°K (300°C). The next two materials, gallium arsenide and gallium phosphide, have a larger bandgap and a corresponding higher maximum operating temperature. Except for the excellent carrier mobility characteristics for gallium arsenide, the characteristics are in the fair range. The carbide family (cubic silicon and 6H) exhibit a much higher maximum operating temperature. Both exhibit fair carrier mobility which limits their use to lower frequencies. However, at 20 KHZ frequency the power switching signal would probably still be considered acceptable. Thermal conductivity and physical stability are both very respectable for these two materials. For diamond, the maximum operating temperature and bandgap do not tract as in the other cases, because diamond experiences a phase change near 1373°K (1100°C). While diamond indicates excellent and good characteristics for thermal conductivity and physical stability, more research is required to move the diamond from long-term to commercially available category.

III. Conclusions

This brief study indicates that greater research emphasis must be placed on the wider bandgap materials such as the silicon carbide family so that the electronic components temperature can be increase. This is especially important for space power systems where power levels could reach the megawatt range as human activity in space increases with time.

Nuclear heat sources operating at high temperature (greater than 1000°K) appear to be the only viable method for generating high power levels over long periods of time with a reasonable size mass. Unfortunately, the conversion from heat to electricity occurs at dc. A second conversion from dc to ac is required in order to operate the electrical power system at higher voltage and frequency. This second conversion could be accomplished by using high frequency electronic converters that are designed at efficiencies greater than 95%. Placing the electronic converter in a high temperature environment (near or at the heat source) would minimize the mass of the dc segment of the power system.

If reliable high frequency turbine driven alternators are developed to operate over many years, this may be one possible strategy to eliminate the electronic power converter. However, the alternator's mass may be substantially larger when compared to the mass of the converter assuming equal power outputs.

References

[9.1] Powell, J.A., "Silicon Carbide, A High Temperature Semiconductor," TM83514, Cleveland Electronic Conference (CECON '83), Cleveland, Ohio, October, 1983.

[9.2] Wiley, J.D. et al., "Amorphous Metallizations for High Temperature Semiconductor Device Applications," IEEE Transactions on Industrial Electronics, Vol. IE-29, No. 2, May 1982.

TABLE 9.1. A Comparison of Some Commercially Available Electron Materials

1-Fair 2-Good 3-Very good 4-Excellent

Material	Bandgap (ev)	Maximum Operating Temperature °K (°C)	Carrier Mobility	Operating Thermal Conductivity	Physical Stability
Silicon	1.1	573 (300)	2	2	2
Gallium Arsenide	1.4	733 (460)	4	1	1
Gallium Phosphide	2.2	1148 (875)	1	1	1
Cubic Silicon Carbide	2.3	1198 (925)	1	3	4
6H Silicon Carbide	2.9	1513 (1240)	1	3	4
Diamond	5.5	1373 (1100)	2	4	3

Chapter 10

HIGH POWER VACUUM SWITCHING DEVICES

I. Introduction

In the previous chapter attention was focused on semiconducting materials that operated at temperatures in the vicinity of 1400°K. Although the operational temperature is acceptable, radiation damage is very important since the electron-hole transport process is dependent on the semiconductor crystalline structure. In space, where radiation could be significant or near a source of radiation such as a nuclear reactor source, the radiation damage will alter the electrical characteristics of semiconductors over time. When using semiconductor devices as a power switch, such as in a 20-KHz converter, radiation damage may be sufficient to disrupt the power conversion and render the electrical power system useless.

Hard vacuum tube and thyration switching have been used in terrestrial applications, but are limited to low current in the case of the hard vacuum tube switch and the requirement of commutation for dc interruptibility for the thyration type devices. However, the USSR [10.1] has developed a switch that is capable of plasma interruption at large anode voltages. They have developed commercial devices capable of switching 300 amperes at 12 kV with a 100-KHz repetition frequency.

It appears that high voltage/high current switching devices would be very useful in the conversion of dc to ac power, switching large blocks of power, and protecting electrical power systems during major faults. This type of switch would be a good candidate for high power space systems such as on the surface of the Moon.

Historically, either hard-vacuum thermionic-cathode or gas-discharge plasma switches have been employed for switching high power. Although the hard-vacuum switch has a fast closing and opening response at high voltage, it has two major faults. They are: (1) low switching current and (2) high cathode heater power. On the other hand, plasma switches, such as the thyration, offer high current at relatively low anode voltage. However, they have poor opening characteristics. For example, once the plasma has been generated, it is very difficult to extinguish the plasma.

Solid-state power switching devices, such as bipolar and MOSFET transistors, SCRs and gate turn-off thyristors (GTO), are capable of switching 100 amperes at 1 kV, but at very large currents and voltage they do not have the switching capacity. Also, solid-state devices are prone to radiation damage.

Table 10.1 [10.2] lists the pulse power capabilities of various types of switches that are commercially available. Accordingly, the Crossatron [10.2] exhibits all the capabilities shown.

II. Crossatron Principles

The structure of the Crossatron is a four-element device, shown in Figure 10.1, that is arranged in a coaxial configuration, consisting of a cold cathode, source grid, control grid and anode. The plasma is produced by a cross of electric and magnetic fields which are respectively established by the potential difference between the source grid and cold cathode and a set of permanent magnets located on the outside of the switch. This cross-field configuration essentially confines the plasma between the cold cathode and the source grid which serves as the anode for the local discharge. Switch action is controlled by pulsing the control grid with a voltage that is higher than the plasma voltage allowing conduction to the anode. Typical anode-cathode voltage has a range from 200 to 500 volts in the conduction mode. Demonstrated tube performance has shown a capability of withstanding an open-circuit voltage of 90,000 volts. The ratio of conduction to open circuit voltage is approximately 0.005 which is very small. Helium or hydrogen gas at pressures of 0.02 to 0.05 Torr is used to establish the plasma. The important features of the Crossatron are the elimination of the cathode heater power and the instant start operation.

Table 10.2 [10.3] lists the demonstrated and projected performance of a Crossatron. Note that the present pulse repetition frequency is 16 KHz, which is commensurate with the 20 KHz space power system frequency.

III. Conclusions

This chapter focuses attention on the possibility of using devices other than solid-state switches, especially when the operating voltages and currents are very large. In the case of space electrical power systems that must operate for many years, such as the lunar base colonies, a nuclear source for generating heat energy will be required. Solid-state electrical characteristics will be affected by possible radiation damage from the nuclear source and, in time, may cause the electrical power system to fail either partially or totally.

A low pressure vacuum-type switch that is commercially available under the trade name Crossatron (Hughes Aircraft Company) has been investigated in this chapter. It appears that the principle of being able to control the plasma offers the possibility of switching large blocks of power or using this principle to convert dc to ac at megawatt levels at pulse repetition frequencies commensurate with present day space power system frequency (20 KHz).

The principle used in the Crossatron seems to demonstrate all the features that define a high power and high frequency switching device.

References

[10.1] Dvornikov, V. D. and et al., "Technika Experiments", No. 4, July-August, 1972.

[10.2] Schumacher, R. W. and Harvey, R. J., "Crossatron Modulator Switch", Conference Record of the Sixteenth IEEE Power Modulator Symposium, Arlington, VA, 1984.

[10.3] Schumacher, R. W. and Harvey, R. J., "The Crossatron Modulator Switch: An Efficient, Long-Life Component For Pulsed-Power Systems", Fifth IEEE Pulse-Power Conference, Arlington, VA, 1985.

Table 10.1. Pulse-Power Switch Capabilities [10.2]

Table 10.1. Pulse-Power Switch Capabilities [10.2]

Switch Type	Instant Start	Low Standby Power	Low Control Power	Low Conduction Voltage	Interruptable dc Current	High Voltage	High Current	High PRF*	Electro-Mechanic "Rugged"
Hand Vacuum Tube					•	•		•	•
Thyratron		•	•	•		•	•	•	•
Ignition	•	•	•	•		•	•		•
Vacuum Spark Gap	•	•	•	•		•	•		•
Pressurized Spark Gap	•	•	•	•		•	•		•
SCR	•	•	•	•			•	•	
Transistor	•	•	•	•	•			•	
Gate Turn-off Thyristor	•	•	•	•	•				
Crossatron	•	•	•	•	•	•	•	•	•

* PRF - Pulse Repetition Frequency

C-2

Table 10.2. Proven and Projected Performance for Crossatron Switches [10.3]

Crossatron Switch Parameter	Proven Performance	Projected Performance
Open Circuit Voltage (kV)	90	200
Conduction Voltage (V)	200-500	30
Interrupted Current (A)	500	50,000
Conduction Current (A)	1,500	50,000
Closing Time (ns)	20	20
Opening Time (ns)	50	20
Pulse Repetition Frequency (KHz)	16	1,000

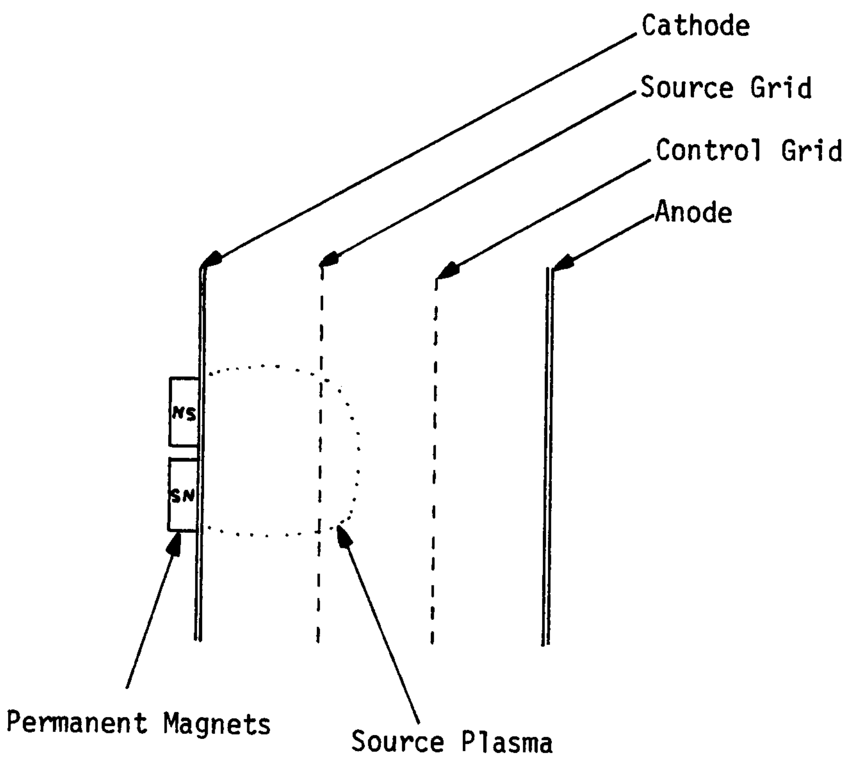

Figure 10.1 Crossatron Modulator Switch Configuration

Chapter 11

OPTIMAL OPERATION OF ELECTRIC POWER SYSTEMS

I. Introduction

The main objective of any electrical power system, whether terrestrial or non-terrestrial, is to accommodate the demand for power in a reliable manner. High power electrical power systems will have several conversion units that will convert heat eneregy into electrical energy using such devices as electronic power conversion or alternators. The total system power input, which may be derived from a nuclear source for a non-terrestrial power system, must be used judiciously; otherwise, the nuclear fuel will have to be replaced more frequently.

The mathematical relationship between the generated power and the total system power input is very complex. However, it is reasonable to assume that the input power increases monotonically with power. The strategy is to minimize the total input power for a given power demand and transmission line loss.

II. Optimal Operation of a Long Electrical Power System

The input power to an electrical power system is measured in terms of megajoules/hour (MJ/h), and the generated electrical power in megawatts (mw). The functional relationship between input and generated power is nonlinear and can be approximated by the following general quadratic expression for a single generator where F and P represent respectively the input and generated power. The determination of A_0, A_1, and A_2 depends on data that relates F to the generation level P.

$$F(P) = A_0 + A_1 P + A_2 P^2 \qquad (11.1)$$

The objective of this chapter is to obtain the most economical loading of "m" generating units such that

$$F_T = \sum_{i=1}^{m} (A_{0i} + A_{1i} P_i + A_{2i} P_i^2) \tag{11.2}$$

(where F_T = total input power) is minimized under the constraint that there is a power demand P_D and a transmission line loss P_L. The power balance including losses is

$$P_D = \sum_{i=1}^{m} P_i - P_L \tag{11.3}$$

where the power loss is assumed to be a function of the power generation alone. The Lagrange multiplier technique can be used to minimize F_T.

The value of F can be expressed as follows using the Lagrange multiplier λ

$$F = \sum_{i=1}^{m} (F_i + \lambda \ (P_D + P_L - \sum_{i=1}^{m} P_i)) \ . \tag{11.4}$$

The optimality conditions are obtained by setting the partial derivatives of F with respect to P_i to 0. This results in the following equation

$$\frac{\partial F_i}{\partial P_i} + \lambda \left(\frac{\partial P_L}{\partial P_i} - 1 \right) = 0 \tag{11.5}$$

If the transmission line losses are negligible $\alpha P_L/\alpha P_I = 0$, then $\partial F_i/\partial P_i = \lambda$. The implication for the lossless case is that individual generating units should share the load such that $\partial F_i/\partial P_i$ are all equal. For the lossy case the Lagrange multiplier is

$$\lambda = \left(\frac{1}{1 - \frac{\partial P_L}{\partial P_i}} \right) \frac{\partial F_i}{\partial P_i} \qquad (i=1 \ldots . \ m) \ . \tag{11.6}$$

The bracketed factor is termed a penalty because F_i is penalized by the corresponding incremental transmission line losses $(\partial P_L/\partial P_i \geq 0)$. Maintaining a high efficient system is of paramount importance, especially for the electrical power systems that are located on another planets.

The functional behavior of loss P_L will now be addressed. Consider the system shown in Figure 11.1 where two generators are tied to the demand bus through transmission lines of resistance R_{1T}, R_{2T}, and R_{3T}, respectively. Note R_{1T}, R_{2T}, and R_{3T} are total line resistances and not per unit resistance values. Assuming the lines are respectively ℓ_1, ℓ_2, and ℓ_3 in length, the total line resistance can be expressed in terms of per unit resistance as follows:

$$R_{1T} = R_1\ell_1 \tag{11.7a}$$

$$R_{2T} = R_2\ell_2 \tag{11.7b}$$

$$R_{3T} = R_3\ell_3 \tag{11.7c}$$

The total power loss can be written in the following manner [11.1]:

$$P_L = B_{11}P_1^{\,2} + 2B_{12}P_1P_2 + B_{22}\,P_2^{\,2} \tag{11.8}$$

where

$$B_{11} = \frac{R_{1T}}{|V_1|^2(PF)_2^2} + \frac{R_{3T}}{|V_3|^2(PF)_3^2}$$

$$B_{22} = \frac{R_{2T}}{|V_1|^2(PF)_2^2} + \frac{R_{3T}}{|V_3|^2(PF)_3^2}$$

$$B_{12} = \frac{R_{3T}}{|V_3|^2(PF)_3^2}$$

where $(PF)_i$ denotes the power factor at the i^{th} bus. The power demand is approximately equal to $P_1 + P_2$, assuming the transmission line losses are small. The coefficients in Equation (11.8) are small if $R_{qT}/(|V_q| \cdot PF_q)^2$ is small which reflects the requirement of (1) a small per unit transmission line resistance, especially if the power system services a relatively low load density over a vast area; (2) a large operating voltage at the q^{th} node; (3) a large power factor at the 8th node (maximum is unity).

A small R_{qT} demands that the transmission line lengths be short (a rather spaciously compact electrical power system) with large cross-sectional conductor areas (a massive transmission line system). If the transmission lines can operate in a superconductive mode, the coefficients approach zero. Even if this condition can exist there will be devices such as transformers or voltage regulators located along the transmission that will contribute to the losses from the generators to the loads.

The product $(|V_q|(PF)_q)^2$ inversely affects the value of the power loss coefficients. Note that this product is squared which has even a greater affect on the coefficients. Maintaining unity power factor at the qth node will require some form of power factor correction at the node which increases the total electrical power system mass. Operating the node at high voltages will reduce the coefficients. However, as the voltage increases, the transmission line support mass increases. For high voltage terrestrial electrical power systems, the support towers would be an example of support mass.

The power loss P_L (Equation 11.8) can be generalized to what is commonly referred to as the loss formula for a more complex power system. The loss formula is

$$P_L = \sum_{i=1}^{m} \sum_{j=1}^{m} B_{ij} P_i P_j \quad . \qquad (11.9)$$

When $i=j$, $P_i P_j = P_i^2$ and $B_{ij} = B_{ii}$, represents, respectively, the power supplied by the i^{th} generator and the sum of contributions of each transmission line from the i^{th} generator to the demand power bus. For $i \neq j$, $P_i P_j$ and B_{ij} represents, respectively, the cross multiplication of the powers from the i^{th} and j^{th} generators and the contribution of the common transmission lines that transmit both the i^{th} and j^{th} power. See Figure 11-1 for a three-line system and the definitions of the B-coefficients in Equation (11.8).

III. Conclusions

The important problem of minimizing fuel consumption in supplying a known power demand is a main driver, especially when the electrical power system is located on the Moon or on some other planet. Assuming the total fuel available is fixed, minimizing the fuel consumption rate extends the time between refueling the power system.

In this chapter a simple electrical power system was investigated that included transmission line losses. For the minimum fuel consumption case, results indicate that all generators, that are operating below their rated limit, must each operate to maintain a constant product of penalty factor and incremental cost.

Results indicate operating all electrical nodes at unity power factor, at the highest possible voltage, and smallest line resistance will reduce the penalty factor. However, the total electrical power system mass will increase because power factor correcting devices must be added, support structure mass will be driven upwards with increasing voltage, and transmission line mass increases with decreasing per unit line resistance.

One possible solution to penalty reduction is operating the transmission line in a superconducting mode. Research must be done on increasing the superconducting temperature to approximately 250°K while still maintaining a high current density and a flexible transmission line.

Reference

[11.1] El-Hawary M.E., "Electric Power Systems: Design and Analysis," Reston Publishing Company, Inc.., 1983.

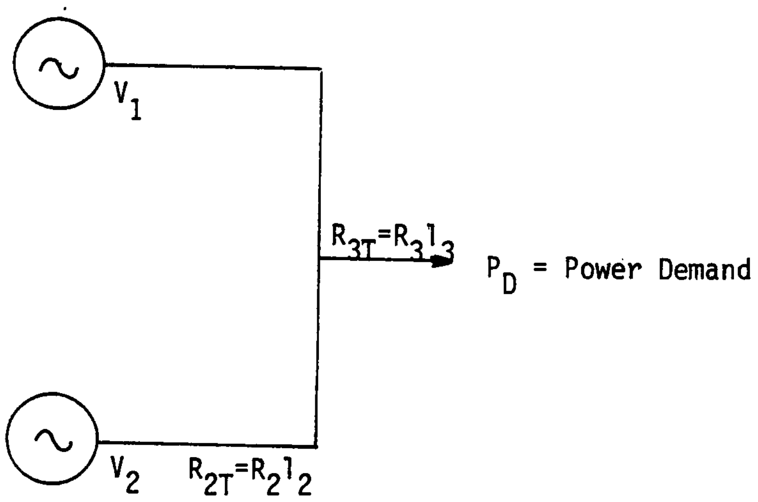

Figure 11.1 A Three-Line Electrical Transmission Line System.

Chapter 12

SYSTEM RELIABILITY

I. INTRODUCTION

A quantitive measure of the performance of a system in terms of its design goals is reflected by the system reliability, which has an upper bound of unity. Reliability can be defined as the probability of successful system operation under the conditions of intent. An ideal system would have a reliability of unity.

Placing identical components in parallel is an example of a design technique called redundancy and improves the system reliability beyond that of any one parallel component. However, there is a penalty, such as dollar cost, mass, and volume, for this increase in reliability. If all components must operate in order to maintain system reliability the redundancy is called active redundancy. There are other types of redundancy that can be used such as inactive redundancy, sometimes called standby redundancy, and voting redundancy. Inactive redundancy switches from a defective to an operational unit with the switching process continuing until all units are defective. On the other hand, voting redundancy, which is a special form of active redundancy, is a system where several parallel outputs are monitored by a decision-making device which provides the required system function as long as a predetermined number of parallel outputs are in agreement.

Reliability allocation, in contrast to placing components in parallel, focuses attention on the allocation of individual component reliability so as to meet a prescribed system reliability to minimize, for example, dollar cost, mass, and/or volume. This chapter will investigate a scheme that minimized the total penalty of a series system while meeting a predetermined reliability. Although the series model is simple, it does shed light on more complex systems that require dynamic programming techniques rather than the technique presented in this chapter.

II. RELIABILITY ALLOCATION

The model shown in Figure 12-1 is a series system with N components where the ith component has R_i reliability ($1 \leq i \leq N$). The system reliability is

$$R_S(t) = \prod_{i=1}^{N} R_i(t) \tag{12.1}$$

where the time functional notation indicates that as the system ages the reliability changes.

Assume each component in the N-series system has an exponential failure time distribution where the reliability of the ith component is $R_i(t) = \exp(-\lambda_i t)$ and λ_i represents the failure rate. The system reliability is

$$R_S(t) = \exp\left(-\sum_{i=1}^{N} \lambda_i t\right). \tag{12.2}$$

It can be shown that the mean time before failure for the ith component is

$$(MTBF)_i = {}^{1}/{\lambda_i} \tag{12.3}$$

and

$$\sum_{i=1}^{N} \lambda_i = -\frac{\ln(R_s(T))}{T} \tag{12.4}$$

where time t has been replaced by a specific time T.

Consider the following minimization problem where the objective is to determine the allocation of the component MTBF which will minimize the total penalty such that for a given time T, the reliability of the system at t = T is $R_S(T)$. The penalty equation can be expressed by the following equation

$$\text{minimize } \left(\sum_{i=1}^{N} g_i(\lambda_i)\right) \qquad (12.5)$$

where $g_i(\lambda_i)$ will generally be nonlinear which implies that either the Lagrange multiplier or dynamic programming technique will be required.

For purpose of illustration, assume $g_i(\lambda_i) = a_i (MTBF)_i$ where $(MTBF)_i = {}^1/\lambda_i$. Using the Lagrange multiplier technique, the total minimum system [12.1] penalty $P_{S,min}$ is

$$P_{s,min} = \frac{-T\left(\sum_{i=1}^{N} a_i^{1/2}\right)^2}{\ell n(R_s(T))} \qquad (12.6)$$

and

$$(MTBF)_i = \frac{-T \sum_{j=1}^{N} a_j^{1/2}}{a_i \, \ell n(R_s(T))} \qquad (12.7)$$

According to Equation (12.6) increasing the time interval T or the system reliability $R_s(T)$ increases $P_{s,min}$. If $P_{s,min}$ is interpreted as a mass penalty, the minimum system mass increases linearly with operation time interval and inversely with the natural logarithm of reliability. The coefficient a_i reflects the penalty paid for increasing $(MTBF)_i$ and is a function of the technology at the time the system is being constructed.

Ideally, $\sum_{i=1}^{N} a_i^{1/2}$ should be as small as possible. Also, it is noted that as N increases $P_{s,min}$ increases.

The MTBF for the ith component (Equation 12.7) is functionally related to the time interval and system reliability in the same manner as in Equation (12.6). However, (MTBF) is proportional to $\sum_{j=1}^{N} a_j^{1/2}$ and inversely related to a_i. Assuming a_i decreases (technological breakthroughs), its impact effects $(MTBF)_i$ more so than any other (MTBF). It has a minor effect on all MTBFs because any MTBF depends on $\sum_{j=1}^{N} a_j^{1/2}$ which includes a_i.

III. RELATIONSHIP BETWEEN NORMALIZED SYSTEM TEMPERATURE AND SYSTEM PARAMETERS

In this section we will establish a relationship between system temperature and the normalized mean time before failure, (MTBF)/T, employing the results from Section II.

Assume a system consisting of N series components with the penalty coefficient a_i having a dimension of mass per unit time. The minimum system penalty $P_{s,min}$ (see Equation 12.6) becomes the minimum system mass $M_{s,min}$ and can be expressed by

$$M_{s,min} = \frac{\left(\sum_{i=1}^{N} a_i^{1/2}\right)^2}{Q} \qquad (12.8)$$

where $Q = \ell n(1/R_s(T))/T$. If Q decreases, which corresponds to either increasing the system reliabiilty $R_s(T)$ or increasing the system operational time T, $M_{s,min}$ increases for a given $\sum_{i=1}^{N} a_i^{1/2}$. since a_i is dependent on the technology at the time the system is designed, the developing technology must reduce a_i which in turn reduces $\sum_{i=1}^{N} a_i^{1/2}$ for a fixed number of components N. The value of $M_{s,min}$ is also a function of N. If it is assumed that $a_i = a$ for all i, $(\sum_{i=1}^{N} a_i^{1/2})^2 = aN^2$ which indicates that $M_{s,min}$ increases as the square of the number of cascaded components. Technology must be developed to maintain a reasonable number of series system components. This general model is applicable to electrical power systems.

The system mass can be related to the average operating system temperature, system power, and a geometrical factor relating system surface radiative area to its volume. This model, although somewhat simplistic, does provide insight about certain system tradeoffs.

Inside an electrical power system, which includes all loads, there is a power source capable of delivering Pin. For a non-terrestrial power system this power must be eventually radiated into space. Employing the Stefan-Boltzmann radiative law, the system mass is

$$M_s = \frac{\rho \, Pin}{\sigma \varepsilon f \Theta_s^4 (r^4 - 1)} \qquad (12.9)$$

where ρ = average system density (kg/m^3)

Pin = input power (watts)

σ = $5.67 \cdot 10^{-8}$ (w/m^2-k^4)

ε = radiator emissivity

Θ_s = sink temperature = 250°K

f = system surface area/system volume (1/m)

r = ratio of average system temperature to sink temperature (Θ/Θ_s).

Equating Equations (12.8) and (12.9) and solving for r^4 we have

$$r^4 = \frac{\rho \text{ Pin } Q}{\sigma\varepsilon f \Theta_s^4 \left(\sum_{i=1}^{N} a_i^{1/2} \right)^2} + 1 \; . \quad (12.10)$$

Treating Q as an independent variable, the slope of the above equation is

$$\text{SLOPE} = \frac{\rho \text{ Pin}}{\sigma\varepsilon f \Theta_s^4 \left(\sum_{i=1}^{N} a_i^{1/2} \right)^2} \; . \quad (12.11)$$

As the electrical input power increases, the product f. $\left(\sum_{i=1}^{N} a_i^{1/2} \right)^2$ must track with power; otherwise the system temperature will become large for a given ρ, $\Theta_s{}^4$, ε, and Q. Since $M_{s,min}$ is proportional and the slope is inversely proportional to $\left(\sum_{i=1}^{N} a_i^{1/2} \right)^2$, the value of f must track, rather strongly, with Pin in order to maintain a small value for $M_{s,min}$ and r^4.

IV. CONCLUSIONS

High strength materials with low mass density must be developed in order to reduce ρ. For lunar base electrical power systems, where the nights are fourteen days long, it appears the energy source must be self-contained, such as a nuclear reactor. Because the reactor is massive, (shielding is required to protect personnel and electronic equipment from radiation damage) this drives the average system mass density is driven upwards.

The system geometrical factor f must be large in order to maintain a reasonable average system temperature. High power electrical power systems must be geometrically flat with a large radiative surface area, otherwise, high temperature component technology must be developed.

Reference

[12.1] Rau, J.G., "Optimization and Probability in Systems Engineering" Van Nostrand Reinhold Co., 1970.

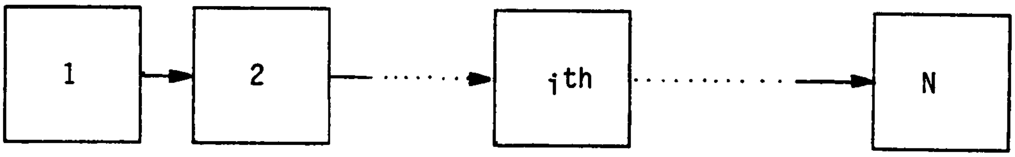

Figure 12.1 Series System of Order N

Chapter 13

EFFECT OF REDUCING THE SPATIAL SEPARATION BETWEEN THE ELECTRICAL HEAT SOURCE AND THE ELECTRONIC POWER CONVERTER

I. Introduction

This chapter will investigate the radiant energy transfer between a power source radiator and an electronic power converter radiator in an electrical power system as a function of radiator separation. The transfer of radiated energy from the higher temperature source radiator to the electronic power converter radiator causes the temperature of the latter radiator to increase as the spatial separation between the two radiators decreases.

The degree of energy coupling between radiators is determined by the configuration factor which in turn depends on the geometry and orientation of the radiators. A general expression relating the radiator temperature to its isolated temperature is presented as a function of the configuration factor. Isolated temperature is defined to be the radiator temperature when the radiator is completely isolated from all radiators.

II. System Analysis

Ideally, it would be advantageous to place the electrical power system unit as close to the heat source as possible to reduce the system losses. In this section, the model shown in Figure 13.1 will be used. Let the conversion from DC to AC have an efficiency of n_e, while the source efficiency is n_s. Separate radiators are used to remove heat loss from the source and converter. If the two radiators are separated by a significant distance, both will effectively be viewing the background which acts as an infinite heat sink. The source radiator temperature is much larger than the converter radiator temperature, usually a factor of approximately three.

14. The reason for this large temperature differential is that the converter radiator temperature is determined essentially by the operating electronic operating temperature, which by today's technology, can be as low as 350°K, while the source temperature can be 1000°K or higher.

As the distance between these two radiators decreases, the transfer of radiated energy between the two radiators increases. Since the source radiator is radiating more power, it will have a greater effect on the converter radiator temperature as compared to the reverse case.

According to [13.1] the following set of equations describe the functional behavior of both radiator temperatures in terms of configuration factor and other system parameters:

$$\frac{x_1}{x_{10}} = \frac{1 + F_{1-2}\,\varepsilon_2\Gamma - \left(\frac{A1}{A2}\right)(F_{1-2})^2(1-\varepsilon_1)}{1-\left(\frac{A1}{A2}\right)(F_{1-2})^2} \tag{13.1}$$

and

$$\frac{x_2}{x_{20}} = \frac{1 + \frac{A1}{A2}F_{1-2}\,\varepsilon_2\left(\frac{1}{\Gamma}\right) - \left(\frac{A1}{A2}\right)(F_{1-2})^2(1-\varepsilon_2)}{1-\left(\frac{A1}{A2}\right)(F_{1-2})^2} \tag{13.2}$$

where F_{1-2} = configurator factor from source (1) to converter (2) radiator

$\varepsilon 1$ = source radiator emissivity

$\varepsilon 2$ = converter radiator emissivity

A1 = source radiator area (m^2)

A2 = converter radiator area (m^2)

x_1 = $T_1^4 - T_s^4$ (^{o}k)

$x_2 = T_2^4 - T_s^4$ (^oK)

$x_{10} = T_{10}^4 - T_s^4$ (^oK)

$x_{20} = T_{20}^4 - T_s^4$ (^oK)

T_1 = radiator source temperature (^oK)

T_2 = radiator converter temperature (^oK)

T_{10} = isolated radiator source temperature (^oK)

T_{20} = isolated radiator converter temperature (^oK)

T_s = sink or background temperature (^oK)

As radiator separation increases, $F_{1-2} \rightarrow 0$, $x_1 \rightarrow x_{10}$, and $x_2 \rightarrow x_{20}$.

The model for the configuration factor is shown in Figure 13.2. It was selected because the configuration factor can be expressed in closed form. The configuration factor F_{1-2} can be expressed in terms of two other configuration factors accordingly

$$F_{1-2} = F_{1-(2+3)} - F_{1-3} \quad (13.3)$$

The first term represents the configuration factor between radiator 1 and radiator (2 + 3), while the second term represents the configuration factor between radiators 1 and 3. The two terms are subtracted to remove the affect of radiator 1 to radiator 3 since radiator 3 is not physically present.

The general configuration faction expression [13.2] for both terms can be expressed by

$$F = \frac{1}{\pi L}\left(L\tan^{-1}\left(\frac{1}{L}\right) + N\tan^{-1}\left(\frac{1}{N}\right) - \sqrt{N^2+L^2}\tan^{-1}\left(\frac{1}{N^2+L^2}\right) + 0.25\ln\right.$$

$$\left.\left(\left(\frac{(1+L^2)\ (1+N^2)}{1+N^2+L^2}\right)\cdot\left(\frac{L^2(1+L^2+N^2)}{(1+L^2)(L^2+N^2)}\right)^{(L)^2}\cdot\left(\frac{N^2(1+L^2+N^2)}{(1+N^2)(L^2+N^2)}\right)^{(N)^2}\right)\right) \quad (13.4)$$

where $L = c/b$

$N = N_2$ or N_3 depending on the configuration to be determined

$N_1 = a/b$

$N_2 = (a+d)/b = \frac{a}{b}(1+d/b) = N_1(1+d/a)$

$N_3 = d/b$

From the above definitions and Equations (13.1) - (13.3) it is obvious that as $d\to\infty$, $N_2\to N_3$, $F_{1-2}\to 0$, $x_1\to x_{10}$, and $x_2\to x_{20}$ which is the case for isolated radiators.

Returning to Figure 13.1, it will be assumed that the converter is an electronic high frequency inverter, the transmission line between the source and inverter is DC, and the transmission line between the inverter and load is an AC transmission line. Besides frequency shifting, the electronic inverter will be capable of increasing the line voltage by a factor of 5. Table 13.1 lists the values for system parameters used in the analysis. A 1000-volt ac operating voltage was selected because the operating voltage must track with output power; otherwise, the AC transmission line would become very massive. A rather tight voltage regulation of 1% was assumed. High power electrical systems, capable of operating over a few decades, will require a nuclear power source which has a rather low efficiency of approximately 10%. A 1000°K source radiator temperature was selected to represent a typical source temperature. As the required power level increases, the source temperature must track with power in order to maintain a reasonable source radiator mass. A 350°K isolated temperature was selected for the electronic radiator to reflect a present-day operating semiconductor temperature of approximately 125°C. Analysis has shown that the source radiator temperature is almost independent of radiator separation with temperature variation of approximately several degrees. This is insignificant when compared to the nominal radiator temperature of 1000°K.

A computer program, written in BASIC (Appendix A), was developed to solve for electronic radiator temperature as a function of separation distance d. Power levels, from 0.1 to 10 megawatts, and two radiator widths (b= 1 and 10) were selected.

III. Results

Figures 13.3 - 13.6 illustrate the behavior of radiator 2 temperature versus radiator separation in d(meters) for the indicated output power and radiator widths. The computer results indicated that for d>10 meters, temperature T_2 was approaching T_{20} = 350°K asymptotically. For distances greater than 10 meters (~30 feet) radiator 2 was seeing essentially the background or sink and its temperature was not affected by the presence of radiator 1.

Figures 13.3 - 13.5 show that for a given radiator width b = 1, the temperature profile first increases when the power changes from 0.1MW to 10MW. However, the temperature profile decreases when the power level increased from 1 to 10MW (see Figures 13.4 and 13.5). The reason for this anomaly is the fact that for a fixed distance d, where $1 \leq d \leq 10$ meter, the radiation pattern of radiator 1 changes because dimension c must track with output power level placing radiator 2 at a lower radiation pattern (radiation 1) level. In other words, for a given separation distance, radiator 2 begins to find itself in the quasi-shadow of radiator 1. At d =

10 meters the temperature of radiator 2 is approximately the same for 1 and 10MW, (Figures 13.4 and 13.5) when the vertical scale factor is taken into account.

For a given power output level and spacing, increasing the width b causes more radiative energy to be transferred from radiator 1 to radiator 2 which in turn increases the temperature of radiator 2. This is illustrated by comparing Figure 13.5 with Figure 13.6.

IV. Conclusion

Reducing the distance between the source and electronic power converter increases the radiator temperature and decreases the mass of the electronic power converter's radiator. However, the penalty for this mass reduction is that the electronic components must operate at a higher temperature. With proper orientation of both radiators, the exchange of radiant energy between the high and low temperature radiators can be minimized.

Table 13.1 Model Parameters

1. Radiator

   Emissivity

   $\varepsilon_1 = 0.8$

   $\varepsilon_2 = 0.8$

   Mass Density

   $\rho_{R1} = 10\ kg/m^2$

   $\rho_{R2} = 8\ kg/m^2$

   Temperature

   $T_{10} = 1000°K$

   $T_{20} = 350°K$

2. Transmission line

   Efficiency

   $N_{T1} = 0.99$

   $N_{T2} = 0.99$

   Voltage regulation

   A.C. line = 1%

   Operating line voltage

   A.C. line = 1000 volts

   D.C. line = 200 volts

3. Electronic converter efficiency = 90%

4. Source efficiency = 10%

5. Load power factor = unity

6. Distance from the source to load = 200 meters

7. Background temperature = 250°K

References

[13.1] Siegel, R. and Howell, J. R. , "Thermal Radiation Heat Transfer", McGraw-Hill Book Company, 1981.

[13.1] Sparrow, E.M. and Cess, R.D., "Radiation Heat Transfer", Hemisphere Publishing Company, 1978.

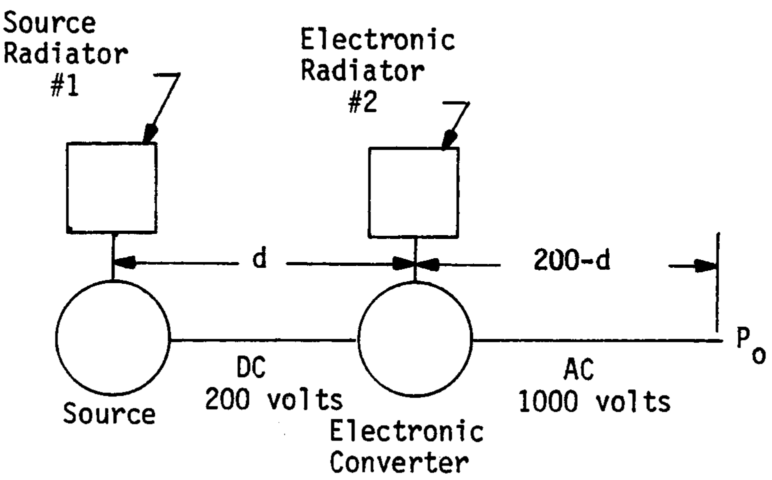

(See Table 13.1 for model parameters)

Figure 13.1 Model of an electrical power system.

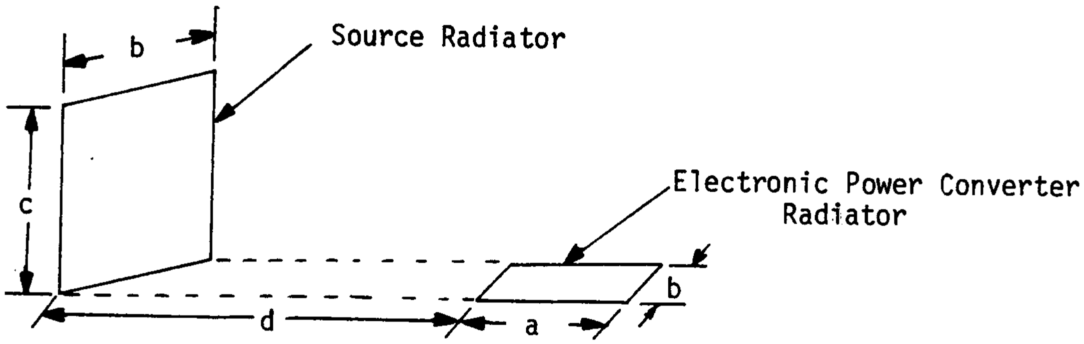

Figure 13.2 Model for the configuration factor.

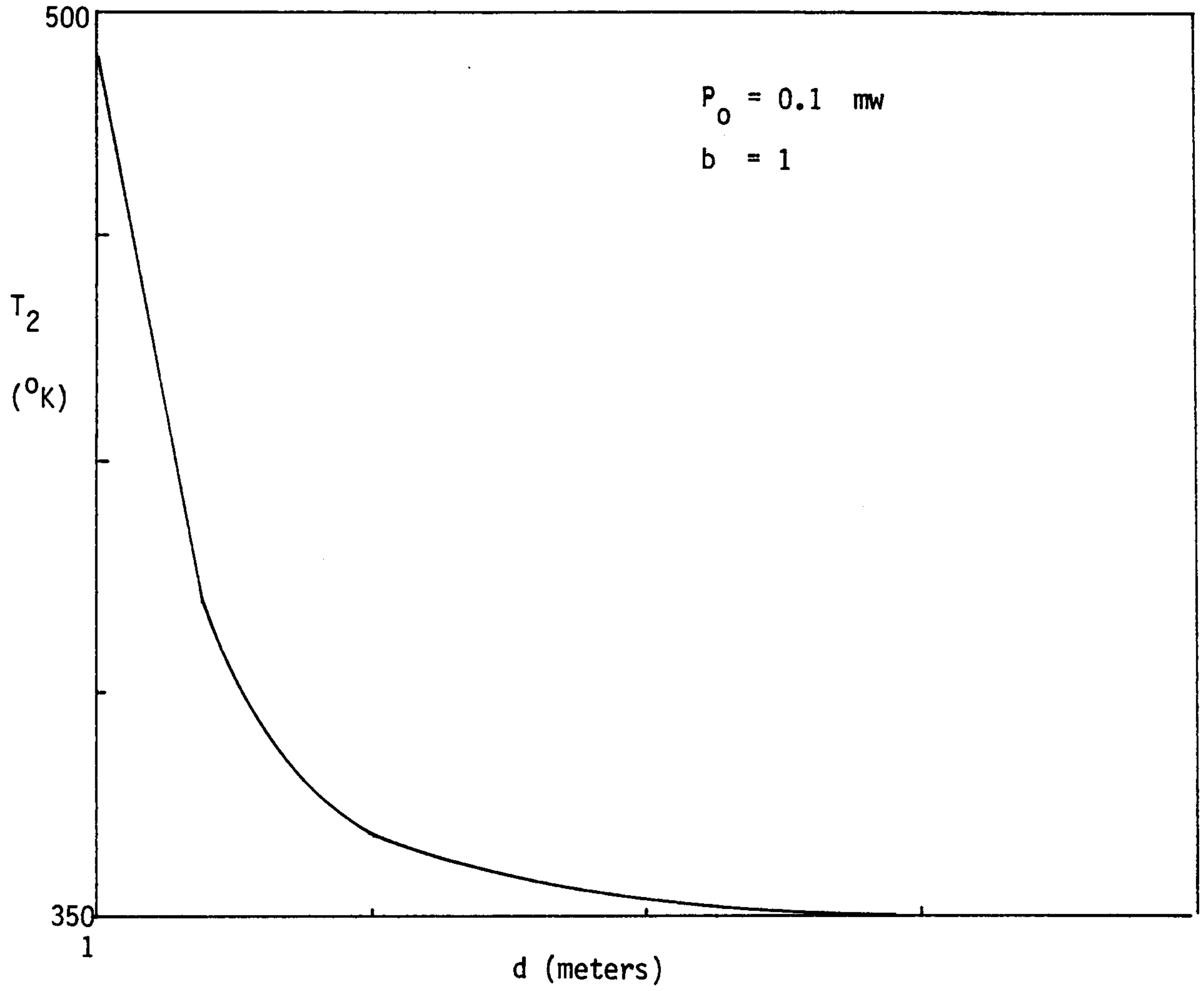

Figure 13.3 Electronic temperature vs. Radiator separation.

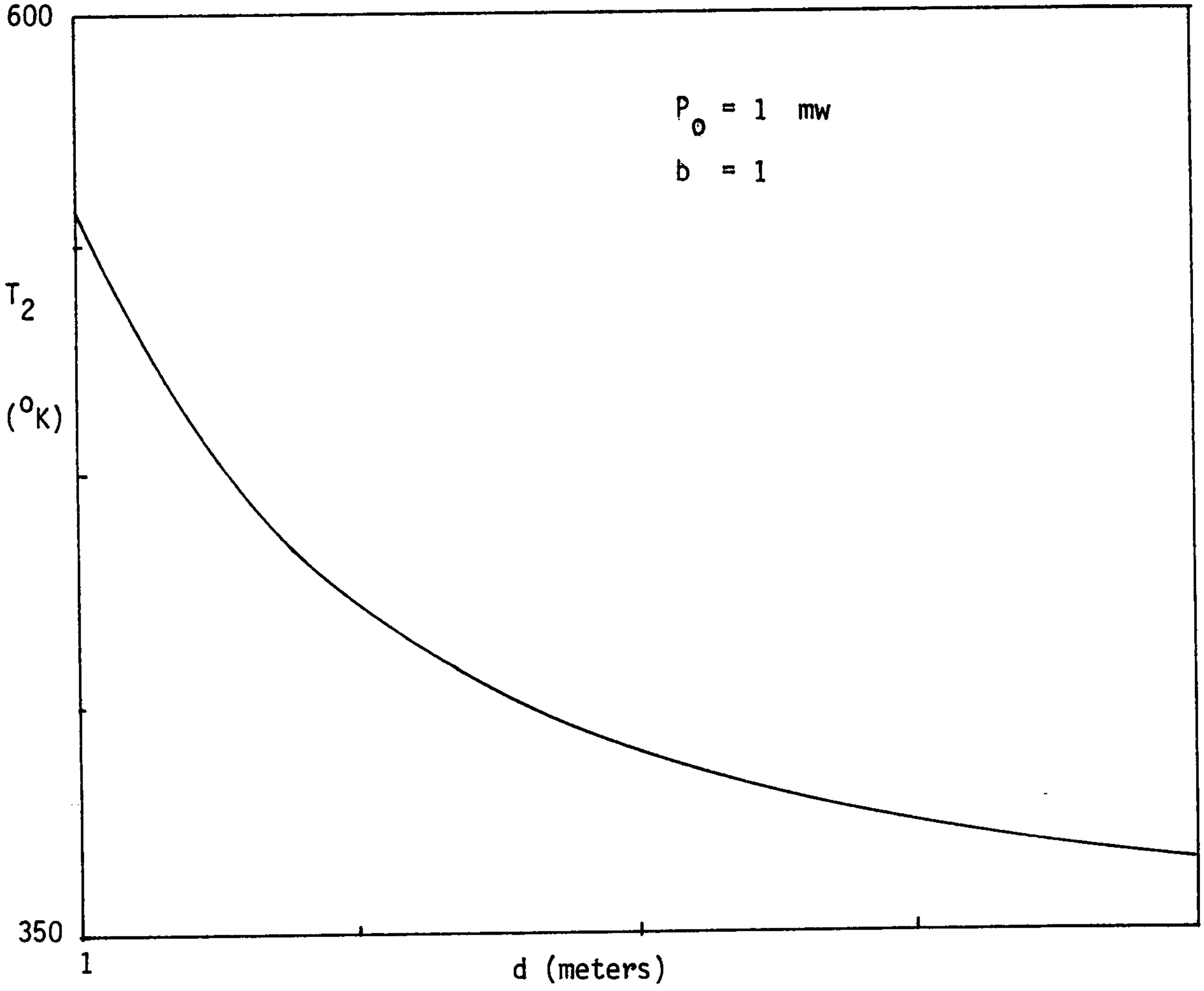

Figure 13.4 Electronic radiator temperature vs. Radiator separation.

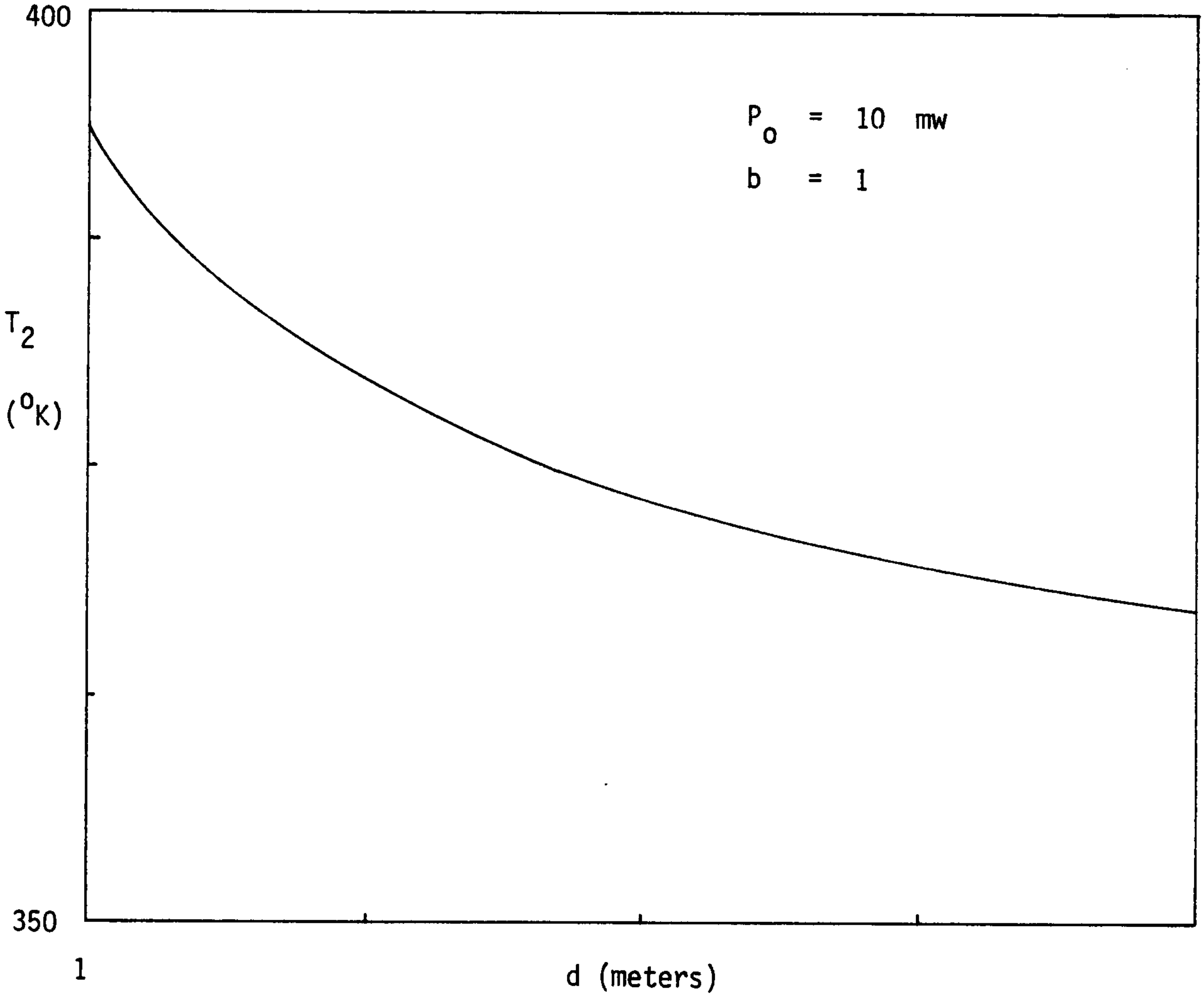

Figure 13.5 Electronic radiator temperature vs. Radiator separation.

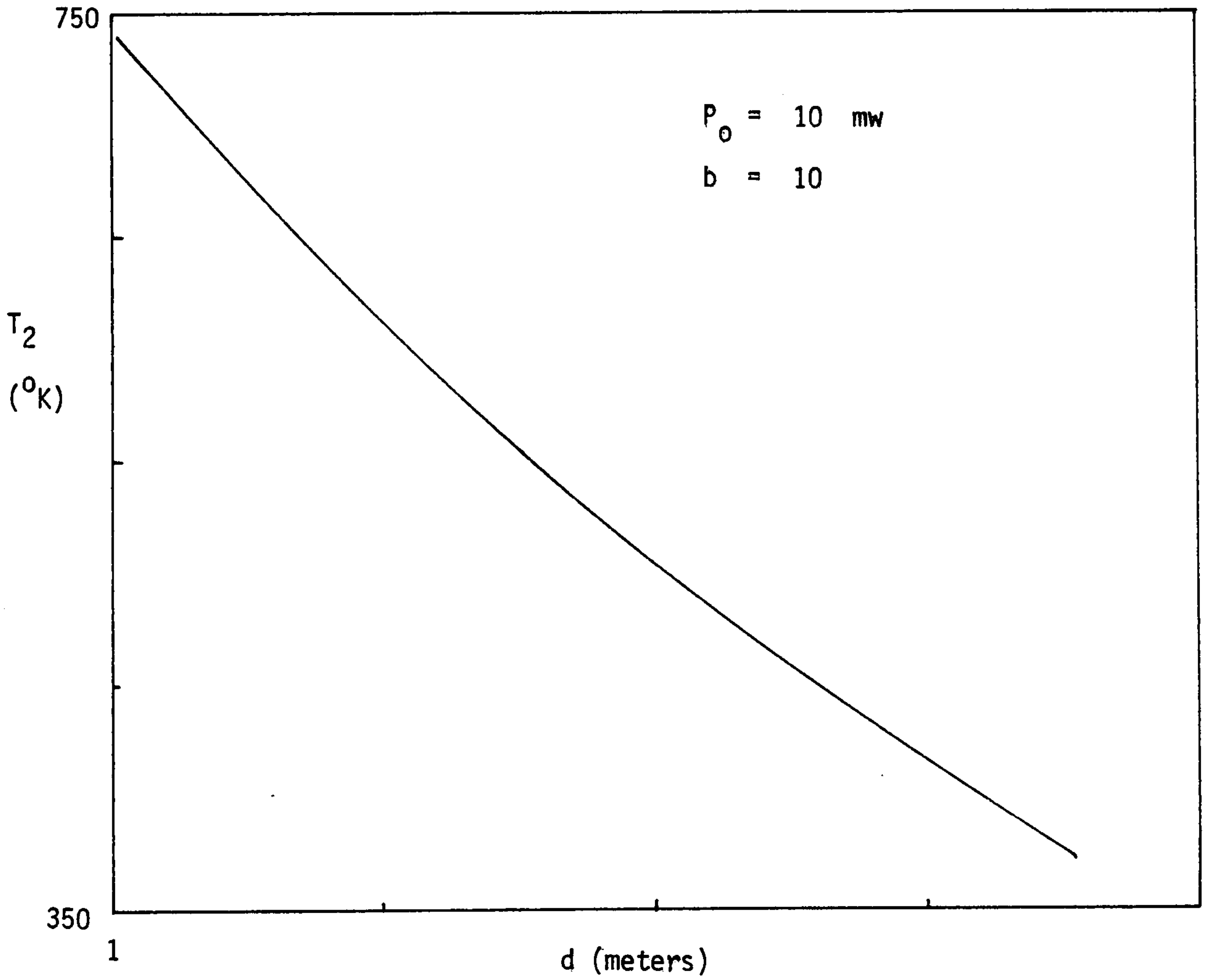

Figure 13.6 Electronic radiator temperature vs. Radiator separation

```
10 PRINT " L=c/b"
20 PRINT " Y=X1/X20, X=X2/X20"
30 PRINT " N1=a/b=(C3*A1)/b^2*(X1/X2), N1=C3*L*Y/X"
40 PRINT " N2=N1+N3"
50 PRINT " P10=10^5 WATTS, P0 OUTPUT POWER"
60 INPUT P0
70 PRINT "N3=d/b"
80 PRINT "b=K"
90 INPUT K
100 PRINT "d=L3"
110 INPUT L3
120 IF L3=1 THEN 150
130 N4=200/K
140 GOTO 160
150 N4=10/K
160 N3=L3/K
170 P10=100000
180 K1=P0/(K*P10)
190 L=K1/K
200 L1=L^2
210 T10=1000
220 T20=350
230 T30=250
240 R=((T20/T30)^4-1)/((T10/T30)^4-1)
250 E1=0.1
260 E=0.8
270 E2=0.9
280 E3=0.99
290 J=3.1415926
300 GOSUB 400
310 IF N3>N4 THEN 340
320 N3=N3+N4/20
330 GOTO 300
340 END
400 X10=T10^4-T30^4
410 X20=T20^4-T30^4
```

```
420  Y=X10/X20
430   C3=(1/E2-1)*E3*E2/(1/E1-1)
440  C4=L*C3
450   A1=1/L
460  X=1
470   A2=ATN(A1)
480   A3=1/N3
490   A4=ATN(A3)
500  A5=1/SQR(L^2+N3^2)
510   A6=ATN(A5)
520  A7=N3^2
530  A8=((1+L^2)*(1+A7)/(1+A7+L^2))*(L^2*(1+L^2+A7)/((1+L^2)*(L^2
     +A7)))^L1
540   A9=(A7*(1+L^2+A7)/((1+A7)*(L^2+A7)))^A7
550   A10=A8*A9
560  F1=(L*A2+N3*A4-SQR(A7+L^2)*A6+0.25*LOG(A10))/(J*L)
570  B1=(Y*C4+N3*X)/X
580   B2=1/B1
590  B=B1^2
600  B3=ATN(B2)
610  B4=SQR(L1+B)
620  B5=1/B4
630  B6=ATN(B5)
640  B7=((1+L1)*(1+B)/(1+L1+B))*(L1*(1+L1+B)/((1+L1)*(L1+B)))^L1
650  B8=(B*(1+L1+B)/((1+B)*(L1+B)))^B
660  B9=B7*B8
670  F2=(L*A2+B1*B3-B4*B6+0.25*LOG(B9))/(J*L)
680  F=F2-F1
690  G=E/(C3*Y*R)
700  H=(1-E)/(C3*Y)
710  I=1/(C3*Y)
720  N1=C4*Y/X
730  Z=(1+G*X*F-H*F^2*X)/(1-F^2*X*I)
740  IF Z<=X THEN 770
750  X=X+0.1
760  GOTO 570
```

```
770 GOSUB 1000
780 X2=Z1*X20
790 T2=(X2+T30^4)^0.25
800 L3=K*N3
810 PRINT "L3=" ; L3 ; "N1=" ; N1 ; "F4=" ; F4 ; "T2=" ; T2
820 RETURN
1000 N2=N1+N3
1010 D1=1/L
1020 D2=ATN(D1)
1030 D3=1/N2
1040 D4=ATN(D3)
1050 D5=1/SQR(N2^2+L^2)
1060 D6=ATN(D5)
1070 D7=N2^2
1080 D8=((1+L^2)*(1+D7)/(1+D7+L^2))*(L^2*(1+L^2+D7)/((1+L^2)*(L^2
     +D7)))^L1
1090 D9=(D7*(1+L^2+D7)/((1+D7)*(L^2+D7)))^D7
1100 D10=D8*D9
1110 F3=(L*D2+N2*D4-SQR(D7+L^2)*D6+0.25*LOG(D10))/(J*L)
1120 F4=F3-F1
1130 C=L/N1
1140 Z1=(1+(C*F4*E)/R-C*F4^2*(1-E))/(1-C*F4^2)
1150 RETURN
```

Chapter 14

SYSTEM SPECIFIC MASS, RELIABILITY AND OPERATIONAL TEMPERATURE AND THEIR INTERACTIONS

I. Introduction

System specific mass, reliability, and operational temperature are very important to the success of any project. This chapter investigates the inner relationship among these three features.

II. Parametric Analysis

The model used to study the behavior of specific mass, system reliability, failure rate, and system time interval is shown in Figure 14.1. The system consists of N-cells cascaded together with each cell containing up to three identical components. The maximum of three parallel components was selected to reflect a system that would be used in a manned space project. Typically, two parallel components would be used in each cell for an unmanned space mission.

All the components in each cell are assumed to be active, with none in a standby mode. This constraint allows for a simpler analysis. If each independent component has an exponential failure time distribution with a constant failure rate; and if all of the N-cells are identical, the system reliability [14.1] can be expressed in the following manner

$$R_s = (1-(1-e^{-\lambda T})^M)^N \qquad (14.1)$$

where R_s = system reliability

λ = component failure rate

T = system operational time interval

M = number of identical components in a cell (M=1,2,3)

N = number of identical cells.

Increasing the value of M increases R_s, while increasing N decreases R_s. Increasing the product λT decreases the system reliability. For systems that must operate over a very long time interval, the failure rate must be very small in order to maintain a respectable system reliability. If the component temperature is increased, the failure rate will, in general, decrease causing the value of R_s to decrease.

Assuming the specific mass of each identical component is k, all components are in an active mode, and the system power output is P_o, the system specific mass k_s is given by

$$k_s = N k . \qquad (14.2)$$

The reason why k_s is independent of M is due to the fact that, for any given cell, the output power for a component is P_o/M and there are M components in a cell. Strategically, it is important to maintain a small value for N in order to have a respectable system specific mass. However, there are constraints imposed on the system that force the value of N upwards. For example, an electrical power system may require a tight tolerance on voltage regulation, which would require the addition of regulators, driving the system specific upwards and the system reliability downwards.

Table 14.1 illustrates the behavior of λT as a function of N, M, and R_s. For M=1 there is no redundancy built into the system. Any component failure causes the system to become inoperable. For a given R_s and N, the λT product is the smallest when compared to M=2 or 3 systems.

For a given N, the λT product increases as the system shifts from unmanned (M=2) to manned (M=3). The system specific mass is constant for a given N. It should be noted that for M=2, if any component fails and is removed, the output power level is halved. For M=3 system, the power level is 2/3 original level for one component failure.

Increasing the system length (N=10 to N=40) and focusing on the manned system (M=3), the λT product decreases as the system length increases for a given R_s. Systems that have a large operational time interval, T large, must have components that have a very low failure rate.

The trend is to operate a non-terrestrial electrical power system at higher temperatures in order to reduce the radiator mass. However, the penalty in using this strategy is an increase in the component failure rate. Technology must be developed such that as system temperature rises, the failure rate remains essentially constant; otherwise, the system time interval will have to be shortened for a given system reliability.

III. Conclusions

In this chapter system reliability and system specific mass have been investigated. Although the model employed had a simplistic format, results tract with what might be expected from more complex systems that have more built in sophisticated redundant systems.

The system specific mass is related to the individual component specific mass. The relationship depends on the actual system configuration and the system specifications such as voltage regulation or system autonomy. As the output power level increases, the electrical power system will become very massive unless the specific mass remains in an acceptable range. Tightening system specifications tends to introduce more cascade cells, which in turn, increases the system specific mass.

Since the amount of mass in a non-terrestrial power system is important, system operation temperature is very important. Increasing the temperature tends to decrease the system specific mass. However, the failure rate rises driving the system time interval downwards for a given system reliability.

Reference

[14.1] Rau, J. G. "Optimization and Probability in Systems Engineering", Van Nostrand Reinhold Company, 1970.

Table 14.1 Failure Rate Time Product Versus System Reliability

R_s	λT			λT		
		N=10			N=40	
	M=1	2	3	M=1	2	3
0.5	0.069	0.299	0.521	0.017	0.140	0.298
0.6	0.051	0.252	0.459	0.013	0.121	0.266
0.7	0.036	0.207	0.396	0.009	0.099	0.232
0.8	0.022	0.161	0.329	0.005	0.070	0.195
0.9	0.011	0.107	0.246	0.003	0.053	0.140

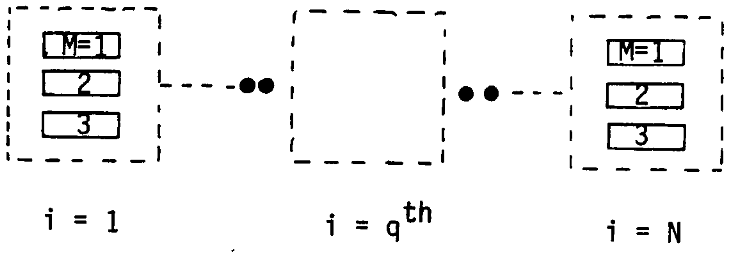

Figure 14.1 Series-parallel system of order (M,N).

Chapter 15

TRADEOFFS IN SYSTEM AVAILABILITY

I. Introduction

All physical systems have certain commonalities. They must be available when needed and operate at prescribed temperature for a designate amount of time. Mass cost is the penalty that must be paid to increase this availaility and essentially involves a tradeoff between system mean time to failure (MTBF) and system mean time to repair (MTTR). Ideally, MTBF should be as large and MTTR as small as possible.

II. Mathematical Model

The two system characteristics, MTBF and MTTR, can be functionally related by the introduction of the system uptime ratio. Consider a system that is initially functioning, upon failure it is repaired, and then returned to its operational state. It can be shown that the uptime ratio (UTR) is given by

$$UTR = \frac{MTBF}{MTBF + MTTR} \tag{15.1}$$

As indicated previously, ideally MTBF $\rightarrow \infty$ and MTTR $\rightarrow 0$ setting the upper bound for UTR at unity. Assume a lower bound, B_0, for UTR. Solving for MTBF in Equation (15.1) we have

$$MTBF \geq \left(\frac{B_0}{1-B_0}\right) MTTR \quad . \tag{15.2}$$

Generally speaking, if the system temperature is increased, MTBF decreases driving the UTR downward. There is a lower bound on MTTR, say MTTR $\geq B_1$, because no physical system on the average can be repaired in zero time. If a failure occurs in an electric power system, it requires time to locate and repair the fault, even when computers are performing the fault analysis.

There is always an upper bound on MTBF, say MTBF $\leq B_2$, due to state-of-the-art or in the case of space power systems mass and/or volume constraints. If it is assumed that the system reliability is of the form $R_s(T)=\exp(-T/MTBF)$, where T equals system operating time, and $R_s(T) > R_{s1}$, where R_{s1} is the minimum system reliability, the MTBF lower bound is $T/\ln(1/R_{s1})$.

The shaded area in Figure 15.1 represents the feasibility region for the above boundary constraints. Assuming for the moment that the technological and MTTR barriers are constant (both B_1 and B_2 are constant), the shaded region decreases if B_o, T, or R_{s1} is increased. For a long term space manned voyage the electrical power system must have all the above parameters as large as possible, which means that technology must keep ahead of the lower boundaries, B_o and $T\ell m\ (1/R_{s1})$.

There is a trend to operate systems at higher temperature to reduce the radiation surface area and the corresponding radiator mass. However, this thruss does drive the lower boundary $T/\ell m\ (1/R_{s1})$ higher because of the downward shifting of all the component MTBFs that effect the system reliability.

The bound, B_1, will always have a physical limitation due to the fact that maintenance and/or repair involve some form of manual activities, even for systems that are highly automated with computers defining the type and degree of failure. One possible technique for reducing B_1 is to have more personnel available to make the appropriate repairs. This scenairo adds to the personnel mass, which is a premium in space. Reducing personnel mass causes the standby redundant system mass to increase if the system reliability is to remain relatively constant.

III. One Unit System Availability

Consider an extra-terrestrial electrical power system as a one unit system with a constant system failure rate λ (λ = 1/MTBF) and a constant system repair rate μ (μ = 1/MTTR). Let the system availability be given by A(T) = p (T) when p (T) denotes the probability that at time T the system is operating. In terms of λ and μ the system availability is given by the following expression

$$A(T) = \left(\frac{1}{1 + \lambda/\mu}\right) \left(1 - (1- p(1 + \lambda/\mu)\, e^{-(1+ \lambda/\mu)\mu T}\right) \qquad (15.3)$$

where p represents the initial system probability. It can be shown that as $\mu T \to 0$, A(0) = p and as $\mu T \to \infty$, $A(\infty) = 1/(1 + \lambda/\mu) = 1/(1 + MTTR/MTBF)$. Note that UTR = $A(\infty)$.

Solving Equation (15.3) for μT results in the following expression

$$\mu T = \frac{1}{1 + \lambda/\mu}\ \ln \left(\frac{1 - p\ (1 + \lambda/\mu)}{1 - A(T)(1+\lambda/\mu)}\right) \qquad (15.4)$$

Since $\mu T > 0$, it can be demonstrated that $p > A(T)$ and $1 \geq p > A(\infty)$ = UTR.Increasing UTR for the electrical power system, forces the initial system probability closer to unity. The consequence of this stratedy demands a large MTBF and a small MTTR. Since the system MTBF characterizes the entire electrical power system, the individual component MTBFs must be larger than the system MTBF assuming the components are cascaded.

IV. Mass Cost Function

The tradeoff discussion from the previous sections suggest possibly two mass penalty functions. They are as follows [15.1]:

TYPE I Penalty

$$M(MTTR, MTBF) = A_1 + A_2 (MTBF) + A_3/(MTTR)$$

$$= A_1 + A_2 \left(\frac{B_O}{1-B_O}\right)(MTTR) + A_3/(MTTR) \qquad (15.5)$$

It can be shown that $\partial M/\partial MTTR < 0$ if $A_3/(MTTR)^2 > A_2\left((B_O/(1-B_O)\right)$. and $\partial m/\partial MTTR > 0$ if $A_3/(MTTR)^2 < A_2\left((B_0)\right)$.

TYPE II Penalty

$$M\ (MTTR, MTBF) = A_4 + A_5\ (MTBF) + A_6(MTTR-M_O)^2 \qquad (15.6)$$

where M_O is a constant.

The typical problem is to maximize UTR subject to a mass cost constraint such as $M(MTTR, MTBF) \leq M_1$, where the mass cost function is less than or equal to a predetermined value M_1. In the case of TYPE I system mass cost function and using the Langrange multiplier technique, it can be shown that UTR_{max} occurs at

$$MTTR_1 = 2A_3/(M_1-A_1)$$

$$MTBF_1 = (M_1-A_1)/(2A_2)$$

$$UTR_{max} = 1/\left(1 + 4A_2A_3/(M_1-A_1)^2\right)$$

$$M(MTTR_1, MTBF_1) = M_1$$

For a TYPE II mass cost function and the constraint $M(MTTR, MTBF) \leq M_1$, it can be shown that $UTTR_{max}$ occurs at

$$MTTR = 0$$

$$MTBF = \left(M_1-A_4-A_4M_O^2\right)/A_5$$

provided that $M_1 > A_4 + A_6M^2$. If $M_1 > A_4 + A_6M_O^2$ cannot be achieved, then the optimal point is

$$\text{MTTR}, \frac{M_1 - A_4 - A_6(\text{MTTR} - M_O)^2}{C_2}$$

where $$\text{MTTR} = \left((A_4 - M_1 + A_6 M_O^2)/A_6\right)^{1/2}$$

V. Conclusions

A mathematical model of a generalized system, which might represent a electrical power in space, has been analyzed in terms of MTTR, MTBF, and a set of upper and lower bounds. It is obvious from the results that if technological advances do not track with system specifications (such as a longer operational system time interval, higher system reliability, and larger uptime system ratio), the system feasibility region will decrease.

Two different mass cost functions where investigated. With appropriate constraints it was shown that the UTR can be maximized for a given mass cost upper bound.

Reference

[15.1] Rau, John G. "Optimization and Probability in Systems Engineering", Van Nostrand Reinhold Company, 1970.

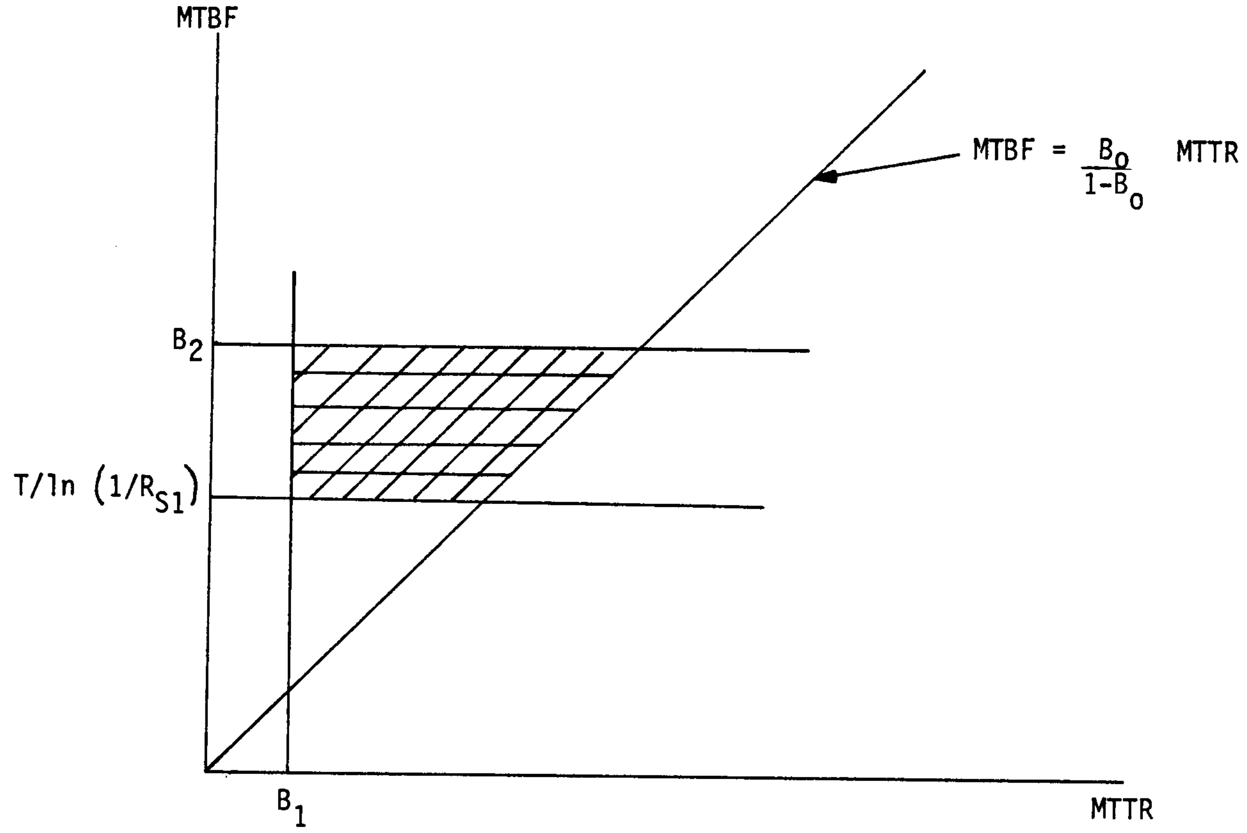

Figure 15.1 Bounded Feasibility Region

Chapter 16

CONCLUDING REMARKS

Projecting the U.S. Space Program into the 21st century requires new technologies that must be developed in order to maximize the information return from space systems that must function over several decades with a sophistication unheard of on Earth. Robotics will play a very important role in aiding man to gather this information, especially in situations where personnel might be exposed to hazards that might be life-threatening.

Initially, robotics will be used for space adventure not touched by humans in order to set the necessary parameters for manned systems that would follow. This strategy was used to place man on the Moon in the late sixties. Regardless where our adventure takes us it must be done in a manner that maximizes man's saftey in space. In other words, if a space program is to be successful it must be very reliable. Unfortunately, reliability and cost, whether it is dollars, mass, etc., are at odds with each other. High reliability generally means a costly system.

When the automotive industry was in its infancy around the turn of the century, the automobile was massive and rather unreliable. Today the automobile is quite reliable with a sizeable mass reduction. This was accomplished through many iterations and permutations of design that gives the automobile its high degree of reliability it enjoys today. There are many differences between the automotive industry and space systems. First, the space system must have a reliability approaching unity. Second, a serious failure in space is almost certain to cause a major disaster because personnel cannot leave the space system and return to a more primitive state like walking after the automobile has failed. Third, the space system will have to have more autonomy as compared to an automobile because routine and fault analysis will be processed by a computer rather than personnel. Personnel should only be in the very outer loop to make final discussion that cannot be resolved by computers.

It appears that reliability technology will have to be developed based on model simulation of the physical space system because they are not a volume endeavor like the automotive industry. For example, an electrical space power system is a low-volume endeavor with only a relatively few units built as compared to terrestrial power systems. The space power system will have the same type of user demands as its counterpart on Earth, except that the extra-terrestrial power system will not have a continental power grid similar to the one on Earth. Electrical energy will have to be allocated in a prioritized manner among the users.

All physical systems have an ideal performance characteristic (Chapters 12, 14, 15), which can be defined as its target value τ. Let the variable Y be the measured value of this performance characteristic, and let the expected value of Y, E[Y], be equal to a nominal value of η. Ideally, $E[Y] = \eta = \tau$. Since all systems exhibit variance, the variance of Y is denoted by σ^2 and it has four components. They are:

- Variability in the measurements
- Variability due to the failure of the system components
- Variability due to usage
- Variability due to the final environment of the system

In the case of a space electrical power system, a sufficient number of measurements of key system parameters must be conducted and analyzed by computers to determine the present system status and trends that the system might be experiencing. This information would indicate the degree of system stability and any near future instability. Technology will have to be developed in instrumentation, computer software and hardware and the determination of the key system parameters.

All well-designed electrical power systems should have components that would fail beyond the specified useful life span of the system. Physical system components can fail before the end of the life span. Critical failed system components must be removed and replaced with operative components or the failed component removed and new set of system strategies developed to operate the system as close to the target as possible.

In the case of a space electrical power system, user power demand must be coordinated in order to prevent the system from exceeding its specifications. This can be accomplished through a prioritized user computer system that identifies users that must remain electrically connected at all cost and the other users that are prioritized in importance and scheduling.

Finally, a system, such as a space power electrical system, may find itself in an environment that causes the system variability to increase and thus causing η to deviate from its target τ. Technology must be developed to test the system in all possible environments. To perform tests on a complete system would be a very arduous task. However, if computer simulation software programs can be developed that account for all the system nonlinearities and anomalies, scenarios can be performed on the computer-simulated system that would reflect the behavior of the physical system.

There is always a pentality associated with adjustment of the system design or parameters. It can be shown that the expected pentality $E[P(Y)] = K\,(Y-T)^2 = K\sigma^2$ where K is some constant and P(Y) is the pentality function.

Reducing the variance, σ^2, has a positive effect on the pentality. If the system has fixed bias, δ, due to poor design or poor manufacturing, the nominal value, η, and target, τ, will be separated by the bias δ. Under this condition the $E[P(Y)] = K(\sigma^2 + \delta^2)$. Note that the pentality is not zero when $\sigma = 0$ because of the fixed bias δ.

Taguchi's [16.1] approach to optimizing the system design, in the case of a space power system, is to carefully choose settings of k factors $\underline{X} = [X_1, X_2, \ldots, X_k]$ first to maximize a performance measure ζ, and then determine the factors that have no or very little influence on ζ to adjust or tune η so that $\eta \rightarrow \tau$. In many cases $\zeta = 10 \log (\eta/\sigma)^2$ where $(\eta/\sigma)^2$ can be considered a signal power-to-noise power ratio. As defined, the performance measure, ζ, depends on a ratio. Hence, no modelling of either η^2 or σ^2 is required, only the ratio is important.

The problem is to separate the k factors $\underline{X}$ into four groups: $\underline{X} = [\underline{X}_1, \underline{X}_2, \underline{X}_3, \underline{X}_4]$ where

- $\underline{X}_1$ =factors affecting η only
- $\underline{X}_2$ =factors affecting $(\eta/\sigma)^2$ only
- $\underline{X}_3$ =factors affecting σ^2 only
- $\underline{X}_4$ =factors with no detectable affects

The approach to optimizing a system design based on Taguchi's method has been used quite successfully in Japan for approximately two decades.

After separating $\underline{X}$ into four groups, the strategy is to find the best settings of $\underline{X}$ that accomplish the following goals:

- A product design that is on target
- A system that has minimum variance
- A system that is operating at the minimum penalty.

This approach to optimizing a system design based on Taguchi's method has been used quite successfully in Japan for approximately two decades and is gaining momentum for adoption in the United States.

It was demonstrated that system availability is strongly tied to the following boundries:

- Operating time interval
- Reliability
- Uptime ratio
- Mean time before failure (MTBF)
- Mean time to repair a failure (MTTR)
- State-of-the-art

As space systems move outward into our solar system, the system operating time, reliability, and uptime ratio will increase. These quantities must drive the mean time before failure upwards and mean time to repair a failure downwards. If the state-of-the-art does not lead this boundary the system feasibility region will shrink.

Increasing the system MTBF and decreasing the system MTTR can be a strong driver on the individual system component's MTBF and MTTR (Chapter 15). The relationship between the component mean time specifications and the mean time system specification is intimately tied to the system topology. For example, if a comparison is made between a manned and unmanned space system, the manned system topology will be more complex because of the higher required reliability. This in turn, drives the system mass upwards. System structures will have to be developed using some sort of a dynamic approach such that components can be reconfigured to satisfy systems demands and system reliability without significantly increasing system mass.

Increasing the system's operating temperature reduces the size of the radiators, especially for the high power low efficiency nuclear sources (Chapters 3,6,7,13). However, the structural integrity and all electronic component characteristics must tract with increase temperature; otherwise, early component failure will occur causing the system characteristics to exceed the system design limits.

Technologies in the area of composite and ceramic material should be developed. Composite materials can be formed in such a manner so that they offer great strength in a prescribed direction. This allows for a significant mass reduction. This investigator has shown through hot-cold heat cycling that the number cycles and the hot-cold temperature differential has an adverse affect on the stress-strain modulus of a boron-aluminum composite. Results did indicate that for a given temperature differential and one heat cycle, the change in the modulus was insignificant as compared to a non-cycled composite material. Debonding of the fibers from the material was a major contributer modulus degradation.

High temperature ceramics materials maintain their strength an elevated temperature, but they tend to shatter on heavy impacts. Development of ceramics, that exhibit some degree of plasticity at high temperatures in order to absorb the impact energy and still preserve high temperature strength, would be an asset to the space program. Such materials would be lighter than their metallic counterparts causing the specific system mass to decrease.

A substantial redundancy/mass penalty is paid for a manned space system, especially one that is designed to operate over a very long period of time. In other words, personnel are probably the most expensive item in the system if all the necessary support material is included. In order to reduce this expense, a high level autonomous system must be developed to offset man's presence in space. This would free the personnel from mundance activity and allow them the opportunity to gather as much information about their mission as possible.

Of all the subsystems that comprise a space system, the electric power system will have probably the largest mass component. The electric power system is the heart of the space system and if it is not functioning properly, the entire system, including the personnel, are in jeopardy (Chapters 2,4,8).

The only plausible method for reducing dedicated power personnel is to use some form of automation with a layer of autonomy (Chapter 5). Automation is the self-operation of a process, in this case an electrical power system, without the aid of any outside controls. Autonomy is automation with the added feature of self-government that considers such items as

- Planning
- Problem solving
- Decision making
- Self-maintenance

This all takes place under variable or even abnormal conditions that can extend over a period of time. Power faults occur when the user demand exceeds the power capacity of the system and nothing is done about the situation or user demand is on schedule, but an electrical component failed causing a disruption in the service to the users.

The user power demand can be avoided by properly scheduling the users so that there are no surges in power demand (Chapter 11). The user scheduling can be a prioritized lists that changes with time.

The case of a component failure is more serious because of the indeterministic nature of the failure. However, if device signature technology can be developed so that the autonomous system watches for tell-tail flags and takes appropriate action prior to component failure; almost all catastrophic situation can be avoided (Chapter 5).

The total electrical power demand will grow as space activity increases, such as more complex experiments and added personnel just to name a few drivers. The inter-connecting transmission lines mass could become a sizeable portion of the entire electrical power system's mass, especially if the power system extends over a large service area (Chapters 2,7). Transmission line efficiency, operating voltage and frequency, and voltage regulation have a high impact on the transmission line mass due to the transmission line resistivity.

Superconducting technology that would have the following physical transmission line characteristics would be an asset to transmission line mass reduction.

- Flexible superconductive transmission line
- Match the superconductive temperature to the inter-planetary environment so that no added cooling is required
- Increase the current density without paying the penalty of lowering the superconduction temperature.

Presently, superconductors ($90^{o}K$) are in the oxide family and are brittle and do not meet all the necessary requirements for transmission line applications.

For a given total electrical power output operating in a non-superconductive mode, increasing the operating line voltage reduces the transmission line mass; a similar strategy is used in terrestrial power systems planning. However, better insulation technology will have to be developed because of the hostile space environment. Results have indicated that radiation and plasma are just two of the many factors that shorten the life span of insulators.

High frequency power generation decreases the electrical system power mass by reducing inductive mass devices such as transformers and regulators. Depending on the source of energy there are essentially two methods for generating high frequency power

- Heat source: converting heat energy into high frequency electrical energy via a turbine-alternator
- DC source: converting dc energy to high frequency electrical energy via electronic switching.

High frequency alternators, in the form of induction generators, have been around for decades. The specific mass of these generators will have to be reduced before they can be used in a space power system. Because there are moving parts, bearing and lubrication technology will have to be developed in order for the alternators to operate over tens of years without failure. The same technology applies to the turbine side of the conversion system. The space station, in its later evolution, will be using this type of technology and should provide a good data base for further research and development.

The conversion of heat energy to high frequency power from a nuclear source is accomplished via dc to high frequency using an electronic converter (Chapters 7,9,10). The dc link should be as short as possible placing the electronic converter component in a hostile temperature and radiation environment. This is detrimental to the semiconduction process since the it depends strongly on crystalline structure, which deteriorates with increasing temperature and radiation damage. Semiconducting materials that operate at high temperature and are not strongly susceipitble to radiation effects will have to be developed.

High power vacuum switch devices have been used in terrestrial electric power system for many years (Chapter 10). There are commercial devices available that can interrupt 500-ampere current with a nominal voltage drop from 200 to 500 volts at a 16 KHZ pulse repetition frequency. Projections indicate that a 50,000-ampere current with a 30-volt nominal voltage drop at 1000 KHZ is conceivable. The advantage of vacuum switching is the fact that there is no crystalline structure to be disturbed by high temperature and radiation levels. Also, these devices are not based on hot cathode electron emission. In passing it is to be noted that the USSR has been very active in high power vacuum switching for many years.

Raising the power system operating frequency does have drawbacks. For example, electromagnetic interference is a very important item when voltage sensitive electronic devices are on board the space vehicle. Proper shielding and transmission line configuration will help reduce some of the electromagnetic interference, but much effort has to be made to minimize venerable interference.

Although high frequency power systems are less massive, fault diagnosis will have to be performed in a shorter period of time. This necessiates faster computers and better instrumentation transducers to monitor the power system's activity. Transducer time response will have to be scaled downwards to respond to various kinds of power faults.

Assuming all the above technologies are in place, the main objective of any electrical power system is to accomodate the demand for power in a reliable manner. Optimal operation of an electric power system

(Chapters 1,11) is very important in order to use the source of energy wisely. Results indicate that operating all electrical nodes at the highest voltage possible, smallest transmission line resistance, and as close to unity power factor as possible results in the best system operation.

BIBLIOGRAPHY

The bibliography listed in this section of the report includes information entered from 1962 to 1987 and was compiled using NASA/RECON (REmote CONsole) computerized bibliographic retrieval system. The entries were sorted by publication date in descending order.

Each entry consists of the following format where applicable:

Title..............................UTTL
Author.............................AUTH
Corporation........................CORP
Report Number......................RPT#
Publication Date...................YEAR/MONTH/DAY

SEARCH TITLE: HEAT SHIELDING

DESCRIPTION:

1. Space Power Reactors
2. Thermonuclear Power
3. Thermoelectric Power
4. Heat Shielding

The above entries were combined using Boolean logic to refine a search strategy, and it was used with the above set numbers only.

Logic Statement: (1+2+3)*4

UTTL: Calculation of carbon ablation on a re-entry body during supersonic/subsonic flight
AUTH: A/HUNTER, L. W.; B/PERINI, L. L.; C/CONN, D. W.; D/BRENZA, P. T.
87A17833
CNT#: N00024-85-C-5301
86/10/00

UTTL: A calculation of carbon ablation on a reentry body during supersonic/subsonic flight
AUTH: A/HUNTER, L. W.; B/PERINI, L. L.; C/CONN, D. W.; D/BRENZA, P. T.
85A37578
RPT#: AIAA PAPER 85-0904
CNT#: N00024-85-C-5301
85/06/00

UTTL: Energy technology
AUTH: A/BRESLOW, M.
CORP: Los Alamos Scientific Lab., N. Mex.
81N76941
RPT#: LA-8797-PR
81/04/00

UTTL: Hybrid thermonuclear reactor configuration driven by a relativistic electron beam and having a liquid first wall
AUTH: A/MURAVEV, Y. V.; B/NEDOSEYEV, S. L.; C/ROMANOV, P. V.; D/RUDAKOV, L. I.; E/RYUTOV, V. D.; F/TSYGANKOV, Y. A.; G/SHATALOV, G. Y.
CORP: Department of Energy, Washington, D. C.
79N32077
RPT#: DOE-TR-166
78/00/00

UTTL: Advanced heat source development for static and dynamic radioisotope space power systems
AUTH: A/SCHUMANN, F. A.; B/OSMEYER, W. E.
75A46008
75/00/00

UTTL: Atmosphere-entry behavior of a modular, disk-shaped, isotope heat source.
AUTH: A/VORREITER, J. W.; B/PITTS, W. C.; C/STINE, H. A.; D/BURNS, J. J.
73A38387
73/00/00

UTTL: Reference design for a thermoelectric isotope power unit employing heat pipe modules
AUTH: A/FRAAS, A. P.; B/LAVERNE, M. E.
CORP: Oak Ridge National Lab., Tenn.
72N21958
RPT#: ORNL-TM-2959
CNT#: W-7405-ENG-26
71/11/00

UTTL: Isotope kilowatt program Quarterly progress report, period ending 30 Jun. 1970
CORP: Oak Ridge National Lab., Tenn.
71N15031
RPT#: ORNL-TM-3099
CNT#: W-7405-ENG-26
70/09/00

UTTL: Uni-directional heat rejection RTG parametric study, Voyager Task C
CORP: General Electric Co., Philadelphia, Pa.
75N78227
RPT#: NASA-CR-145843 TID/SNG-6
CNT#: JPL-95112
66/12/30

SEARCH TITLE: INVERTED CONVERTERS

DESCRIPTION:

1. Inverted Converters
2. Spacecraft Power Supplies

The above entries were combined using Boolean logic to refine a search strategy, and it was used with the above set numbers only.

Logic Statement: 1*2

UTTL: Description of a 20 Kilohertz power distribution system
AUTH: A/HANSEN, I. G.
CORP: National Aeronautics and Space Administration. Lewis Research Center, Cleveland, Ohio.
86N31584
RPT#: NASA-TM-87346 NAS 1.15:87346
86/08/00

UTTL: Description of a 20 kilohertz power distribution system
AUTH: A/HANSEN, I. G.
CORP: National Aeronautics and Space Administration. Lewis Research Center, Cleveland, Ohio.
87A18115
86/00/00

UTTL: Multiprimary winding inverter with low harmonic content
AUTH: A/CARPIO, J.; B/CASTRO, M.; C/MARTINEZ, S.; D/PEIRE, J.; E/ALDANA, F.
CORP: Universidad Politecnica de Madrid (Spain).
86N17439
85/05/00

UTTL: Design considerations for large space electric power systems
AUTH: A/RENZ, D. D.; B/FINKE, R. C.; C/STEVENS, N. J.; D/TRINER, J. E.; E/HANSEN, I. G.
CORP: National Aeronautics and Space Administration. Lewis Research Center, Cleveland, Ohio.
83N24552
RPT#: NASA-TM-83064 E-1535 NAS 1.15:83064
83/04/00

UTTL: Large-signal dynamic-stability analysis of synchronised current-controlled modulators - Application to sine-wave high-power inverters
AUTH: A/CAPEL, A.; B/MARPINARD, J. C.; C/JALADE, J.; D/VALENTIN, A.
83A33475
83/00/00

UTTL: System study concerning the definition of standard spacecraft power interface characteristics
AUTH: A/HUFNAGEL, H.
CORP: Messerschmitt-Boelkow-Blohm G.m.b.H., Ottobrunn (West Germany).
83N25785
RPT#: MBB-RT-221 ESA-CR(P)-1713
CNT#: ESTEC-4599/81/NL-PP(SC)
82/06/00

UTTL: Hardware evaluation of a spacecraft ac power distribution system
AUTH: A/SCHRADE, J.
CORP: Dornier-Werke G.m.b.H., Friedrichshafen (West Germany).
81N27197
RPT#: ESA-CR(P)-1410
CNT#: ESTEC-3021/NL-HP
80/07/00

UTTL: Assessment of short and medium term improvements to the Spacelab power system. Volume 1: Executive summary
CORP: AEG-Telefunken, Wedel (West Germany).
79N31512
RPT#: ESA-CR(P)-1193-VOL-1
CNT#: ESA-3538/78-F-HEW(SC)
78/10/26

UTTL: Transistor inverters for satellite onboard networks of higher power
AUTH: A/AUBRAM, S.; B/GRUMBRECHT, P.; C/ROLLE, S.
78A40865
78/00/00

UTTL: A modulator for the Seasat-A radar altimeter
AUTH: A/ISHIKAWA, K. Y.; B/MCCOWN, C. T.; C/STRONKA, G. E.
CORP: Hughes Aircraft Co., Torrance, Calif.
83N75212
78/00/00

UTTL: Development of a 2 kW ac power system with multiple applications
AUTH: A/DENZINGER, W.; B/SCHRADE, J.
CORP: Dornier-Werke G.m.b.H., Friedrichshafen (West Germany).
77N32241
RPT#: ESA-CR(P)-960
CNT#: ESA-2293/74-AK

77/03/00

UTTL: Development of a three-phase dc/ac-inverter with sinusoidal output voltage at 400 Hz for the European Space Laboratory Spacelab
AUTH: A/GOHRBANDT, B.; B/LANGE, D.
78A37974
77/00/00

UTTL: The 400 Hz sine wave power inverter for Spacelab
AUTH: A/GOHRBRANDT, B.
CORP: AEG-Telefunken, Wedel (West Germany).
78N15118
77/00/00

UTTL: High-efficiency 400 Hz 3-phase static inverter for 3KVA nominal and 6KVA peak power
AUTH: A/DENZINGER, W.
CORP: Dornier-Werke G.m.b.H., Friedrichshafen (West Germany).
78N15117
77/00/00

UTTL: Square wave ac power generation and distribution of high power spacecraft
AUTH: A/MULLER, W.; B/DENZINGER, W.
CORP: Dornier-Werke G.m.b.H., Friedrichshafen (West Germany).
78N15106
77/00/00

UTTL: Square-wave power generation and distribution
AUTH: A/DENZINGER, W.
CORP: Dornier-Werke G.m.b.H., Friedrichshafen (West Germany).
76N10234
74/09/00

UTTL: Ac power systems in the kilowatt range
AUTH: A/HEHNEN, R.
CORP: AEG-Telefunken, Hamburg (West Germany).
76N10233
74/09/00

UTTL: Research on reliable and radiation insensitive pulse-drive sources for all-magnetic logic systems
AUTH: A/BAER, J. A.; B/HECKLER, C. H., JR.
CORP: Stanford Research Inst., Menlo Park, Calif.
85N74053
RPT#: DE85-900318 NP-5900318
62/06/00

SEARCH TITLE: TETHERED SATELLITES

DESCRIPTION:

1. Space Power Reactors
2. Spacecraft Shielding
3. Heat Shielding
4. Tethered Satellites

The above entries were combined using Boolean logic to refine a search strategy, and it was used with the above set numbers only.

Logic Statement: (1+2+3)*4

UTTL: Applications of low-earth-orbit power transmission
AUTH: A/ARNDT, G. D.; B/KERWIN, E. M.
CORP: National Aeronautics and Space Administration. Lyndon B. Johnson Space Center, Houston, Tex.
87A22770
86/00/00

UTTL: Orbital atomic oxygen effects on thermal control and optical materials - STS-8 results
AUTH: A/WHITAKER, A. F.; B/LITTLE, S. A.; C/HARWELL, R. J.; D/GRINER, D. B.; E/DEHAYE, R. F.; F/FROMHOLD, A. T., JR.
CORP: National Aeronautics and Space Administration. Marshall Space Flight Center, Huntsville, Ala.; Auburn Univ., Ala.
85A19737
RPT#: AIAA PAPER 85-0416
85/01/00

UTTL: Space Systems Technology Conference, Costa Mesa, CA, June 5-7, 1984, Technical Papers
84A34004
84/00/00

UTTL: Thermal control of tethered satellite in a very low altitude aerodynamic mission
AUTH: A/BORRIELLO, G.; B/CHIARELLI, C.; C/PELLIS, G.; D/AL-ASTRABADI, F.
CORP: Aeritalia S.p.A., Torino (Italy).
84N19444
83/12/00

SEARCH TITLE: SPACECRAFT POWER SUPPLIES

DESCRIPTION:

1. Inverted Converters
2. Transmission Lines
3. Power Conditioning
4. Thermonuclear Power
5. Thermionic Power Generation
6. Thermoelectric Power
7. Lunar Spacecraft
8. Nuclear Electric Power
9. Spacecraft Power Supplies

The above entries were combined using Boolean logic to refine a search strategy, and it was used with the above set numbers only.

Logic Statement: (1+2+3+4+5+6+7+8)*9+3*(4+6)

Energy to the 21st century :
3 v. (xxii, 2669 p.) : ill. ; 28 cm.
81V11386

Laser interaction and related plasma phenomena v. 4A :
AUTH: A/Schwarz, Helmut J.
lxxv, 602 p. : ill.
80V10502

Proceedings.
186 p. illus. 28 cm.
75V47943

Proceedings.
188 p. illus. 28 cm.
75V47942

Thermionic electrical power generation;
3 v. ; 29 cm.
75V28530

Proceedings of the 16th Intersociety Energy Conversion Engineering Conference, Atlanta, Georgia, August 9-14, 1981 /
3 v. (various pagings) : ill. ; 28 cm.
81V28904

Record :
152 p. : ill. ; 28 cm.
83V55711

Power supply of flight vehicles /
AUTH: A/Balagurov, V. A.
536 p.
84V54744

UTTL: Space nuclear power systems 1985; Proceedings of the Second Symposium, Albuquerque, NM, Jan. 14-16, 1985. Volumes 3 & 4
AUTH: A/EL-GENK, MOHAMED S.; B/HOOVER, MARK D.
87A21801
87/00/00

UTTL: Microwave power transmission for use in space
AUTH: A/GLASER, PETER E.
87A27180
86/12/00

UTTL: Opportunities for commercial space power
AUTH: A/STITT, D. N.; B/GOSS, R. J.; C/GLASER, P. E.
87A15905
RPT#: IAF PAPER 86-157
86/10/00

UTTL: Space power systems for the next decade
AUTH: A/DOUGHERTY, T. A.; B/VAN OMMERING, G.; C/POLLARD, H. E.
87A15901
RPT#: IAF PAPER 86-153
86/10/00

UTTL: The development and flight performances of China's satellites power systems
AUTH: A/LIU, L.-H.
87A15899
RPT#: IAF PAPER 86-151
86/10/00

UTTL: Solar dynamic power supply for orbiting systems with free-piston Stirling engine
AUTH: A/KUCZERA, H.
87A15896
RPT#: IAF PAPER 86-145
86/10/00

UTTL: A high reliability battery management system
AUTH: A/MOODY, M. H.
CORP: Canadian Astronautics Ltd., Ottawa (Ontario).
87N11094
86/09/00

UTTL: Description of a 20 Kilohertz power distribution system
AUTH: A/HANSEN, I. G.
CORP: National Aeronautics and Space Administration. Lewis Research Center, Cleveland, Ohio.
86N31584
RPT#: NASA-TM-87346 NAS 1.15:87346
86/08/00

UTTL: Advances in defining a closed Brayton conversion system for future Ariane 5 space nuclear power applications
AUTH: A/TILLIETTE, Z. P.
86A48110
RPT#: ASME PAPER 86-GT-15
86/06/00

UTTL: Inertial fusion power for space applications
AUTH: A/MEIER, W. R.; B/HOGAN, W. J.; C/HOFFMAN, N. J.; D/MURRAY, K. A.; E/OLSON, R. E.
CORP: Lawrence Livermore National Lab., Calif.; Rockwell International Corp., Canoga Park, Calif.; Sandia National Labs., Albuquerque, N. Mex.
87N14969
RPT#: DE86-011879 UCRL-94138 CONF-860810-22
CNT#: W-7405-ENG-48
86/05/19

UTTL: Power system technologies for the manned Mars mission
AUTH: A/BENTS, DAVE; B/PATTERSON, MICHAEL J.; C/BERKOPEC, F.; D/MYERS, IRA; E/PRESLER, A.
CORP: National Aeronautics and Space Administration. Lewis Research Center, Cleveland, Ohio.
87N17789
86/05/00

UTTL: PEGASUS: A multi-megawatt nuclear electric propulsion system
AUTH: A/COOMES, EDMUND P.; B/CUTA, JUDITH M.; C/WEBB, BRENT J.; D/KING, DAVID Q.; E/PATTERSON, MIKE J.; F/BERKOPEC, FRANK
CORP: National Aeronautics and Space Administration. Lewis Research Center, Cleveland, Ohio.
87N17787
86/05/00

UTTL: A programmable transformer coupled converter for high-power space applications
AUTH: A/KAPUSTKA, R. E.; B/BUSH, J. R., JR.; C/GRAVES, J. R.; D/LANIER, J. R., JR.
CORP: National Aeronautics and Space Administration. Marshall Space Flight Center, Huntsville, Ala.
86A49486
86/01/00

UTTL: Estimated burst power requirements for selected SDI missions
AUTH: A/MCCULLOCH, W. H.
CORP: Sandia National Labs., Albuquerque, N. Mex.
86N30955
RPT#: DE86-005438 SAND-85-1840C CONF-860102-6
CNT#: DE-AC04-76DP-00789
86/00/00

UTTL: Thermionic nuclear reactor systems
AUTH: A/KENNEL, E. B.
87A18181
86/00/00

UTTL: Thermoelectric converter modeling in nuclear space power conversion and regulation
AUTH: A/YADAVALLI, S. R.
87A18160
86/00/00

UTTL: Load following and reliability studies of thermoelectric SP-100 systems
AUTH: A/EL-GENK, M. S.; B/SEO, J. T.; C/BUKSA, J. J.
87A18159
CNT#: F290601-84-C-0080
86/00/00

UTTL: Thermoelectric converter for SP-100 space reactor power system
AUTH: A/TERRILL, W. R.; B/HALEY, V. F.
CORP: General Electric Co., Philadelphia, Pa.
87A18158
CNT#: JPL-956473 JPL-956851
86/00/00

UTTL: Comparison of concepts for a 300 kWe nuclear power system
AUTH: A/KIRPICH, A.; B/BIDDISCOMBE, R.; C/CHAN, J.; D/MCNAMARA, E.
87A18155
86/00/00

UTTL: A Space Station power management system architecture
AUTH: A/DECKER, D. K.; B/CAMPBELL, J. F.
87A18152
86/00/00

UTTL: Expert systems for on-array power management
AUTH: A/TRUMBLE, T.M.
87A18135
86/00/00

UTTL: Space power system scheduling using an expert system
AUTH: A/BAHRAMI, K. A.; B/BIEFELD, E.; C/COSTELLO, L.; D/KLEIN, J. W.
CORP: Jet Propulsion Lab., California Inst. of Tech., Pasadena.
87A18134
86/00/00

UTTL: An evaluation of inverter topologies for high power spacecraft
AUTH: A/NATARAJAN, T.
87A18120
86/00/00

UTTL: Description of a 20 kilohertz power distribution system
AUTH: A/HANSEN, I. G.
CORP: National Aeronautics and Space Administration. Lewis Research Center, Cleveland, Ohio.
87A18115
86/00/00

UTTL: Multimegawatt power distribution considerations
AUTH: A/GOTO, S. K.; B/HAYDEN, J. H.
87A18113
86/00/00

UTTL: Hubble Space Telescope power distribution and intercabling
AUTH: A/DICKASON, R. J.; B/COSTA, F. V.
87A18112
86/00/00

UTTL: Large capacity Ni-H2 battery cells
AUTH: A/MILLER, L.
87A18102
86/00/00

UTTL: Military space power systems technology for the twenty-first century
AUTH: A/BARTHELEMY, R. R.; B/MASSIE, L. D.; C/BORGER, W. U.
87A18065
86/00/00

UTTL: Aspects of Cs, Ba Knudsen ultrahigh-temperature TEC
AUTH: A/MORRIS, J. F.
87A18062
86/00/00

UTTL: STAR-C - Space Thermionic Advanced Reactor-Compact
AUTH: A/SNYDER, H. J., JR.
87A18060
86/00/00

UTTL: IECEC '86; Proceedings of the Twenty-first Intersociety Energy Conversion Engineering Conference, San Diego, CA, August 25-29, 1986. Volumes 1, 2, & 3
87A18026
86/00/00

UTTL: A new approach to optimum sizing and in-orbit utilization of spacecraft photovoltaic power system
AUTH: A/IMAMURA, M. S.; B/KHOSHAIM, B. H.
86A15713
RPT#: IAF PAPER 85-156
85/10/00

UTTL: Alternative space power systems
AUTH: A/WESTPAL, W.; B/KRUELLE, G.
86A35194
85/09/00

UTTL: Power supplies for primary electric propulsion missions
AUTH: A/JONES, R. M.; B/SCOTT-MONCK, J. A.
CORP: Jet Propulsion Lab., California Inst. of Tech., Pasadena.
85A34002
85/06/00

UTTL: Leasecraft power system
AUTH: A/CHETTY, P. R. K.
85A39464
85/05/00

UTTL: Uniform power distribution interfaces for future spacecraft
AUTH: A/CAPART, J. J.; B/OSULLIVAN, D. M.
85A42698
85/05/00

UTTL: Design of high-voltage, high-power, solid state remote power controllers for aerospace applications
AUTH: A/STURMAN, J. C.
CORP: National Aeronautics and Space Administration. Lewis Research Center, Cleveland, Ohio.
86N17456
85/05/00

UTTL: Application of current-control modulator (MC2) control feedback for 12 GHz 20 W Electric Power Conditioner (EPC) for Telecom satellite
AUTH: A/DESNE, J. P.; B/PEYROTTE, C.
CORP: Alcatel Thomson Espace, Courbevoie (France).
86N17455
85/05/00

UTTL: The 230W Traveling Wave Tube Amplifier (TWTA) power supply design
AUTH: A/GASPARINI, A.; B/BONATI, A.
CORP: Fabrica Italiana Apparecchi Radio S.p.A., Milan.
86N17453
85/05/00

UTTL: The results of some end of life tests on the OTS battery
AUTH: A/LEGGETT, P.; B/LECHTE, H.; C/SEPERS, A.
CORP: European Space Agency. European Space Research and Technology Center, ESTEC, Noordwijk (Netherlands).
86N17448
85/05/00

UTTL: Multiprimary winding inverter with low harmonic content
AUTH: A/CARPIO, J.; B/CASTRO, M.; C/MARTINEZ, S.; D/PEIRE, J.; E/ALDANA, F.
CORP: Universidad Politecnica de Madrid (Spain).
86N17439
85/05/00

UTTL: The ERS-1 power system
AUTH: A/HAINES, J. E.; B/MCCARTHY, C.; C/PONCIN, A.
CORP: European Space Agency. European Space Research and Technology Center, ESTEC, Noordwijk (Netherlands).
86N17437
85/05/00

UTTL: Alternating currrent buses for low Earth orbits: A viable alternative
AUTH: A/EGGERS, G.
CORP: AEG-Telefunken, Wedel (West Germany).
86N17435
85/05/00

UTTL: Spaceborne power systems preference analyses. Volume 2: Decision analysis
AUTH: A/SMITH, J. H.; B/FEINBERG, A.; C/MILES, R. F., JR.
CORP: Jet Propulsion Lab., California Inst. of Tech., Pasadena.
85N24518
RPT#: NASA-CR-175645 JPL-PUB-85-5-VOL-2 NAS 1.26:175645
CNT#: NAS7-918
85/01/15

UTTL: Advanced energy storage systems
AUTH: A/CHALLITA, A.; B/BARBER, J. P.; C/MCCORMICK, T. J.
CORP: IAP Research, Inc., Dayton, Ohio.
85N26915
RPT#: AD-A152244 IAP-TR-83-7 AFRPL-TR-84-099
CNT#: F04611-82-C-0029
85/01/00

UTTL: Space nuclear power
AUTH: A/ANGELO, J. A., JR.; B/BUDEN, D.
86A47276
85/00/00

UTTL: EURECA battery discharge regulator
AUTH: A/BORELLI, V.
86A40439
85/00/00

UTTL: An a.c. power distribution for satellite
AUTH: A/ROCCUCCI, S.; B/MENEGHINI, G.; C/TURRINI, L.
86A40438
85/00/00

UTTL: PESC '85; Annual Power Electronics Specialists Conference, 16th, Universite de Toulouse III, France, June 24-28, 1985, Record
86A40426
85/00/00

UTTL: Computerized data acquisition and analysis for measuring thermal diffusivity
AUTH: A/CHMIELEWSKI, A.; B/WOOD, C.; C/VANDERSANDE, J.
CORP: Jet Propulsion Lab., California Inst. of Tech., Pasadena.
86A24910
85/00/00

UTTL: Static and dynamic high power, space nuclear electric generating systems
AUTH: A/WETCH, J. R.; B/BEGG, L. L.; C/KOESTER, J. K.
CORP: Space Power, Inc., Sunnyvale, Calif.
86A24905
85/00/00

UTTL: An artificial intelligence approach to autonomous power system maintenance and control
AUTH: A/ADAMS, T. L.; B/DAMBROSIO, B.; C/FEHLING, M. R.; D/SCHWARTZBERG, S.; E/BARTON, J.
86A24842
85/00/00

UTTL: Performance analysis of radiation cooled dc transmission lines for high power space systems
AUTH: A/SCHWARZE, G. E.
CORP: National Aeronautics and Space Administration. Lewis Research Center, Cleveland, Ohio.
86A24811
85/00/00

UTTL: Space Station power system issues
AUTH: A/GIUDICI, R. J.
CORP: National Aeronautics and Space Administration. Marshall Space Flight Center, Huntsville, Ala.
86A24789
85/00/00

UTTL: A nuclear reactor electrical power system for a manned Space Station in low earth orbit
AUTH: A/SILVERMAN, S. W.
86A24788
85/00/00

UTTL: The application and use of nuclear power for future spacecraft
AUTH: A/WETCH, J. R.; B/BEGG, L. L.; C/DICK, R. S.
86A24780
85/00/00

UTTL: SP-100 program developments
AUTH: A/SCHNYER, A. D.; B/SHOLTIS, J. A., JR.; C/WAHLQUIST, E. J.; D/VERGA, R. L.; E/WILEY, R. L.
CORP: National Aeronautics and Space Administration, Washington, D.C.; Department of Energy, Washington, D. C.; Department of Defense, Washington, D. C.
86A24779
85/00/00

UTTL: Space Station Power System Advanced Development
AUTH: A/FORESTIERI, A. F.; B/BARAONA, C. R.; C/VALGORA, M. E.
CORP: National Aeronautics and Space Administration. Lewis Research Center, Cleveland, Ohio.
86A24778
85/00/00

UTTL: Military space power systems technology trends and issues
AUTH: A/BARTHELEMY, R. R.; B/MASSIE, L. D.
86A24777
85/00/00

UTTL: Intersociety Energy Conversion Engineering Conference, 20th, Miami Beach, FL, August 18-23, 1985, Proceedings. Volumes 1, 2, & 3
86A24776
RPT#: SAE P-164
85/00/00

UTTL: Review of the design status of the SP-100 space nuclear power system
AUTH: A/EL-GENK, M. S.; B/WOODALL, D. M.; C/DEAN, V. F.; D/LOUIE, D. L. Y.
86A20740
CNT#: F29601-82-K-0055

85/00/00

UTTL: Evolution of systems concepts for a 100 kWe class Space Nuclear Power System
AUTH: A/KATUCKI, R.; B/JOSLOFF, A.; C/KIRPICH, A.; D/FLORIO, F.
CORP: General Electric Co., Philadelphia, Pa.
86A20738
CNT#: JPL-956473
85/00/00

UTTL: Space nuclear power systems 1984; Proceedings of the First Symposium, Albuquerque, NM, January 11-13, 1984. Volumes 1 & 2
AUTH: A/EL-GENK, M. S.; B/HOOVER, M. D.
86A20726
85/00/00

UTTL: Large power systems for space platform application
AUTH: A/RATH, J.
85A42557
RPT#: AAS PAPER 84-310
85/00/00

UTTL: Performance analysis of radiation cooled dc transmission lines for high power space systems
AUTH: A/SCHWARZE, G. E.
CORP: National Aeronautics and Space Administration. Lewis Research Center, Cleveland, Ohio.
85N28222
RPT#: NASA-TM-87040 E-2596 NAS 1.15:87040
85/00/00

UTTL: General-purpose heat source development: Safety test program. Postimpact evaluation, design iteration test 5
AUTH: A/GEORGE, T. G.; B/SCHONFELD, F. W.
CORP: Los Alamos Scientific Lab., N. Mex.
85N22129
RPT#: LA-10232-SR
CNT#: W-7405-ENG-36
84/12/00

UTTL: The DFS-Kopernikus solar generator
AUTH: A/DIESSNER, F.
CORP: Deutsche Forschungs- und Versuchsanstalt fuer Luft- und Raumfahrt, Bonn (West Germany).
85N22591
84/11/00

UTTL: The DFS-Kopernikus solar generator electrical design
AUTH: A/PREUSS, L.
CORP: Messerschmitt-Boelkow-Blohm G.m.b.H., Ottobrunn (West Germany).
85N22590
84/11/00

UTTL: Power division and optimum system design method of dual-frequency system
AUTH: A/HE, Z.-H.
85A13242
RPT#: IAF PAPER 84-386
84/10/00

UTTL: Inertial energy storage for spacecraft
AUTH: A/RODRIGUEZ, G. E.
CORP: National Aeronautics and Space Administration. Goddard Space Flight Center, Greenbelt, Md.
84N33669
84/09/00

UTTL: General-purpose heat source development: Safety test program. Postimpact evaluation, design iteration test 1
AUTH: A/SCHONFELD, F. W.
CORP: Los Alamos Scientific Lab., N. Mex.
85N22131
RPT#: LA-9680-SR
CNT#: W-7405-ENG-36
84/04/00

UTTL: Thermoelectric and thermionic conversion technology
AUTH: A/MONDT, J. F.; B/AMBRUS, J. H.
CORP: Jet Propulsion Lab., California Inst. of Tech., Pasadena.
85N13905
84/04/00

UTTL: Space power management and distribution status and trends
AUTH: A/REPPUCCI, G. M.; B/BIESS, J. J.; C/INOUYE, L.
CORP: TRW, Inc., Redondo Beach, Calif.
85N13896
84/04/00

UTTL: Technology status of thermionic fuel elements for space nuclear power
AUTH: A/HOLLAND, J. W.; B/YANG, L.
CORP: GA Technologies, Inc., San Diego, Calif.
85N13893
84/04/00

UTTL: Study report on a modular photovoltaic power supply system for space application
AUTH: A/BAUNE, M.; B/BITTNER, H.; C/EGGERS, G.; D/GOERGENS, B.; E/HUETTMANN, H. J.; F/HUSE, K.; G/MANSHOLDT, U.; H/ROTH, M.; I/SCHNEIDER, K.; J/WESTPHAL, W.
CORP: Erno Raumfahrttechnik G.m.b.H., Bremen (West Germany).
84N28904
RPT#: BMFT-FB-W-84-010 ISSN-0170-1339
84/03/00

UTTL: PESC '84 - Annual Power Electronics Specialists Conference, 15th, Gaithersburg, MD, June 18-21, 1984, Record
86A31264
84/00/00

UTTL: Design of the next generation of communications satellites
AUTH: A/RUSCH, R. J.
87A18383
84/00/00

UTTL: Thermionic converter power generation test
AUTH: A/FUKUDA, R.; B/HAYASHI, K.; C/KASUGA, Y.; D/SHIMIZU, S.
87A18290
84/00/00

UTTL: In-core thermionic reactor for space power applications
AUTH: A/HOMEYER, W. G.; B/MERRILL, M. H.
85A45515
84/00/00

UTTL: Technology status of thermionic fuel elements for space nuclear power
AUTH: A/HOLLAND, J. W.; B/YANG, L.
85A45503
84/00/00

UTTL: STC/DBS power subsystem control loop stability analysis
AUTH: A/PECK, S. R.; B/DEVAUX, R. N.
85A45439
84/00/00

UTTL: Power conditioning and processing for the European Direct Broadcast Olympus 1 Satellite
AUTH: A/HAINES, J. E.; B/FORATTINI, F.
85A45410
84/00/00

UTTL: STC-DBS electrical power subsystem
AUTH: A/PECK, S. R.; B/CALLEN, P.; C/PIERCE, P.; D/WYLIE, T.
85A45409
84/00/00

UTTL: Microprocessor control of photovoltaic systems
AUTH: A/MILLNER, A. R.; B/KAUFMAN, D. L.
CORP: TriSolar Corp., Bedford, Mass.
85A45408
CNT#: DEN3-310
84/00/00

UTTL: Autonomy requirements for satellite power systems
AUTH: A/TRUMBLE, T. M.; B/WISE, J. F.; C/GJERMUNDSEN, E.
85A45405
84/00/00

UTTL: Space Station automation and autonomy
AUTH: A/CARLISLE, R. F.
CORP: National Aeronautics and Space Administration, Washington, D.C.
85A45398
84/00/00

UTTL: Minimizing spacecraft power loss due to single-point failures
AUTH: A/BILLERBECK, W.
85A45396
84/00/00

UTTL: IECEC '84: Advanced energy systems - Their role in our future; Proceedings of the Nineteenth Intersociety Energy Conversion Engineering Conference, San Francisco, CA, August 19-24, 1984. Volumes 1, 2, 3, & 4
85A45351
84/00/00

UTTL: Solar dynamic power for Space Station
AUTH: A/MCKENNA, R.; B/NIGGEMANN, R.; C/THOLLOT, P.
85A39258
RPT#: SAE PAPER 841524
84/00/00

UTTL: Photovoltaic Specialists Conference, 17th, Kissimmee, FL, May 1-4, 1984, Conference Record
85A35601
84/00/00

UTTL: The status of power supplies for primary electric propulsion in the U.S.A.
AUTH: A/JONES, R. M.; B/SCOTT-MONCK, J. A.
CORP: Jet Propulsion Lab., California Inst. of Tech., Pasadena.
85A16450
84/00/00

UTTL: Power supply unit of pulsed plasma engine
AUTH: A/MURAKAMI, H.; B/HIRATA, M.
85A16417
84/00/00

UTTL: Space know-how, twenty years' space experience
CORP: AEG-Telefunken, Wedel (West Germany).
85N12926
84/00/00

UTTL: Space station energy sizing
AUTH: A/RICE, R. R.
CORP: National Aeronautics and Space Administration. Lyndon B. Johnson Space Center, Houston, Tex.
84N12233
83/12/00

UTTL: GSFC flywheel status
AUTH: A/RODRIGUEZ, G. E.
CORP: National Aeronautics and Space Administration. Goddard Space Flight Center, Greenbelt, Md.
84N12230
83/12/00

UTTL: APPLE power system
AUTH: A/KANTHIMATHINATHAN, T.; B/SRINIVASAMURTHY, N.; C/AGRAWAL, B. L.; D/MATHUR, R. S.; E/SURESH, M. S.; F/EKKUNDI, R. S.; G/BHATIA, R. S.; H/CHANDRAMOHAN, M.
84A44808
83/11/00

UTTL: Experimental and systems studies of the alkali metal thermoelectric converter for aerospace power
AUTH: A/BANKSTON, C. P.; B/COLE, T.; C/JONES, R.; D/EWELL, R.
CORP: Jet Propulsion Lab., California Inst. of Tech., Pasadena.
84A10500
83/10/00

UTTL: Power conditioning system of an international amateur radio satellite
AUTH: A/REDL, R.; B/BANFALVI, A.
83A47247
RPT#: IAF PAPER 83-61
83/10/00

UTTL: Simplified power processing for ion-thruster subsystems
AUTH: A/WESSEL, F. J.; B/HANCOCK, D. J.
CORP: Hughes Research Labs., Malibu, Calif.
83A36384
RPT#: AIAA PAPER 83-1394
CNT#: NAS3-22447
83/06/00

UTTL: Assessment of flywheel energy storage for spacecraft power systems
AUTH: A/RODRIGUEZ, G. E.; B/STUDER, P. A.; C/BAER, D. A.
CORP: National Aeronautics and Space Administration. Goddard Space Flight Center, Greenbelt, Md.
83N33941
RPT#: NASA-TM-85061 NAS 1.15:85061 G-83F0229
83/05/00

UTTL: Nuclear energy in space
AUTH: A/LOEB, H.
CORP: Lawrence Livermore National Lab., Calif.
83N36894
RPT#: DE83-011128 UCRL-TRANS-11841
CNT#: W-7405-ENG-48
83/04/00

UTTL: Design considerations for large space electric power systems
AUTH: A/RENZ, D. D.; B/FINKE, R. C.; C/STEVENS, N. J.; D/TRINER, J. E.; E/HANSEN, I. G.
CORP: National Aeronautics and Space Administration. Lewis Research Center, Cleveland, Ohio.
83N24552
RPT#: NASA-TM-83064 E-1535 NAS 1.15:83064
83/04/00

UTTL: Research on spacecraft electrical power conversion
AUTH: A/WILSON, T. G.
CORP: Duke Univ., Durham, N. C.
83N19227
RPT#: NASA-CR-169974 NAS 1.26:169974
CNT#: NGL-34-001-001
83/01/31

UTTL: Nickel-cadmium battery operation on a satellite with insufficient loading
AUTH: A/FABER, J.; B/BAKER, D.; C/JONES, S.
83A16829
RPT#: AIAA PAPER 83-0525
83/01/00

UTTL: Spectrum management considerations of adaptive power control in satellite networks
AUTH: A/SAWITZ, P.; B/SULLIVAN, T.
CORP: Operations Research, Inc., Silver Spring, Md.
85A28235
CNT#: NASW-3583
83/00/00

UTTL: Sodium-sulfur cells for high-power spacecraft batteries
AUTH: A/HASKINS, H. J.; B/MCCLANAHAN, M. L.; C/MINCK, R. W.
84A30173
83/00/00

UTTL: Solar array power to weight performance of 1- to 10-kilowatt, flat-folded flexible wings
AUTH: A/DILLARD, P. A.; B/CAMPELL, M. L.
84A30146
83/00/00

UTTL: Computer memory power control for the Galileo spacecraft
AUTH: A/DETWILER, R. C.
CORP: Jet Propulsion Lab., California Inst. of Tech., Pasadena.
84A30135
83/00/00

UTTL: Spacecraft automated electrical power subsystem simulator
AUTH: A/MOSER, R. L.; B/GINGERICH, D. E.; C/BUCHANAN, E. E.
84A30133
83/00/00

UTTL: The economics of autonomy in the EPS
AUTH: A/BARTON, J. R.; B/RAUER, D. K.
84A30131
83/00/00

UTTL: An electronic power conditioner for a 12 GHz/260 W TWT for DBS
AUTH: A/HUEBNER, K.-H.; B/LIEBISCH, W.
84A30128
83/00/00

UTTL: Adaptive satellite power amplifier operation for TDMA down-links
AUTH: A/EAVES, R. E.
84A17757
83/00/00

UTTL: FLTSATCOM - A power subsystem in evolution
AUTH: A/LINDENMAN, G. A.
84A30115
83/00/00

UTTL: Power subsystems for a low earth orbit station
AUTH: A/DUBOIS, Y.; B/ESPACE, M.
84A30105
83/00/00

UTTL: Future military space power systems and technology
AUTH: A/BARTHELEMY, R. R.; B/MASSIE, L. D.
84A30103
83/00/00

UTTL: Combustion converter development for topping and cogeneration applications
AUTH: A/GOODALE, D.; B/LIEB, D.; C/MISKOLCZY, G.; D/MOFFAT, A.
84A30036
CNT#: DE-AC02-76ET-11292
83/00/00

UTTL: Energy conversion for megawatt space power systems
AUTH: A/EWELL, R.
CORP: Jet Propulsion Lab., California Inst. of Tech., Pasadena.
84A30030
83/00/00

UTTL: IECEC '83; Proceedings of the Eighteenth Intersociety Energy Conversion Engineering Conference, Orlando, FL, August 21-26, 1983. Volume 1 - Thermal energy systems
84A30026
83/00/00

UTTL: PESC '83; Annual Power Electronics Specialists Conference, 14th, Albuquerque, NM, June 6-9, 1983, Record
84A18409
83/00/00

UTTL: Large-signal dynamic-stability analysis of synchronised current-controlled modulators - Application to sine-wave high-power inverters
AUTH: A/CAPEL, A.; B/MARPINARD, J. C.; C/JALADE, J.; D/VALENTIN, A.
83A33475
83/00/00

UTTL: Component technology for space power systems
AUTH: A/FINKE, R. C.
CORP: National Aeronautics and Space Administration. Lewis Research Center, Cleveland, Ohio.
82A44750
RPT#: IAF PAPER 82-408
82/09/00

UTTL: Power supplies, conditioning and distribution on UOSAT
AUTH: A/SLOWIKOWSKI, J. Z.; B/BLEWETT, M. J.
82A44572
82/09/00

UTTL: The APC, a basis for a power control unit using microprocessors
AUTH: A/CLAUSEN, N. A.
CORP: Terma Elektronisk Industri A/S, Lystrup (Denmark).
83N21016
82/09/00

UTTL: Simulation of the behavior of the Telecom 1 satellite input circuits in AMRT mode
AUTH: A/BARDE, H.
CORP: Engins Matra, Toulouse (France).
83N21009
82/09/00

UTTL: The Marecs/ECS power subsystem
AUTH: A/HAINES, J. E.
CORP: British Aerospace Dynamics Group, Stevenage (England).
83N21008
82/09/00

UTTL: Fourth ESTEC spacecraft power-conditioning seminar
AUTH: A/BATTRICK, B.; B/ROLFE, E.
CORP: European Space Agency, Paris (France).
83N21006
RPT#: ESA-SP-186 ISSN-0379-6566
82/09/00

UTTL: Direct Energy Conversion, a current awareness bulletin
CORP: Department of Energy, Oak Ridge, Tenn.
82N32860
RPT#: PB82-946616 DOE/DEC-82/16
82/08/30

UTTL: Design study of a high power rotary transformer
AUTH: A/WEINBERGER, S. M.
CORP: General Electric Co., Philadelphia, Pa.
83N16630
RPT#: NASA-CR-168012 NAS 1.26:168012 GE-82SDS4222
CNT#: NAS3-23155
82/07/00

UTTL: Military spacecraft thermal management - The evolving requirements and challenges
AUTH: A/MAHEFKEY, T.
82A37452
RPT#: AIAA PAPER 82-0827
82/06/00

UTTL: Research needs: Prime-power for high energy space systems
AUTH: A/TURCHI, P. J.
CORP: R and D Associates, Arlington, Va.
83N14156
RPT#: AD-A119243 AFOSR-82-0717TR
CNT#: F49260-82-C-0008 AF PROJ. 2308
82/06/00

UTTL: System study concerning the definition of standard spacecraft power interface characteristics
AUTH: A/HUFNAGEL, H.
CORP: Messerschmitt-Boelkow-Blohm G.m.b.H., Ottobrunn (West Germany).
83N25785
RPT#: MBB-RT-221 ESA-CR(P)-1713
CNT#: ESTEC-4599/81/NL-PP(SC)
82/06/00

UTTL: Reentry thermal testing of a general purpose heat source fueled clad
AUTH: A/PETERSON, D. E.; B/FRANTZ, C. E.
CORP: Los Alamos Scientific Lab., N. Mex.
83N23146
RPT#: DE82-014125 LA-9227
CNT#: W-7405-ENG-36
82/03/00

UTTL: A study of the selection of microcomputer architectures to automate planetary spacecraft power systems
AUTH: A/NAUDA, A.
CORP: Jet Propulsion Lab., California Inst. of Tech., Pasadena.
82N17259
RPT#: NASA-CR-168412 JPL-PUB-82-1
CNT#: NAS7-100
82/01/01

UTTL: Power conversion: Overview
AUTH: A/LAYTON, J. P.
CORP: Layton (J. Preston), Princeton Junction, N.J.
83N15898
82/00/00

UTTL: Thermal management of large pulsed power systems
AUTH: A/HASLETT, B.
CORP: Grumman Aerospace Corp., Bethpage, N.Y.
83N15889
82/00/00

UTTL: A survey of recent advances in and future prospects for thermionic energy conversion
AUTH: A/LAWLESS, J.
CORP: Carnegie-Mellon Univ., Pittsburgh, Pa.
83N15888
82/00/00

UTTL: Thermionic technology for spacecraft power: Progress and problems
AUTH: A/HUFFMAN, F.; B/LIEB, D.; C/REAGAN, P.; D/MISKOLCZY, G.
CORP: Thermo Electron Corp., Waltham, Mass.
83N15887
82/00/00

UTTL: Thermionic conversion for space power application
AUTH: A/YANG, L.; B/FITZPATRICK, G. O.
CORP: General Atomic Co., San Diego, Calif.; Rasor Associates, Inc., Sunnyvale, Calif.
83N15886
82/00/00

UTTL: Status of thermoelectronic laser energy conversion, TELEC
AUTH: A/BRITT, E. J.
CORP: Rasor Associates, Inc., Sunnyvale, Calif.
83N15864
82/00/00

UTTL: Effects of reactor design, component characteristics and operating temperatures on direct conversion power systems
AUTH: A/FITZPATRICK, G. O.; B/BRITT, E. J.
CORP: Rasor Associates, Inc., Sunnyvale, Calif.
83N15857
82/00/00

UTTL: Power requirements for manned space stations
AUTH: A/WOODCOCK, G. R.; B/SILVERMAN, S.
CORP: Boeing Aerospace Co., Seattle, Wash.
83N15842
82/00/00

UTTL: Proceedings of the AFOSR Special Conference on Prime-Power for High Energy Space Systems, volume 1
AUTH: A/TURCHI, P. J.
CORP: R and D Associates, Rosslyn, Va.
83N15841
RPT#: AD-A118887 AFOSR-82-0655TR-VOL-1
CNT#: F49620-82-C-0008
82/00/00

UTTL: Baseline power system design for the Giotto spacecraft
AUTH: A/LEVINS, D.; B/OSULLIVAN, D.; C/LO GALBO, P.
84A18397
82/00/00

UTTL: A programmable power processor for high power space applications
AUTH: A/LANIER, J. R., JR.; B/GRAVES, J. R.; C/KAPUSTKA, R. E.; D/BUSH, J. R., JR.
CORP: National Aeronautics and Space Administration. Marshall Space Flight Center, Huntsville, Ala.
84A18394
82/00/00

UTTL: Application of beam power technology to a space station
AUTH: A/ARNDT, G. D.; B/SUDDATH, J. H.
CORP: National Aeronautics and Space Administration. Lyndon B. Johnson Space Center, Houston, Tex.
84A15642
82/00/00

UTTL: The NASA program in Space Energy Conversion Research and Technology
AUTH: A/MULLIN, J. P.; B/FLOOD, D. J.; C/AMBRUS, J. H.; D/HUDSON, W. R.
CORP: National Aeronautics and Space Administration, Washington, D.C.
83A27326
82/00/00

UTTL: Thermoelectric conversion for space nuclear power
AUTH: A/EWELL, R.; B/STAPFER, G.
CORP: Jet Propulsion Lab., California Inst. of Tech., Pasadena.
83A27222
82/00/00

UTTL: Testing of the GPHS electrically heated thermoelectric converter
AUTH: A/KELLY, C. E.; B/AMBROSE, G. R.
83A27217
82/00/00

UTTL: Development of improved hydrogen recombination in sealed nickel-cadmium aerospace cells
AUTH: A/RITTERMAN, P. F.
CORP: TRW, Inc., Redondo Beach, Calif.
83A27198
CNT#: NAS3-21253
82/00/00

UTTL: Viking Lander NiCd battery special reconditioning sequences
AUTH: A/BRITTING, A. O., JR.
83A27196
82/00/00

UTTL: High voltage distribution and grounding in high power spacecraft
AUTH: A/DUNBAR, W. G.
CORP: Boeing Aerospace Co., Seattle, Wash.
83A27156
CNT#: NAS8-33432
82/00/00

UTTL: High voltage power electronics packaging on NASA's Space Telescope
AUTH: A/YADAVALLI, S. R.; B/WESTROM, J. L.; C/WILLIAMS, J. W.
83A27155
82/00/00

UTTL: Recent advances in interpretation of corona test results
AUTH: A/BURNHAM, J.
83A27154
82/00/00

UTTL: Solar array switching power management
AUTH: A/CASSINELLI, J. E.; B/SMITH, L. D.; C/VALGORA, M.
CORP: TRW Defense and Space Systems Group, Redondo Beach, Calif.; National Aeronautics and Space Administration. Lewis Research Center, Cleveland, Ohio.
83A27132
82/00/00

UTTL: Comparison of evolving photovoltaic and nuclear power systems for earth orbital applications
AUTH: A/ROCKEY, D. E.; B/JONES, R. M.; C/SCHULMAN, I.
CORP: Jet Propulsion Lab., California Inst. of Tech., Pasadena.
83A27131
CNT#: NAS7-100
82/00/00

UTTL: IECEC '82; Proceedings of the Seventeenth Intersociety Energy Conversion Engineering Conference, Los Angeles, CA, August 8-12, 1982. Volumes 1, 2, 3, 4 & 5
83A27126
82/00/00

UTTL: Power-system simulation for low-orbit spacecraft - The EBLOS computer program
AUTH: A/CAPEL, A.; B/FERRANTE, J.; C/CORNET, J.; D/LEBLANC, P.
83A13848
82/00/00

UTTL: Nuclear energy in space
AUTH: A/LOEB, H.
83A11837
82/00/00

UTTL: Nuclear energy in space
AUTH: A/LOEB, H. W.
83A11780
82/00/00

UTTL: Current control modulators - General theory on specific designs
AUTH: A/CAPEL, A.; B/CLIQUE, M.; C/FOSSARD, A. J.
82A15090
81/11/00

UTTL: Nickel cadmium batteries. Citations from the NTIS data base
CORP: National Technical Information Service, Springfield, Va.
82N72595
RPT#: PB82-801259 NTIS/PS-79/0647
81/10/00

UTTL: Thermionic energy conversion. Citations from the NTIS data base
CORP: National Technical Information Service, Springfield, Va.
82N71624
RPT#: PB81-808891 NTIS/PS-79/0596
81/08/00

UTTL: International Energy Agency Small Solar Power Systems (SSPS) project review
AUTH: A/BAKER, A. F.
CORP: Sandia National Labs., Livermore, Calif.
81N32643
RPT#: SAND-81-8216
CNT#: DE-AC04-76DP-00789
81/05/00

UTTL: Phonon scattering at grain boundaries in heavily doped fine-grained silicon-germanium alloys
AUTH: A/ROWE, D. M.; B/SHUKLA, V. S.; C/SAVVIDES, N.
81A33499
81/04/30

UTTL: An evaluation of nuclear electric propulsion for planetary exploration missions
AUTH: A/NAGORSKI, R. P.; B/BOAIN, R. J.
CORP: Jet Propulsion Lab., California Inst. of Tech., Pasadena.
81A32901
RPT#: AIAA PAPER 81-0705
CNT#: NAS7-100
81/04/00

UTTL: Extended operating range of the 30-cm ion thruster with simplified power processor requirements
AUTH: A/RAWLIN, V. K.
CORP: National Aeronautics and Space Administration. Lewis Research Center, Cleveland, Ohio.
81A32897
RPT#: AIAA PAPER 81-0692
81/04/00

UTTL: RCA Satcom in-orbit experience
AUTH: A/STEWART, D.
CORP: RCA Labs., Princeton, N. J.
81N21526
81/03/00

UTTL: Viking lander five year summary
AUTH: A/BRITTING, A.
CORP: Jet Propulsion Lab., California Inst. of Tech., Pasadena.
81N21524
81/03/00

UTTL: Energy for space applications
AUTH: A/MULLIN, J. P.
81A46242
RPT#: AAS PAPER 81-083
81/03/00

UTTL: Space nuclear power - A strategy for tomorrow
AUTH: A/BUDEN, D.; B/ANGELO, J. A., JR.
81A22764
RPT#: AIAA PAPER 81-0450
81/02/00

UTTL: Radiatively coupled thermionic and thermoelectric power system concept
AUTH: A/SHIMADA, K.; B/EWELL, R.
CORP: Jet Propulsion Lab., California Inst. of Tech., Pasadena.
81A20683
RPT#: AIAA PAPER 81-0217
CNT#: NAS7-100
81/01/00

UTTL: A high voltage, high power pulsed TWT power supply for space application
AUTH: A/SOPPER, P.
83A11022
81/00/00

UTTL: An automatic protection of spacecraft high power lines - The electronic solid state switch /ELS3/
AUTH: A/CAPEL, A.; B/SULLIVAN, D. O.; C/LEVINS, D.; D/FERRANTE, J. G.; E/ROSSEL, P.
83A11005
81/00/00

UTTL: Utilization of outer space and international law
AUTH: A/REIJNEN, G. C. M.
82A15588
81/00/00

UTTL: The electronic solid-state switch /ELS3/ - An automatic protection for spacecraft high-power lines
AUTH: A/CAPEL, A.; B/OSULLIVAN, D.; C/LEVINS, D.; D/ROSSEL, P.; E/FERRANTE, J. G.
82A15219
81/00/00

UTTL: The in-flight performance of the Solar Maximum Mission Electrical Power System
AUTH: A/BRODERICK, R. J.
CORP: National Aeronautics and Space Administration. Goddard Space Flight Center, Greenbelt, Md.
82A11843
81/00/00

UTTL: Advanced high temperature thermoelectrics for space power
AUTH: A/LOCKWOOD, A.; B/EWELL, R.; C/WOOD, C.
CORP: Jet Propulsion Lab., California Inst. of Tech., Pasadena.; University of Northern Illinois, De Kalb.
82A11823
81/00/00

UTTL: Thermionic application for future air force space power systems
AUTH: A/MAHEFKEY, T.
82A11822
81/00/00

UTTL: The evaluation of four solar-array-powered multi-kW power conditioners for Space Shuttle Orbiter application
AUTH: A/WRIGHT, M. C.
82A11772
81/00/00

UTTL: The systems impact of a concentrated solar array on a Jupiter orbiter
AUTH: A/ROCKEY, D. E.; B/BAMFORD, R.; C/HOLLARS, M. G.; D/KLEMETSON, R. W.; E/KOERNER, T. W.; F/MARSH, E. L. ; G/PRICE, H.; H/UPHOFF, C.
CORP: Jet Propulsion Lab., California Inst. of Tech., Pasadena.
82A11770
CNT#: NAS7-100
81/00/00

UTTL: Power management of multi-hundred kilowatt spacecraft power systems
AUTH: A/DECKER, D. K.; B/FLECK, G. W.; C/GRAVES, J.
CORP: TRW Defense and Space Systems Group, Redondo Beach, Calif.; National Aeronautics and Space Administration. Marshall Space Flight Center, Huntsville, Ala.
82A11769
81/00/00

UTTL: Advances in space power research and technology at the National Aeronautics and Space Administration
AUTH: A/MULLIN, J. P.; B/RANDOLPH, L. P.; C/HUDSON, W. R.; D/AMBRUS, J. H.
CORP: National Aeronautics and Space Administration, Washington, D.C.
82A11755
81/00/00

UTTL: Satellite power systems /SPS/ energy conversion and power management
AUTH: A/NUSSBERGER, A. A.
82A11742
81/00/00

UTTL: Programmable Power Processor /P3/
AUTH: A/LUKENS, F. E.; B/MOSER, R. L.
82A11739
81/00/00

UTTL: Series vs. shunt regulators for power control in satellite power systems
AUTH: A/SHEIE, J. R.; B/CORBETT, R. E.; C/GLASS, M. C.
82A11738
81/00/00

UTTL: High power solar array switching regulation
AUTH: A/DECKER, D. K.; B/CASSINELLI, J.; C/VALGORA, M.
CORP: TRW Defense and Space Systems Group, Redondo Beach, Calif.; National Aeronautics and Space Administration. Lewis Research Center, Cleveland, Ohio.
82A11736
81/00/00

UTTL: In-space inertial energy storage design
AUTH: A/STUDER, P. A.; B/EVANS, H. E.
CORP: National Aeronautics and Space Administration. Goddard Space Flight Center, Greenbelt, Md.
82A11708
81/00/00

UTTL: Intersociety Energy Conversion Engineering Conference, 16th, Atlanta, GA, August 9-14, 1981, Proceedings. Volumes 1, 2 & 3
82A11701
81/00/00

UTTL: Distributed processing on the Space Shuttle - A case study
AUTH: A/SCHOONMAKER, P. B.
CORP: McDonnell-Douglas Technical Services Co., Inc., Houston, Tex.
82A10099
RPT#: AIAA 81-2140
CNT#: NAS9-16105 NASA ORDER C-1322
81/00/00

UTTL: Dispersed solar thermal generation employing parabolic dish-electric transport with field modulated generator systems
AUTH: A/RAMAKUMAR, R.; B/BAHRAMI, K.
CORP: Oklahoma State Univ., Stillwater.; Jet Propulsion Lab., California Inst. of Tech., Pasadena.
81A42451
81/00/00

UTTL: Field emission electric propulsion power conditioning unit design concept, volume 2
AUTH: A/GASPARINI, A.; B/DEVAMBEZ, F.; C/VALENTIAN, D.
CORP: Societe Europeenne de Propulsion, Vernon (France).
82N32401
RPT#: SEP-TS/SL/340/DV/30-063/80-V2 ESA-CR(P)-1556-VOL-2
CNT#: ESTEC-3983/79/NL-AK
81/00/00

UTTL: Field emission electric propulsion power conditioning unit design concept, volume 1
AUTH: A/GASPARINI, A.; B/DEVAMBEZ, F.; C/VALENTIAN, D.
CORP: Societe Europeenne de Propulsion, Vernon (France).
82N32400
RPT#: SEP-TS/SL/340/DV/30-063/80-V1 ESA-CR(P)-1556-VOL-1
CNT#: ESTEC-3983/79/NL-AK
81/00/00

UTTL: Initial guidelines and estimates for a power system with inertial (flywheel) energy storage
AUTH: A/SLIFER, L. W., JR.
CORP: National Aeronautics and Space Administration. Goddard Space Flight Center, Greenbelt, Md.
81N29532
RPT#: NASA-TM-82134
80/12/00

UTTL: Space nuclear electric power systems
AUTH: A/BENNETT, G. L.; B/LOMBARDO, J. J.; C/ROCK, B. J.
81A33535
RPT#: AAS PAPER 80-220
80/10/00

UTTL: The Magsat power system
AUTH: A/ALLEN, W. E.
81A16484
80/09/00

UTTL: Power management
AUTH: A/GRAVES, J.
CORP: National Aeronautics and Space Administration. Marshall Space Flight Center, Huntsville, Ala.
80N33475
80/09/00

UTTL: Study of power management technology for orbital multi-100KWe applications. Volume 2: Study results
AUTH: A/MILDICE, J. W.
CORP: General Dynamics/Convair, San Diego, Calif.
80N28862
RPT#: NASA-CR-159834-VOL-2 GDC-ASP-80-015
CNT#: NAS3-21757
80/07/15

UTTL: Hardware evaluation of a spacecraft ac power distribution system
AUTH: A/SCHRADE, J.
CORP: Dornier-Werke G.m.b.H., Friedrichshafen (West Germany).
81N27197
RPT#: ESA-CR(P)-1410
CNT#: ESTEC-3021/NL-HP
80/07/00

UTTL: Research on design feasibility of high-power light-weight dc-to-dc converters for space power application
AUTH: A/WILSON, T. G.
CORP: Duke Univ., Durham, N. C.
80N29190
RPT#: NASA-CR-163375 SASR-6
CNT#: NSG-3157
80/05/31

UTTL: Cell short circuit, preshort signature
AUTH: A/LURIE, C.
CORP: TRW, Inc., Redondo Beach, Calif.
80N20850
80/04/00

UTTL: RCA Satcom: In-orbit experience
AUTH: A/DEBAYLO, P. W.; B/GASTON, S. J.
CORP: RCA American Communications, Inc., Piscataway, N. J.
80N20837
80/04/00

UTTL: NATO: In-orbit experience
AUTH: A/CAPULLI, J. J.
CORP: Space and Missile Systems Organization, Los Angeles Air Force Station, Calif.
80N20836
80/04/00

UTTL: Application of small-signal modeling and measurement techniques to the stability analysis of an integrated switching-mode power system
AUTH: A/WONG, R. C.; B/OWEN, H. A., JR.; C/WILSON, T. G.; D/RODRIGUEZ, G. E.
CORP: Duke Univ., Durham, N. C.; National Aeronautics and Space Administration. Goddard Space Flight Center, Greenbelt, Md.
81A32961
CNT#: NAS5-25351
80/00/00

UTTL: NTS-2 solar cell experiment after two years in orbit
AUTH: A/STATLER, R. L.; B/WALKER, D. H.
81A27268
80/00/00

UTTL: Summary results of the ATS-6 solar cell flight experiment
AUTH: A/GOLDHAMMER, L. J.; B/SLIFER, L. W., JR.
CORP: Hughes Aircraft Co., El Segundo, Calif.; National Aeronautics and Space Administration. Goddard Space Flight Center, Greenbelt, Md.
81A27209
CNT#: NAS5-24458
80/00/00

UTTL: Current-control modulators - General theory for specific designs
AUTH: A/CAPEL, A.; B/CLIQUE, M.; C/FOSSARD, A. J.
81A26156
80/00/00

UTTL: RTG power source for the International Solar Polar Mission
AUTH: A/COCKFIELD, R. D.; B/HARTMAN, R. F.; C/KELLY, C. E.
80A48305
80/00/00

UTTL: Power processing technology for spacecraft primary ion propulsion
AUTH: A/BIESS, J. J.; B/INOUYE, L. Y.; C/FRYE, R. J.
CORP: TRW Defense and Space Systems Group, Redondo Beach, Calif.; National Aeronautics and Space Administration. Lewis Research Center, Cleveland, Ohio.
80A48265
CNT#: NAS12-2183 NAS3-14383 NAS3-18924 NAS3-20403 NAS3-21372 NAS3-21746
80/00/00

UTTL: Advanced development of a programmable power processor
AUTH: A/LUKENS, F. E.; B/LANIER, J. R., JR.; C/KAPUSTKA, R. E.; D/GRAVES, J.
CORP: Martin Marietta Aerospace, Denver, Colo.; National Aeronautics and Space Administration. Marshall Space Flight Center, Huntsville, Ala.
80A48264
80/00/00

UTTL: Development of Automated Power Systems Management for planetary spacecraft
AUTH: A/BRIDGEFORTH, A. O.
CORP: Jet Propulsion Lab., California Inst. of Tech., Pasadena.
80A48253
CNT#: NAS7-100
80/00/00

UTTL: Optimisation of powerful energy supply systems for application in space
AUTH: A/BLUMENBERG, J.
79A53333
RPT#: IAF PAPER 79-169
79/09/00

UTTL: The on-board computer in diagnosis of satellite power unit
AUTH: A/BELGII, V. V.; B/BUGROVSKII, V. V.; C/KOVACHICH, IU. V.; D/PETROV, B. N.; E/SHEVIAKOV, A. A.
79A53332
RPT#: IAF PAPER 79-168
79/09/00

UTTL: Selection of power plant elements for future reactor space electric power systems
AUTH: A/BUDEN, D.; B/BENNETT, G. A.; C/COOPER, K.; D/DAVIDSON, K.; E/KOENIG, D.; F/LUNDBERG, L. B.; G/MALENFANT, R.; H/MARTZ, H.; I/RANKEN, W. A.; J/RILEY, R. E.
CORP: Los Alamos Scientific Lab., N. Mex.
80N21133
RPT#: LA-7858
CNT#: W-7405-ENG-36
79/09/00

UTTL: Environmental development plan for space applications
CORP: Department of Energy, Washington, D. C.
80N20922
RPT#: DOE/EDP-0057
79/09/00

UTTL: A cesium TELEC experiment at Lewis Research Center
AUTH: A/BRITT, E. J.
CORP: Rasor Associates, Inc., Sunnyvale, Calif.
80N14386
RPT#: NASA-CR-159729 NSR-8-1
CNT#: NAS3-21149
79/09/00

UTTL: Thermionic energy conservation, volume 2. A bibliography with abstracts
AUTH: A/REED, W. E.
CORP: National Technical Information Service, Springfield, Va.
79N30838
RPT#: NTIS/PS-79/0596
79/06/00

UTTL: Spacecraft power systems
AUTH: A/GOLDSMITH, P.
79A43199
79/05/00

UTTL: Module failure isolation circuit for paralleled inverters
AUTH: A/NAGANO, S.
CORP: National Aeronautics and Space Administration. Pasadena Office, Calif.; Jet Propulsion Lab., California Inst. of Tech., Pasadena.
79N24254
RPT#: NASA-CASE-NPO-14000-1 US-PATENT-4,150,425 US-PATENT-APPL-SN-876431 US-PATENT-CLASS-363-56 US-PATENT-CLASS-307-82 US-PATENT-CLASS-363-71 US-PATENT-CLASS-363-97
79/04/17

UTTL: Aerospace power systems - A building surge
AUTH: A/BARTHELEMY, R. R.; B/KOESTER, R. J.; C/STEARNS, J. W.; D/STOFEL, E.
CORP: Air Force Aero Propulsion Lab., Wright-Patterson AFB, Ohio.; Aeronautical Systems Div., Wright-Patterson AFB, Ohio.; Jet Propulsion Lab., California Inst. of Tech., Pasadena.; Hughes Aircraft Co., Culver City, Calif.
79A23044
79/02/00

UTTL: Enhanced power generation by optical solar reflectors on geostationary spinners
AUTH: A/CHETTY, P. R. K.; B/VASAGAM, R. M.
79A25138
79/01/00

UTTL: Tailoring EMI specifications for spacecraft electrical power system compatibility
AUTH: A/BOETTCHER, R. W.; B/JOHNSON, A. K.
81A14292
79/00/00

UTTL: A theoretical method for estimation of power loss due to mismatch in solar cell I-V characteristics
AUTH: A/SRINIVASAMURTHY, N.; B/MALATHI, G.; C/MATHUR, R. S.
80A12763
79/00/00

UTTL: Radioisotope thermoelectric generator cooling in the Shuttle bay
AUTH: A/STIMPSON, L. D.; B/LEVINE, D. I.
CORP: Jet Propulsion Lab., California Inst. of Tech., Pasadena.; Rockwell International Corp., Downey, Calif.
79A51936
CNT#: NAS7-100 NAS9-14000
79/00/00

UTTL: Design optimization of RTG for Solar-Polar Mission
AUTH: A/SCHOCK, A.; B/SOOKIAZIAN, H.
79A51935
CNT#: EN-77-C-02-4281
79/00/00

UTTL: Analytical predictions of RTG power degradation
AUTH: A/NOON, E. L.; B/RAAG, V.
CORP: Jet Propulsion Lab., California Inst. of Tech., Pasadena.; Syncal Corp., Sunnyvale, Calif.
79A51934
CNT#: AT(04-3)-959 NAS7-100
79/00/00

UTTL: Use of modular heat source stack in RTGs
AUTH: A/SCHOCK, A.; B/SHOSTAK, A.
79A51933
CNT#: EN-77-C-02-4281
79/00/00

UTTL: Baseline design of the thermoelectric reactor space power system
AUTH: A/RANKEN, W. A.; B/KOENIG, D. R.
79A51932
79/00/00

UTTL: Application of the Dynamic Isotope Power System to a multimission spacecraft
AUTH: A/KENNEY, W. D.; B/PRICKETT, W. Z.; C/KRUEGER, E. C.
79A51929
79/00/00

UTTL: Development in high efficiency light weight power system electronics
AUTH: A/LUKENS, F. E.
79A51921
79/00/00

UTTL: Advanced Linear Charge Current Control /LC3/ electrical power system
AUTH: A/COLLINS, W. B.; B/NICHOLS, D.; C/LUKENS, F.; D/MASSON, J.
79A51920
CNT#: F040701-78-C-0050
79/00/00

UTTL: Viking Lander power system operational results through the primary and extended mission
AUTH: A/BRITTING, A. O., JR.; B/LEAR, J. W.
79A51908
79/00/00

UTTL: Spacecraft power plants /2nd revised and enlarged edition/
AUTH: A/KULANDIN, A. A.; B/TIMASHEV, S. V.; C/IVANOV, V. P.
79A43841
79/00/00

UTTL: Synchronous orbit power technology needs
AUTH: A/SLIFER, L. W., JR.; B/BILLERBECK, W. J.
CORP: National Aeronautics and Space Administration. Goddard Space Flight Center, Greenbelt, Md.; Communications Satellite Corp., Clarksburg, Md.
79A34739
RPT#: AIAA 79-0916
79/00/00

UTTL: Solar thermoelectric power generation for Mercury orbiter missions
AUTH: A/SWERDLING, M.; B/RAAG, V.
CORP: Jet Propulsion Lab., California Inst. of Tech., Pasadena.; Syncal Corp., Sunnyvale, Calif.
79A34738
RPT#: AIAA 79-0915
CNT#: NAS7-100
79/00/00

UTTL: An economic analysis of a commercial approach to the design and fabrication of a space power system
AUTH: A/PUTNEY, Z.; B/BEEN, J.
CORP: Solarex Corp., Rockville, Md.; National Aeronautics and Space Administration. Lewis Research Center, Cleveland, Ohio.
79A34737
RPT#: AIAA 79-0914
79/00/00

UTTL: The power system
AUTH: A/RAMAKRISHNAN, S. Y.; B/MATHUR, R. S.; C/SUBRAMANIAN, M.; D/KANTHIMATHINATHAN, T.; E/JARPANGAL, S.; F/VENKATARAMANAN, S. T.; G/SAVALGI, N. I.
CORP: ISRO Satellite Centre, Peenya, Bangalore (India).
80N29387
79/00/00

UTTL: Baseline design of the thermoelectric reactor space power system
AUTH: A/RANKEN, W. A.; B/KOENIG, D. R.
CORP: Los Alamos Scientific Lab., N. Mex.
80N13906
RPT#: LA-UR-79-1242 CONF-790803-21
CNT#: W-7405-ENG-36
79/00/00

UTTL: Heat pipe cooling of power processing magnetics
AUTH: A/HANSEN, I. G.; B/CHESTER, M. S.
CORP: National Aeronautics and Space Administration. Lewis Research Center, Cleveland, Ohio.
80N11327
RPT#: NASA-TM-79270 E-223
79/00/00

UTTL: Reduced power processor requirements for the 30-cm diameter Hg ion thruster
AUTH: A/RAWLIN, V. K.
CORP: National Aeronautics and Space Administration. Lewis Research Center, Cleveland, Ohio.
79N33253
RPT#: NASA-TM-79257 E-169 AIAA-PAPER-79-2081
79/00/00

UTTL: The electrical power interface between solar array and power conditioning
AUTH: A/GOHRBRANDT, B.; B/GOERGENS, B.
CORP: AEG-Telefunken, Wedel (West Germany).
79N30741
78/11/00

UTTL: Assessment of short and medium term improvements to the Spacelab power system. Volume 1: Executive summary
CORP: AEG-Telefunken, Wedel (West Germany).
79N31512
RPT#: ESA-CR(P)-1193-VOL-1
CNT#: ESA-3538/78-F-HEW(SC)
78/10/26

UTTL: Photovoltaic power systems workshop
AUTH: A/KILLIAN, H. J.; B/GIVEN, R. W.
CORP: Aerospace Corp., Los Angeles, Calif.
79N10140
78/09/00

UTTL: An economical approach to space power systems
AUTH: A/TEREN, F.
CORP: National Aeronautics and Space Administration. Lewis Research Center, Cleveland, Ohio.
79N10139
78/09/00

UTTL: Power modules and projected power systems evolution
AUTH: A/BRANTLEY, L. W.
CORP: National Aeronautics and Space Administration. Marshall Space Flight Center, Huntsville, Ala.
79N10137
78/09/00

UTTL: Power management and control for space systems
AUTH: A/FINKE, R. C.; B/MYERS, I. T.; C/TERDAN, F. F.; D/STEVENS, N. J.
CORP: National Aeronautics and Space Administration. Lewis Research Center, Cleveland, Ohio.
79N10134
78/09/00

UTTL: Space power technology - Current status and future development trends
AUTH: A/PESCHKA, W.
79A14054
RPT#: DGLR PAPER 78-167
78/09/00

UTTL: Comment on 'Heat-pipe reactors for space power applications'
AUTH: A/ENGLISH, R. E.
CORP: National Aeronautics and Space Administration. Lewis Research Center, Cleveland, Ohio.
78A40826
78/06/00

UTTL: Spacecraft power systems
AUTH: A/ASHIYA, R.
CORP: Indian Space Research Organization, Bangalore.
78N32131
78/04/00

UTTL: Computer simulation on electric power balance of the satellite
AUTH: A/MARUYAMA, T.; B/MATUURA, N.
79A11733
78/03/00

UTTL: Is Europe's space power technology competitive
AUTH: A/CAPART, J. J.
78A45902
78/02/00

UTTL: Development and fabrication of a diffusion welded Columbium alloy heat exchanger
AUTH: A/ZIMMERMAN, W. F.; B/DUDERSTADT, E. C.; C/WEIN, D.; D/TITRAN, R. H.
CORP: General Electric Co., Evendale, Ohio.; National Aeronautics and Space Administration. Lewis Research Center, Cleveland, Ohio.
78A31500
RPT#: AIME PAPER A78-61
CNT#: NAS3-18541
78/02/00

UTTL: Electronics for a focal plane crystal spectrometer
AUTH: A/GOEKE, R. F.
CORP: Massachusetts Inst. of Tech., Cambridge.
78A25313
CNT#: NAS8-30752
78/02/00

UTTL: U.S. broadcast satellites
AUTH: A/BRAHAM, H. S.
78A22447
78/01/00

UTTL: Prospects of thermionic power systems
AUTH: A/SHIMADA, K.
CORP: Jet Propulsion Lab., California Inst. of Tech., Pasadena.
79A10220
CNT#: NAS7-100
78/00/00

UTTL: Status of free-piston Stirling engine/linear alternator power conversion system development
AUTH: A/PILLER, S. J.
79A10212
78/00/00

UTTL: Melting multifoil insulation for KIPS emergency cooling
AUTH: A/DAROOKA, D. K.; B/LOUGHEED, V. R.
79A10191
78/00/00

UTTL: Brayton Isotope Power System - The versatile dynamic power converter
AUTH: A/GABLE, R. D.; B/MCCORMICK, J. E.
79A10190
78/00/00

UTTL: A thermally-integrated spacecraft design approach using nuclear dynamic power systems
AUTH: A/RAAB, B.
79A10184
CNT#: EN-77-C-02-4281
78/00/00

UTTL: Compact fusion reactors using controlled imploding liners
AUTH: A/BURTON, R. L.; B/TURCHI, P. J.
79A10151
78/00/00

UTTL: Developments in modular spacecraft power conditioning for application satellites
AUTH: A/OSULLIVAN, D.; B/WEINBERG, A.
79A10005
78/00/00

UTTL: The modular power subsystem for the multimission modular spacecraft
AUTH: A/HARRIS, D. W.
CORP: National Aeronautics and Space Administration. Goddard Space Flight Center, Greenbelt, Md.
79A10003
78/00/00

UTTL: Intersociety Energy Conversion Engineering Conference, 13th, San Diego, Calif., August 20-25, 1978, Proceedings. Volumes 1, 2 & 3
79A10001
78/00/00

UTTL: Transistor inverters for satellite onboard networks of higher power
AUTH: A/AUBRAM, S.; B/GRUMBRECHT, P.; C/ROLLE, S.
78A40865
78/00/00

UTTL: Heat pipe nuclear reactors for space applications
AUTH: A/KOENIG, D. R.; B/RANKEN, W. A.
78A35629
RPT#: AIAA 78-454
78/00/00

UTTL: High temperature heat pipe research at NASA Lewis Research Center
AUTH: A/TOWER, L. K.; B/KAUFMAN, W. B.
CORP: National Aeronautics and Space Administration. Lewis Research Center, Cleveland, Ohio.
78A35618
RPT#: AIAA 78-438
78/00/00

UTTL: A new battery charger/discharger converter
AUTH: A/MIDDLEBROOK, R. D.; B/CUK, S.; C/BEHEN, W.
CORP: California Inst. of Tech., Pasadena.
79A26972
78/00/00

UTTL: A programmable power processor for a 25 kW power module
AUTH: A/KAPUSTKA, R. E.; B/LANIER, J. R., JR.
CORP: National Aeronautics and Space Administration. Marshall Space Flight Center, Huntsville, Ala.
79A26959
78/00/00

UTTL: Spacecraft electromagnetic environment prediction
AUTH: A/ERICKSON, S. A.
79A25312
78/00/00

UTTL: Development of isotopic generators in Europe
AUTH: A/SCHARMANN, A.; B/SCHALCH, D.
79A17993
78/00/00

UTTL: Microprocessor control for standardized power control systems
AUTH: A/GREEN, D. G.; B/PERRY, E.
CORP: Alabama Univ., Huntsville.; National Aeronautics and Space Administration. Marshall Space Flight Center, Huntsville, Ala.
79A16542
78/00/00

UTTL: Space power for space
AUTH: A/MULLIN, J. P.
CORP: National Aeronautics and Space Administration, Washington, D.C.
79A16143
78/00/00

UTTL: A modulator for the Seasat-A radar altimeter
AUTH: A/ISHIKAWA, K. Y.; B/MCCOWN, C. T.; C/STRONKA, G. E.
CORP: Hughes Aircraft Co., Torrance, Calif.
83N75212
78/00/00

UTTL: Procedure for minimizing the cost per watt of photovoltaic systems
AUTH: A/REDFIELD, D.
CORP: RCA Labs., Princeton, N. J.
78A23636
CNT#: JPL-954352
77/12/00

UTTL: Kilowatt isotope power system: Component test report for the ground demonstration system jet condenser orifice performance
AUTH: A/BRAINARD, E. L.
CORP: Sundstrand Energy Systems, Rockford, Ill.
81N73541
RPT#: DOE/ET-33001-T33
CNT#: DE-AC02-77ET-33001
77/11/08

UTTL: Automatic optimization of operating modes in thermionic electrical power generators
AUTH: A/GALKIN, L. M.; B/PETROV, B. N.; C/ULANOV, G. M.
77A51445
RPT#: IAF PAPER 77-142
77/09/00

UTTL: Optimize out-of-core thermionic energy conversion for nuclear electric propulsion
AUTH: A/MORRIS, J. F.
CORP: National Aeronautics and Space Administration. Lewis Research Center, Cleveland, Ohio.
78N17856
RPT#: NASA-TM-73892
77/09/00

UTTL: Space station systems analysis study. Part 3: Documentation. Volume 7: SCB alternate EPS evaluation, task 10
CORP: McDonnell-Douglas Astronautics Co., Huntington Beach, Calif.
78N10185
RPT#: NASA-CR-151535 MDC-G6954-PT-3-VOL-7
CNT#: NAS9-14958
77/09/00

UTTL: A nickel-cadmium battery reconditioning circuit
AUTH: A/LANIER, R.
CORP: National Aeronautics and Space Administration. Marshall Space Flight Center, Huntsville, Ala.
77N25630
RPT#: NASA-TN-D-8508 M-221
77/06/00

UTTL: Copper-selenide system, P-Type TPM-217
AUTH: A/STAPFER, G.
CORP: Jet Propulsion Lab., California Inst. of Tech., Pasadena.
82N70982
RPT#: DE81-025715 DOE/ET-33003-T5
CNT#: DE-AI03-76ET-33003
77/04/00

UTTL: The 10-75-kWe-reactor-powered organic Rankine-Cycle Electric Power Systems (ORCEPS) study
CORP: TRW Defense and Space Systems Group, Redondo Beach, Calif.
82N70166
RPT#: DE81-026132 DOE/SF-80111-T1 TRW-30415.000
CNT#: DE-AC03-76SF-80111 EY-76-C-03-1336
77/03/30

UTTL: Design problems of spacecraft for communication missions
AUTH: A/COLLETTE, R. C.; B/HERDAN, B. L.
77A28081
77/03/00

UTTL: Nuclear powered satellite design for Shuttle launches
AUTH: A/KAPLAN, M. H.
77A23925
RPT#: AIAA PAPER 77-508
CNT#: ERDA EY-76-S-02-4045
77/03/00

UTTL: Development of a 2 kW ac power system with multiple applications
AUTH: A/DENZINGER, W.; B/SCHRADE, J.
CORP: Dornier-Werke G.m.b.H., Friedrichshafen (West Germany).
77N32241
RPT#: ESA-CR(P)-960
CNT#: ESA-2293/74-AK
77/03/00

UTTL: Design-to-cost philosophy for communication satellites: The example of Phebus power supply
AUTH: A/DUMONT, A.
CORP: Etudes Techniques et Constructions Aerospatiales, Charleroi (Belgium).
77N23318
77/02/00

UTTL: Power supply systems in the multi-kW power range
AUTH: A/GOHRBANDT, B.; B/RATH, J.
CORP: AEG-Telefunken, Wedel (West Germany).
77N23317
77/02/00

UTTL: Proposals for power conditioning systems of high power communication satellites
AUTH: A/GRASYNSKI, K.
79A10897
77/00/00

UTTL: Square wave ac power generation and distribution of high power spacecraft
AUTH: A/MUELLER, W.; B/DENZINGER, W.
79A10895
77/00/00

UTTL: A 2.5 KV high-reliability TWT power supply - Design techniques for high efficiency and low ripple
AUTH: A/ISRAELSEN, B. P.; B/MARTIN, J. R.; C/REEVE, C. R.; D/SCOWN, V. S.
79A10892
77/00/00

UTTL: Designing reliability into high voltage power processors
AUTH: A/WILLIAMS, J. W.
79A10891
77/00/00

UTTL: Power Electronics Specialists Conference, Palo Alto, Calif., June 14-16, 1977, Record
79A10876
77/00/00

UTTL: Development of a three-phase dc/ac-inverter with sinusoidal output voltage at 400 Hz for the European Space Laboratory Spacelab
AUTH: A/GOHRBANDT, B.; B/LANGE, D.
78A37974
77/00/00

UTTL: Reconditioning experience at Marshall Space Flight Center
AUTH: A/PASCHAL, L. E.
CORP: National Aeronautics and Space Administration. Marshall Space Flight Center, Huntsville, Ala.
79N21591
77/00/00

UTTL: Reconditioning on SATCOM
AUTH: A/NAPOLI, J.
CORP: RCA American Communications, Inc., Piscataway, N. J.
79N21590
77/00/00

UTTL: A simple approach to time domain simulation of linear and non-linear circuits
AUTH: A/SPRUIJT, H. J. N.
CORP: European Space Agency. European Space Research and Technology Center, ESTEC, Noordwijk (Netherlands).
78N15132
77/00/00

UTTL: Interactive computer simulation and design of power processing system. FTANAL: An ESTEC software project
AUTH: A/FERRANTE, J. G.; B/CAPEL, A.
CORP: European Space Agency. European Space Research and Technology Center, ESTEC, Noordwijk (Netherlands).
78N15131
77/00/00

UTTL: Modeling and design of dc-dc converters using modern control theory. Part 1: Modelization
AUTH: A/FOSSARD, A. J.; B/CLIQUE, M.
CORP: Ecole Nationale Superieure de l'Aeronautique et de l'Espace, Toulouse (France).
78N15129
77/00/00

UTTL: Software/hardware interface in control and protection of space batteries
AUTH: A/MONTALENTI, P.
CORP: European Space Agency. European Space Research and Technology Center, ESTEC, Noordwijk (Netherlands).
78N15127
77/00/00

UTTL: How essential are advanced techniques for control and protection of NiCd batteries on geostationary mission?
AUTH: A/LECHTE, H.
CORP: European Space Agency. European Space Research and Technology Center, ESTEC, Noordwijk (Netherlands).
78N15126
77/00/00

UTTL: Battery management using microprocessors
AUTH: A/GAYET, C.
CORP: European Space Agency. European Space Research and Technology Center, ESTEC, Noordwijk (Netherlands).
78N15125
77/00/00

UTTL: Thermal assessment of batteries for space application
AUTH: A/LAURSEN, A.
CORP: Danish Research Center for Applied Electronics, Hoersholm.
78N15123
77/00/00

UTTL: Ionizing discharges: Prevention techniques and measurement and detection methods
AUTH: A/MENEGHINI, G.
CORP: Selenia S.p.A., Rome (Italy).
78N15121
77/00/00

UTTL: The design of high voltage transformers for switching mode TWT - EPC's
AUTH: A/PALZ, G.
CORP: Siemens A.G., Munich (West Germany).
78N15120
77/00/00

UTTL: Thick film for future spacecraft
AUTH: A/MARSH, M. J.
CORP: Marconi Space and Defence Systems Ltd., Portsmouth (England).
78N15119
77/00/00

UTTL: The 400 Hz sine wave power inverter for Spacelab
AUTH: A/GOHRBRANDT, B.
CORP: AEG-Telefunken, Wedel (West Germany).
78N15118
77/00/00

UTTL: High-efficiency 400 Hz 3-phase static inverter for 3KVA nominal and 6KVA peak power
AUTH: A/DENZINGER, W.
CORP: Dornier-Werke G.m.b.H., Friedrichshafen (West Germany).
78N15117
77/00/00

UTTL: Multiple PWM boost regulator
AUTH: A/CARRARO, A.
CORP: Compagnia Generale di Elettricita S.p.A., Milan (Italy).
78N15111
77/00/00

UTTL: High power modular regulators
AUTH: A/PONCIN, A.; B/DAVOINE, F.; C/VANVYVE, J.; D/FRERE, J. L.
CORP: Etudes Techniques et Constructions Aerospatiales, Charleroi (Belgium).
78N15108
77/00/00

UTTL: Improved power conditioning unit for regulated bus spacecraft power system
AUTH: A/CHETTY, P. R. K.
CORP: Indian Space Research Organization, Bangalore.
78N15107
77/00/00

UTTL: Square wave ac power generation and distribution of high power spacecraft
AUTH: A/MULLER, W.; B/DENZINGER, W.
CORP: Dornier-Werke G.m.b.H., Friedrichshafen (West Germany).
78N15106
77/00/00

UTTL: The power and control subsystem used with the Marots L-band transistorised power amplifier
AUTH: A/DUNSTER, R. E.
CORP: Marconi Space and Defence Systems Ltd., Portsmouth (England).
78N15105
77/00/00

UTTL: EMC specifications: Their parameters, origin, intent and interpretation
AUTH: A/PURCHASE, J. F.
CORP: European Space Agency. European Space Research and Technology Center, ESTEC, Noordwijk (Netherlands).
78N15100
77/00/00

UTTL: Power supply requirements of transistor power amplifiers in a satellite phased array system
AUTH: A/PETT, R.
CORP: Mullard Ltd., Southampton (England).
78N15099
77/00/00

UTTL: Power subsystem requirements of present and future microwave payloads
AUTH: A/MICA, G.; B/GREINER, W.
CORP: European Space Agency. European Space Research and Technology Center, ESTEC, Noordwijk (Netherlands).
78N15098
77/00/00

UTTL: Spacecraft power conditioning
AUTH: A/HOGSHOLM, A.; B/GUYENNE, T. D.
CORP: European Space Agency, Paris (France).
78N15097
RPT#: ESA-SP-126
77/00/00

UTTL: Heat pipe reactors for space power applications
AUTH: A/KOENIG, D. R.; B/RANKEN, W. A.; C/SALMI, E. W.
CORP: Los Alamos Scientific Lab., N. Mex.
78N14653
RPT#: LA-UR-77-296 CONF-770302-2
CNT#: W-7405-ENG-36
77/00/00

UTTL: Advances in spacecraft power conditioning - New concepts from old
AUTH: A/OSULLIVAN, D.; B/WEINBERG, A.
78A26527
77/00/00

UTTL: Remarks on the stability of the voltage limiter-solar array system of the Sirio satellite
AUTH: A/ROCCUCCI, S.; B/MASTINI, G.
78A12884
77/00/00

UTTL: Conceptual definition of Automated Power Systems Management
AUTH: A/IMAMURA, M. S.; B/SKELLY, L.; C/WEINER, H.
CORP: Martin Marietta Aerospace, Denver, Colo.; Jet Propulsion Lab., California Inst. of Tech., Pasadena.
77A48862
77/00/00

UTTL: The electrical power system for Spacelab
AUTH: A/GOHRBANDT, B.; B/SCHMIDT, E. F.
77A46789
77/00/00

UTTL: Development of a 30-cm ion thruster thermal-vacuum power processor
AUTH: A/HERRON, B. G.
CORP: Hughes Research Labs., Malibu, Calif.
77A15088
RPT#: AIAA PAPER 76-991
CNT#: NAS3-17223
76/11/00

UTTL: Electric power systems for future communications satellites
AUTH: A/ESCH, F. H.; B/BILLERBECK, W. J.; C/CURTIN, D. J.
76A46091
RPT#: IAF PAPER 76-237
76/10/00

UTTL: Mathematical simulation of power conditioning systems. Volume 5: OTS power supply simulation
AUTH: A/PRAJOUX, R.; B/MAZANKINE, J.; C/GOUYON, J. P.; D/CHAUSSON, P.
CORP: Centre National de la Recherche Scientifique, Toulouse (France).
77N32239
RPT#: LAAS-PUBL-1453-VOL-5 ESA-CR(P)-949-VOL-5
CNT#: ESTEC-2299/74-AK
76/09/07

UTTL: Physics and potentials of fissioning plasmas for space power and propulsion
AUTH: A/THOM, K.; B/SCHWENK, F. C.; C/SCHNEIDER, R. T.
CORP: Florida Univ., Gainesville.; MC452981
76A47490
76/08/00

UTTL: Mathematical simulation of power conditioning systems. Volume 4: Systems simulation: Regulated bus, ac distribution, MPPT system
AUTH: A/PRAJOUX, R.; B/MAZANKINE, J.
CORP: Centre National de la Recherche Scientifique, Toulouse (France).
77N32238
RPT#: LAAS-PUBL-1453-VOL-4 ESA-CR(P)-949-VOL-4
CNT#: ESTEC-2299/74-AK
76/07/20

UTTL: Mathematical simulation of power conditioning systems. Volume 3: Simulation of elementary units. Results for boost, buck, buck-boost, shunt PWM
AUTH: A/PRAJOUX, R.; B/MAZANKINE, J.
CORP: Centre National de la Recherche Scientifique, Toulouse (France).
77N32237
RPT#: LAAS-PUBL-1453-VOL-3 ESA-CR(P)-949-VOL-3
CNT#: ESTEC-2299/74-AK
76/07/20

UTTL: Mathematical simulation of power conditioning systems. Volume 2: Simulation of elementary units. Implementation of hybrid simulation system
CORP: Centre National de la Recherche Scientifique, Toulouse (France).
77N32236
RPT#: LAAS-PUBL-1453-VOL-2 ESA-CR(P)-949-VOL-2
CNT#: ESTEC-2299/74-AK
76/07/20

UTTL: Mathematical simulation of power conditioning systems. Volume 1: Simulation of elementary units. Report on simulation methodology
AUTH: A/PRAJOUX, R.; B/MAZANKINE, J.; C/IPPOLITO, J. C.
CORP: Centre National de la Recherche Scientifique, Toulouse (France).
77N32235
RPT#: LAAS-PUBL-1453-VOL-1 ESA-CR(P)-949-VOL-1
CNT#: ESTEC-2299/74-AK
76/07/20

UTTL: General Electric preliminary design review data package for BIPS-ERDA PDR
CORP: AiResearch Mfg. Co., Phoenix, Ariz.
78N75242
RPT#: GE-BIPS-30-001
76/06/01

UTTL: Solid state remote power controllers for 120 VDC power systems
AUTH: A/SUNDBERG, G. R.; B/BAKER, D. E.
CORP: National Aeronautics and Space Administration. Lewis Research Center, Cleveland, Ohio.; Westinghouse Electric Corp., Lima, Ohio.
76A31510
76/04/00

UTTL: Thermoelectric power system
AUTH: A/BYRD, A. W.
CORP: National Aeronautics and Space Administration. Marshall Space Flight Center, Huntsville, Ala.
76N16612
RPT#: NASA-CASE-MFS-22002-1 US-PATENT-3,931,532 US-PATENT-APPL-SN-452769 US-PATENT-CLASS-310-4 US-PATENT-CLASS-136-202 US-PATENT-CLASS-136-210 US-PATENT-CLASS-165-105
76/01/06

C-3

UTTL: Application of the Venable converter to a series of satellite TWT power processors
AUTH: A/ROSTAD, A. S.; B/MCCOWN, C. T.; C/LAWRENCE, D. O.
77A40957
76/00/00

UTTL: The nuclear spinner for Satcom applications
AUTH: A/KARLIN, J. J.; B/RAAB, B.
77A12838
CNT#: E(49-15)-3063
76/00/00

UTTL: A simplified minimum power dissipation approach to regulate the solar array output power in a satellite power subsystem
AUTH: A/SALIM, A. A.
77A12834
76/00/00

UTTL: Sirio SHF experiment - Interfaces between the satellite power plant and travelling wave tube amplifier turn-on problems
AUTH: A/PERROTTA, G. M.-G.
76A45978
76/00/00

UTTL: Electric power conditioning for a thermionic generator
AUTH: A/KLEINKAUF, W.
CORP: European Space Agency, Paris (France).
77N13146
RPT#: ESA-TT-216 DLR-FB-75-44
75/12/00

UTTL: Research on spacecraft electrical power conversion
AUTH: A/WILSON, T. G.
CORP: Duke Univ., Durham, N. C.
75N76702
RPT#: NASA-CR-145459 SR-29
CNT#: NGL-34-001-001
75/09/01

UTTL: 7.5 kW solar array simulator
AUTH: A/ROBSON, R. R.
75A45652
RPT#: AIAA PAPER 75-1240
75/09/00

UTTL: LST power system long life design techniques
AUTH: A/SMITH, O. B.; B/DONOVAN, R. L.; C/OBERG, J. L.
CORP: Martin Marietta Aerospace, Denver, Colo.
76A12809
RPT#: AAS PAPER 75-182
CNT#: NAS8-31312
75/08/00

UTTL: Features of a barium/cesium diode with plane, polycrystalline molybdenum electrodes for thermionic energy conversion
AUTH: A/HENNE, R.
CORP: European Space Agency, Paris (France).
76N10571
RPT#: ESA-TT-171 DLR-FB-75-11
75/06/00

UTTL: Thyristor power processor for the 30 cm mercury electric propulsion engine
AUTH: A/BIESS, J. J.; B/INOUYE, L. Y.; C/SCHOENFELD, A. D. ; D/SHANK, J. H.
75A26588
RPT#: AIAA PAPER 75-433
CNT#: NAS3-14383 NAS3-18924
75/03/00

UTTL: Primary electric propulsion thrust subsystem definition
AUTH: A/MASEK, T. D.; B/WARD, J. W.; C/KAMI, S.
75A26581
RPT#: AIAA PAPER 75-405
CNT#: NAS8-30920 NAS8-30921
75/03/00

UTTL: Power balance and stress problems of internal-conductor systems
AUTH: A/LEHNERT, B.
75A27458
75/02/00

UTTL: AC power. Generation and distribution
AUTH: A/DENZINGER, W.
CORP: Dornier-Werke G.m.b.H., Friedrichshafen (West Germany).
75N33172
RPT#: ESRO-CR(P)-655
CNT#: ESTEC-1844/72-AA
75/01/00

UTTL: Design, manufacture and qualification of modular power conditioning circuits for space application using thick film technology
AUTH: A/KROEGER, H.; B/SPENCER, J.; C/LEWICKI, A.
CORP: Lewicki Microelectronic, Oberdischingen (West Germany).; Dornier-Werke G.m.b.H., Friedrichshafen (West Germany).
76N15265
RPT#: ESA-CR(P)-719
CNT#: ESTEC-1870/73-HP
75/01/00

UTTL: A digital computer simulation and study of a direct-energy-transfer power-conditioning system
AUTH: A/BURNS, W. W., III; B/OWEN, H. A., JR.; C/WILSON, T. G.; D/RODRIGUEZ, G. E.; E/PAULKOVICH, J.
CORP: Duke Univ., Durham, N. C.; National Aeronautics and Space Administration. Goddard Space Flight Center, Greenbelt, Md.
76A34269
CNT#: NGL-34-001-001
75/00/00

UTTL: A 100 watt TWT power conditioning system
AUTH: A/PECK, S. R.
76A34260
75/00/00

UTTL: The ATS-6 power system - An optimized design for maximum power source utilization
AUTH: A/LAVIGNA, T. A.
75A46017
75/00/00

UTTL: Advanced heat source development for static and dynamic radioisotope space power systems
AUTH: A/SCHUMANN, F. A.; B/OSMEYER, W. E.
75A46008
75/00/00

UTTL: Power supply of flight vehicles
AUTH: A/BALAGUROV, V. A.; B/BESEDIN, I. M.; C/GALTEEV, F. F.; D/KOROBAN, N. T.; E/MASTIAEV, N. Z.
75A44376
75/00/00

UTTL: High-voltage and power-conditioning thick-film ceramic circuits for space use
AUTH: A/LEWICKI, A.
CORP: Lewicki Microelectronic, Oberdischingen (West Germany).
76N10262
74/09/00

UTTL: EPC for TWT version of Marots
AUTH: A/WHALLEY, G. W.; B/HODGE, C. J.
CORP: Marconi Co. Ltd., Chelmsford (England).
76N10261
74/09/00

UTTL: Introduction of thick-film technology to power-conditioning circuits for space application
AUTH: A/KROEGER, H.; B/SPENCER, J.; C/LEWICKI, A.
CORP: Dornier-Werke G.m.b.H., Friedrichshafen (West Germany).
76N10259
74/09/00

UTTL: Advances in methods of construction, including thick film multichip integration, for future spacecraft power systems
AUTH: A/MARSH, M. J.
CORP: Marconi Space and Defence Systems Ltd., Portsmouth (England).
76N10258
74/09/00

UTTL: Technology utilized for production of an encapsulated TWT power supply
AUTH: A/MENEGHINI, G.; B/DELPRETE, F.
CORP: Selenia S.p.A., Rome (Italy).
76N10257
74/09/00

UTTL: The COS-B battery control system
AUTH: A/LEIBRANDT, W.
CORP: European Space Agency. European Space Research and Technology Center, ESTEC, Noordwijk (Netherlands).
76N10256
74/09/00

UTTL: Monitoring, control and protection techniques for storage batteries of applications satellites
AUTH: A/LECHTE, H.
CORP: European Space Agency. European Space Research and Technology Center, ESTEC, Noordwijk (Netherlands).
76N10255
74/09/00

UTTL: Effect of electronics on the operational methods of batteries for space
AUTH: A/GOUDOT, D.
CORP: European Space Agency. European Space Research and Technology Center, ESTEC, Noordwijk (Netherlands).
76N10254
74/09/00

UTTL: Considerations on the performance and utilization modes of Ni-Cd batteries onboard satellites
AUTH: A/FONT, S.
CORP: Societe des Accumulateurs Fixes et de Traction, Romainville (France).
76N10253
74/09/00

UTTL: Modelling and stability analysis of a buck-boost switching regulator intended for the power conditioning of a cesium contact ion thruster
AUTH: A/POWELL, D. R.
CORP: Centre National de la Recherche Scientifique, Toulouse (France).
76N10247
74/09/00

UTTL: The Faust-Plaque experiment. Description of the 15 kV converter
AUTH: A/DEGIVRY, J.; B/LEMOINE, J. D.
CORP: Engins Matra, Velizy (France).
76N10243
74/09/00

UTTL: A two-kilowatt EPC for a satellite TWT
AUTH: A/PALZ, G.
CORP: Siemens A.G., Munich (West Germany).
76N10242
74/09/00

UTTL: A boost regulator with a new energy-transfer principle
AUTH: A/WEINBERG, A. H.
CORP: European Space Agency. European Space Research and Technology Center, ESTEC, Noordwijk (Netherlands).
76N10241
74/09/00

UTTL: PWM type shunt regulator
AUTH: A/BARNABA, C.
CORP: Centre National d'Etudes Spatiales, Toulouse (France).
76N10240
74/09/00

UTTL: Design and stability analysis of a PWM shunt regulator
AUTH: A/SCHREGER, A.
CORP: AEG-Telefunken, Hamburg (West Germany).
76N10239
74/09/00

UTTL: Optimisation of dc/dc converter design for constant power output for spacecraft power systems
AUTH: A/CHETTY, P. R. K.
CORP: Indian Space Research Organization, Bangalore.
76N10238
74/09/00

UTTL: Design aspects of the PCU for the GEOS power system
AUTH: A/HOEGSHOLM, A.
CORP: Danish Research Center for Applied Electronics, Hoersholm.
76N10237
74/09/00

UTTL: Modular dc power systems for the 0.5 to 5 kW range
AUTH: A/GOHRBANDT, B.
CORP: AEG-Telefunken, Hamburg (West Germany).
76N10236
74/09/00

UTTL: Modular concept for space power systems
AUTH: A/GARREAU, M.
CORP: Engins Matra, Velizy (France).
76N10235
74/09/00

UTTL: Square-wave power generation and distribution
AUTH: A/DENZINGER, W.
CORP: Dornier-Werke G.m.b.H., Friedrichshafen (West Germany).
76N10234
74/09/00

UTTL: Ac power systems in the kilowatt range
AUTH: A/HEHNEN, R.
CORP: AEG-Telefunken, Hamburg (West Germany).
76N10233
74/09/00

UTTL: Power-conditioning developments for future satellites in the Federal Republic of Germany
AUTH: A/GRASZYNSKI, K.; B/ROEMISCH, N.
CORP: Gesellschaft fuer Weltraumforschung m.b.H., Porz (West Germany).
76N10232
74/09/00

UTTL: Optimal energy conversion: Investigation of a Maximum Power Point Tracking (MPPT) system
AUTH: A/ROBIN-JOUAN, Y.
CORP: Laboratoire Central de Telecommunications, Paris (France).
76N10231
74/09/00

UTTL: Optimisation of voltage regulators for satellites power systems
AUTH: A/CHETTY, P. R. K.
CORP: Indian Space Research Organization, Bangalore.
76N10230
74/09/00

UTTL: The Meteosat project as a modular conception of future systems
CORP: Etudes Techniques et Constructions Aerospatiales, Charleroi (Belgium).
76N10229
74/09/00

UTTL: Power subsystem configurations for geosynchronous applications satellites
AUTH: A/YOUNG, R. W.
CORP: Hawker Siddeley Dynamics Ltd., Stevenage (England).
76N10228
74/09/00

UTTL: Intasat power subsystem
AUTH: A/DIEZ, A.; B/HERBADA, F.
CORP: Construcciones Aeronauticas S.A., Madrid (Spain).
76N10227
74/09/00

UTTL: Spacecraft power-conditioning electronics seminar
AUTH: A/BATTRICK, B. T.; B/NGUYEN, T. D.
CORP: European Space Agency, Paris (France).
76N10225
RPT#: ESA-SP-103
74/09/00

UTTL: Advances in space power generation
AUTH: A/KERR, R. L.; B/REAMS, J. D.
75A13718
RPT#: IAF PAPER 74-086
74/09/00

UTTL: Space power systems - Retrospect and prospect
AUTH: A/LAYTON, J. P.
75A13714
RPT#: IAF PAPER 74-082
74/09/00

UTTL: Skylab technology electrical power system
AUTH: A/WOOSLEY, A. P.; B/SMITH, O. B.; C/NASSEN, H. S.
74A42076
RPT#: AAS PAPER 74-129
74/08/00

UTTL: Interdependence of the Airlock Module/Orbital Workshop thermal control and electrical power systems on Skylab
AUTH: A/MARKUS, J. A.
74A39133
RPT#: ASME PAPER 74-ENAS-35
74/07/00

UTTL: Converter design techniques and applications
AUTH: A/LALLI, V. R.
74A33219
74/05/00

UTTL: Compact reactor power systems
AUTH: A/BRUNINGS, J. E.; B/MASON, D. G.; C/THOMSON, W. B.; D/VAN OSDOL, J. H.
74A29858
CNT#: AT(04-3)-701
74/05/00

UTTL: The analysis, evaluation and optimization of satellite-borne power-supply units with the aid of a computer
AUTH: A/ARBES, J.; B/BAZIN, A.; C/POTIN, B.; D/TESSIER, J.
CORP: Compteurs Schlumberger, Montrouge (France).
75N13911
RPT#: ESRO-CR-205
CNT#: ESTEC-1134/70
74/05/00

UTTL: Thermionic conversion
CORP: Army Foreign Science and Technology Center, Charlottesville, Va.
75N19853
RPT#: AD-A002639 FSTC-HT-23-1822-73
74/02/25

UTTL: The subsystem power conditioning in the satellite Symphonie
AUTH: A/RAHMANN, M.
74A25025
74/02/00

UTTL: Development of a power conditioning and control logic system for the 'T4' ion thruster
AUTH: A/HUNT, R. P.; B/WILLIAMS, J. A.
75A36548
74/00/00

UTTL: The communications technology satellite deployable solar array subsystem
AUTH: A/SACHDEV, S. S.; B/QUITTNER, E.; C/GRAHAM, J. D.
75A24247
74/00/00

UTTL: A high power TWT power processing system
AUTH: A/FARBER, B. F.; B/GOLDIN, D. S.; C/SIEGERT, C.; D/GOURASH, F.
75A23582
CNT#: NAS3-15839
74/00/00

UTTL: Spacecraft integration and problem area studies on nickel hydrogen cells
AUTH: A/LEVY, E., JR.; B/ROGERS, H. H.
75A10568
CNT#: F33615-73-C-2064
74/00/00

UTTL: Battery and cell redundancy considerations for long duration space missions.
AUTH: A/FONO, P.
75A10494
74/00/00

UTTL: Design and performance of the Telesat power subsystem
AUTH: A/WICK, H. M.
75A10483
74/00/00

UTTL: The Atmosphere Explorer power subsystem
AUTH: A/OBENSCHAIN, A.; B/BACHER, J.; C/CALLEN, P.
75A10482
74/00/00

UTTL: Solar electric propulsion spacecraft power subsystem for an Encke comet rendezvous mission
AUTH: A/COSTOGUE, E. N.
75A10481
CNT#: NAS7-100
74/00/00

UTTL: Power subsystem simulation studies for the Timation IIIA spacecraft
AUTH: A/EWEN, W.; B/RUSTA, D.; C/STERNBERG, R.
75A10480
74/00/00

UTTL: A spacecraft integrated power/attitude control system
AUTH: A/KECKLER, C. R.; B/JACOBS, K. L.
75A10479
74/00/00

UTTL: Digital techniques in future spacecraft automated power systems
AUTH: A/IMAMURA, M. S.; B/SHEPPARD, N. R.; C/PATTERSON, T. D.
75A10478
74/00/00

UTTL: Electrical power generation subsystem for Space Shuttle Orbiter
AUTH: A/BLASKI, M. F.; B/OWENS, S. L.
75A10477
74/00/00

UTTL: Feasibility study of the power stage of a maritime satellite
AUTH: A/PALZ, G.; B/SCHMID, E.
CORP: Siemens A.G., Munich (West Germany).
74N26744
RPT#: ESRO-CR(P)-403
CNT#: ESTEC-SC/9/73/HQ
73/12/14

UTTL: Energy supply and energy transformers in satellites and spacecraft
AUTH: A/PESCHKA, W.
74A18189
73/12/00

UTTL: Spacecraft standardization through nuclear power
AUTH: A/FREY, E. J.; B/RAAB, B.; C/SCHOCK, A.; D/CARPENTER, R. T.
CORP: Fairchild Space and Electronics Co., Germantown, Md.
74N31336
73/11/09

UTTL: Prospects of energy conversion and storage derived from space systems technology
AUTH: A/BARGELLINI, P. L.
74A19485
73/10/00

UTTL: Recent developments in the field of thermionic power conversion and its possible effects on power supply systems in space and on earth
AUTH: A/HENNE, R.
74A17195
RPT#: DGLR PAPER 73-092
73/09/00

UTTL: Static dc to dc power conditioning-active ripple filter, 1 MHz dc to dc conversion, and nonlinear analysis
AUTH: A/SANDER, W. A., III
CORP: Duke Univ., Durham, N. C.
74N18867
RPT#: NASA-CR-138994
CNT#: NGL-34-001-001
73/03/23

UTTL: Launch window for ISS
AUTH: A/HIRAI, M.; B/TAKAHIRA, A.; C/SHIRAI, T.; D/HAGIWARA, T.; E/SAWAI, A.; F/WAKASUGI, N.
74A42390
73/00/00

UTTL: The supply of power to station-keeping electric thrusters in geostationary communication satellites
AUTH: A/TONKIN, S. W.; B/JENKINS, R. M.
74A26832
73/00/00

UTTL: Power conditioning and control for the T4 ion thruster
AUTH: A/HUGHES, R. C.; B/DAY, B. P.; C/FEARN, D. G.
74A26819
73/00/00

UTTL: Roll-out solar arrays for high power application
AUTH: A/KARIUS, S.; B/RUESCH, D.
74A24920
73/00/00

UTTL: Electric power for state-of-the-art communications satellites
AUTH: A/BILLERBECK, W. J.
74A18006
73/00/00

UTTL: Bilateral power conditioner.
AUTH: A/CARDWELL, G. I.; B/NEEL, W. O., III
73A42916
CNT#: F33615-70-C-1710
73/00/00

UTTL: Power Electronics Specialists Conference, California Institute of Technology, Pasadena, Calif., June 11-13, 1973, Record.
73A42901
73/00/00

UTTL: Nuclear safety considerations for the design of a shuttle launched 500 to 2000 watt isotope Brayton power system.
AUTH: A/GARATE, J. A.; B/GORLAND, S. H.
73A38432
73/00/00

UTTL: ASDTIC - A feedback control innovation.
AUTH: A/LALLI, V. R.; B/SCHOENFELD, A. D.
73A14901
RPT#: AIAA PAPER 72-1057
CNT#: NAS12-2017 NAS3-14392
72/11/00

UTTL: Optimization of PWM power units
AUTH: A/POTIN, B.
CORP: Compteurs Schlumberger, Montrouge (France).
72N31072
72/07/00

UTTL: Circuits for delayed switching and limitation of transients in the power transistors
AUTH: A/ROCCUCCI, S.; B/MENEGHINI, G.
CORP: Selenia S.p.A., Rome (Italy).
72N31062
72/07/00

UTTL: Standardized design and technology of black boxes for power conditioning electronics
AUTH: A/KOENNEKE, W.
CORP: AEG-Telefunken, Hamburg (West Germany).
72N31057
72/07/00

UTTL: Digital shunt power conditioning system for satellites using large power supplies
AUTH: A/FORATTINI, F.
CORP: European Space Agency. European Space Research and Technology Center, ESTEC, Noordwijk (Netherlands).
72N31055
72/07/00

UTTL: Parallel operation of solar generator with shunt regulator and battery discharge regulator on a constant voltage main bus
AUTH: A/KIENSCHERF, E.
CORP: AEG-Telefunken, Hamburg (West Germany).
72N31054
72/07/00

UTTL: A sequenced PWM controlled power conditioning unit for a regulated bus satellite power system
AUTH: A/CAPEL, A.; B/OSULLIVAN, D. M.
CORP: European Space Agency. European Space Research and Technology Center, ESTEC, Noordwijk (Netherlands).
72N31052
72/07/00

UTTL: Advanced power conditioning using a maximum power point tracking system
AUTH: A/PONCIN, A.
CORP: Etudes Techniques et Constructions Aerospatiales, Charleroi (Belgium).
72N31051
72/07/00

UTTL: Power conditioning of the French FR-1, D-2A, and STRET-1 satellites
AUTH: A/PRIDO, R.
CORP: Centre National d'Etudes Spatiales, Toulouse (France).
72N31047
72/07/00

UTTL: Dynamic behaviour of power conditioning systems for satellites with a maximum-power-point-tracking system
AUTH: A/BOEHRINGER, A.; B/HAUSSMANN, J.
CORP: Dornier-Werke G.m.b.H., Friedrichshafen (West Germany).
72N31046
72/07/00

UTTL: The power system of the Aeros satellite
AUTH: A/MUELLER, W.
CORP: Dornier-Werke G.m.b.H., Friedrichshafen (West Germany).
72N31045
72/07/00

UTTL: Spacecraft power conditioning electronics
CORP: European Space Agency, Paris (France).
72N31043
RPT#: ESRO-SP-84
72/07/00

UTTL: New control technique in dc/dc regulators for space applications.
AUTH: A/CAPEL, A.
72A41081
72/07/00

UTTL: An out-of-core thermionic-converter system for nuclear space power.
AUTH: A/BREITWIESER, R.
72A36187
72/06/00

UTTL: Feedback synthesis of an incore thermionic reactor control system for space.
AUTH: A/DAGBJARTSSON, S.; B/FERG, D.; C/SIEGEL, K.
72A36186
72/06/00

UTTL: A comparison of thermionic reactor designs employing a common thermionic fuel element.
AUTH: A/FISHER, C. R.; B/MERRILL, M. H.
72A36183
CNT#: AT(04-3)-840
72/06/00

UTTL: Voltage-conversion for incore-thermionic-reactors.
AUTH: A/KLEINKAUF, W.
72A36182
72/06/00

UTTL: Controlled dc to dc converter for a space-qualified thermionic-reactor.
AUTH: A/UHING, E.
72A36170
72/06/00

UTTL: Thermionic reactor power systems.
AUTH: A/GIETZEN, A. J.; B/HOMEYER, W. G.
72A36168
CNT#: AT(04-3)-840
72/06/00

UTTL: University role in astronaut life support systems: Space power supply systems
AUTH: A/CHIN, L. Y.
CORP: Massachusetts Inst. of Tech., Cambridge.
72N25144
RPT#: NASA-CR-2061
CNT#: NGR-22-009-312
72/06/00

UTTL: Probe measurements of a cesium plasma in a simulated thermionic energy converter
AUTH: A/SHIMADA, K.
CORP: Jet Propulsion Lab., California Inst. of Tech., Pasadena.
72N25668
RPT#: NASA-CR-126866 JPL-TM-33-551
CNT#: NAS7-100
72/05/15

UTTL: Radioisotope thermionic power supply for spacecraft
AUTH: A/HOMEYER, W. G.; B/GIETZEN, A. J.; C/HEATH, C. A.
72B10212
ARC-10438
72/05/00

UTTL: Improvements in tactical satellite communications.
AUTH: A/DEAN, J. C.
72A27844
72/05/00

UTTL: Maximum power transfer from a solar-cell array by sensing array temperature
AUTH: A/SUSSMAN, M.
CORP: National Aeronautics and Space Administration. Langley Research Center, Hampton, Va.
72N19055
RPT#: NASA-TN-D-6678 L-8110
72/03/00

UTTL: Design, performance, and evaluation of a direct-current contactor for space nuclear electrical systems
AUTH: A/MUELLER, L. A.; B/MEDWID, D. W.; C/KOUTNIK, E. A.; D/POWELL, A. H.
CORP: National Aeronautics and Space Administration. Lewis Research Center, Cleveland, Ohio.
72N18234
RPT#: NASA-TN-D-6699 E-6627
72/03/00

UTTL: Solar cells in satellite power supplies.
AUTH: A/CUSSEN, W. G.
72A24150
72/03/00

UTTL: Space power systems program
AUTH: A/BRILEY
CORP: National Aeronautics and Space Administration. Lyndon B. Johnson Space Center, Houston, Tex.
71M51311
RPT#: H-MSC-H134
CNT#: UNIVAC 1108
72/02/15

UTTL: The subsystem power conditioning for the Symphonie communications satellite
CORP: AEG-Telefunken, Hamburg (West Germany).
73N18085
RPT#: REPT-72-90
72/00/00

UTTL: Transit RTG - A status report.
AUTH: A/LURIE, H.; B/ROCKLIN, S.
73A26041
CNT#: AT(29-2)-2617
72/00/00

UTTL: SNAP-29 Power System/Agena integration study.
AUTH: A/ELMS, R. V., JR.
73A26040
72/00/00

UTTL: The SNAP-19 radioisotopic thermoelectric generator experiment - Flight performance on the Nimbus III observatory.
AUTH: A/FIHELLY, A. W.; B/BAXTER, C. F.; C/LYON, W. C.
73A26037
72/00/00

UTTL: Nuclear thermionic power plants in the 50-300 kWe range.
AUTH: A/VAN HOOMISSEN, J. E.; B/SAWYER, C. D.; C/PRICKETT, W. Z.
73A26027
CNT#: AT(04-3)-771 JPL-952381
72/00/00

UTTL: 100 kWe thermionic power system design.
AUTH: A/GIETZEN, A. J.; B/HOMEYER, W. G.
73A26026
CNT#: AT(04-3)-167
72/00/00

UTTL: Thermionic reactor systems for electric propulsion.
AUTH: A/MONDT, J. F.
73A26025
CNT#: NAS7-100
72/00/00

UTTL: Power system for a 4.1 kilowatt synchronous satellite.
AUTH: A/HNATEK, E. R.; B/BYXBEE, R. C.; C/CORBETT, R. E.
73A26023
72/00/00

UTTL: SNAP-27/ALSEP power subsystem used in the Apollo program.
AUTH: A/REMINI, W. C.; B/GRAYSON, J. H.
73A26021
72/00/00

UTTL: A modular Space Station/Base electrical power system - Requirements and design study.
AUTH: A/ELIASON, J. T.; B/ADKISSON, W. B.
73A26015
CNT#: NAS8-20055
72/00/00

UTTL: Reactor-thermoelectric power systems for NASA Space Station/Space Base.
AUTH: A/GYLFE, J. D.; B/JOHNSON, R. A.; C/KITTERMAN, W. L.
73A26012
72/00/00

UTTL: Concept for a high voltage solar array with integral power conditioning.
AUTH: A/WIENER, P.; B/RASMUSSEN, R.
73A26001
CNT#: NAS3-8997
72/00/00

UTTL: Energy 70; Proceedings of the Fifth Intersociety Energy Conversion Engineering Conference, Las Vegas, Nev., September 21-25, 1970. Volumes 1 & 2.
73A25976
72/00/00

UTTL: Advances in the safety of space nuclear power systems.
AUTH: A/DIX, G. P.
73A23287
72/00/00

UTTL: Modularised power conditioning units for high power satellite applications.
AUTH: A/O'SULLIVAN, D. M.; B/CAPEL, A.
73A22806
72/00/00

UTTL: Autonomous power subsystem design for an Outer Planet Spacecraft.
AUTH: A/ANDREWS, R. E.; B/WICK, H. M.
73A22805
CNT#: NAS7-100
72/00/00

UTTL: Power subsystem performance prediction /PSPP/ computer program.
AUTH: A/WEINER, H.; B/WEINSTEIN, S.
73A22802
72/00/00

UTTL: Zirconium Hydride Space Power Reactor design.
AUTH: A/ASQUITH, J. G.; B/MASON, D. G.; C/STAMP, S.
73A22801
CNT#: AT(04-3)-701
72/00/00

UTTL: Nuclear power system study.
AUTH: A/VAN OSDOL, J. H.; B/WILSON, R. F.; C/HENGLE, J. E. ; D/REARDON, D. E.
73A22799
CNT#: AT(04-3)-701
72/00/00

UTTL: Thermionic reactor power systems.
AUTH: A/GIETZEN, A. J.; B/HOMEYER, W. G.
73A22798
72/00/00

UTTL: System design considerations for a 25kW Space Station power system.
AUTH: A/TURNER, G. F.; B/JOHNSON, A. K.; C/GANDEL, M. G.
73A22784
72/00/00

UTTL: Electrical Power Subsystem definition for shuttle launched modular space station.
AUTH: A/NUSSBERGER, A. A.
73A22781
72/00/00

UTTL: Intersociety Energy Conversion Engineering Conference, 7th, San Diego, Calif., September 25-29, 1972, Proceedings.
73A22751
72/00/00

UTTL: New energy systems for space flight
AUTH: A/PESCHKA, W.
73A17668
72/00/00

UTTL: The liquid metal slip ring experiment for the Communications Technology Satellite.
AUTH: A/LOVELL, R. R.
73A15449
72/00/00

UTTL: Electric power processing, distribution and control for advanced aerospace vehicles.
AUTH: A/KRAUSZ, A.; B/FELCH, J. L.
73A13947
72/00/00

UTTL: A sequenced PWM controlled power conditioning unit for a regulated bus satellite power system.
AUTH: A/CAPEL, A.; B/O'SULLIVAN, D. M.
73A13930
72/00/00

UTTL: Power regulation in the Symphonie satellite
AUTH: A/KIENSCHERF, E.
72A36682
72/00/00

UTTL: Power supply and power converters in satellites and spacecraft
AUTH: A/PESCHKA, W.
72A16745
71/12/00

UTTL: Space power systems performances in vehicles employing nuclear reactors as energy source
AUTH: A/CAMPANARO, P.
CORP: Politecnico di Torino (Italy).
73N74230
RPT#: PUBL-131
71/10/00

UTTL: Power and load priority control concept for a Brayton cycle power system
AUTH: A/KELSEY, E. L.; B/YOUNG, R. N.
CORP: National Aeronautics and Space Administration. Langley Research Center, Hampton, Va.
71N36452
RPT#: NASA-TN-D-6478 L-7865
71/10/00

UTTL: Manufacture and use of atomic batteries
AUTH: A/SCHAEFER, H.
CORP: Air Force Systems Command, Wright-Patterson AFB, Ohio.
72N19064
RPT#: AD-734219 FTD-HT-23-973-71
71/09/22

UTTL: Brief description of the pilot plant installation and the incore-thermionic reactor
CORP: Scripta Technica, Inc., Washington, D. C.
71N35787
RPT#: NASA-TT-F-13744
CNT#: NASW-2036
71/08/00

UTTL: X4 satellite current design features and application
AUTH: A/STANIFORTH, R. G.
71A35330
71/08/00

UTTL: Radioisotope power systems.
72A10387
RPT#: SAE AIR 1213
71/07/30

UTTL: Extended lifetime considerations in radioisotope thermoelectric generators
AUTH: A/JAFFE, H.; B/ORIORDAN, P. A.
71A37929
RPT#: AAS PAPER 71-160
71/06/00

UTTL: Control characteristics and power conditioning of the electrostatic ion propulsion system ESKA-18P
AUTH: A/BAUMGARTH, S. F.; B/KLEINKAUF, W. A.
71A35543
RPT#: DGLR-71-029
71/06/00

UTTL: The potential of nuclear MHD electric power systems
AUTH: A/NICHOLS, L. D.; B/SEIKEL, G. R.
71A30716
RPT#: AIAA PAPER 71-638
71/06/00

UTTL: Status of advanced Rankine power conversion technology
AUTH: A/GUTSTEIN, M. U.; B/HELLER, J. A.; C/PETERSON, J. R.
71A33525
RPT#: GESP-623
71/06/00

UTTL: The incore-thermionic-reactor as power supply for a direct-to-home TV satellite
AUTH: A/RASCH, W.
71A32853
71/05/00

UTTL: A design for thick film microcircuit dc-to-dc converter electronics
AUTH: A/CAPODICI, S.; B/WICK, H. M., JR.
71A30801
71/05/00

UTTL: Heat-rejection radiator mass and its influence in space power systems
AUTH: A/BONNEVILLE, J. M.
71A28597
71/03/00

UTTL: SERT II - Solar array power system
AUTH: A/FALCONER, J. D.; B/SHAW, G. A. D.
71A22901
RPT#: AIAA PAPER 70-1159
71/03/00

UTTL: Design, performance, and evaluation of switchgear for space nuclear electrical systems
AUTH: A/KOUTNIK, E. A.; B/MUELLER, L. A.; C/POWELL, A. H.
CORP: General Electric Co., Cincinnati, Ohio.
71N20394
RPT#: NASA-CR-1719 GESP-372
CNT#: NAS3-9421
71/03/00

UTTL: Prime power systems, part 6
CORP: Hughes Aircraft Co., Culver City, Calif.
71N19649
71/02/00

UTTL: Space vehicle electrical power systems study Interim technical report
AUTH: A/BECHTOLD, G. W.; B/ROBINETTE, S. L.; C/SPANN, G. W.
CORP: Georgia Inst. of Tech., Atlanta.
71N20474
RPT#: NASA-CR-103072
CNT#: NAS8-25192
71/01/22

UTTL: Multi-phase, 2-kilowatt, high-voltage, regulated power supply.
AUTH: A/GARTH, D. R.; B/MULDOON, W. J.; C/BENSON, G. C.; D/COSTAGUE, E. N.
72A11063
71/00/00

UTTL: Pulse width modulated series inverter with inductor-transformer in low power applications.
AUTH: A/LINDENA, S.
72A11060
71/00/00

UTTL: Some design aspects concerning input filters for dc-dc converters.
AUTH: A/YU, Y.; B/BIESS, J. J.
72A11058
71/00/00

UTTL: PCSC '71; Power Conditioning Specialists Conference, California Institute of Technology, Pasadena, Calif., April 19, 20, 1971, Record.
72A11051
71/00/00

UTTL: Performance of the thermoelectric converter for the zirconium hydride reactor space power supply
AUTH: A/DU VAL, R. A.; B/MCCOURT, P. E.; C/ROBERTS, D. R.
71A38951
CNT#: AT/04-3/-701
71/00/00

UTTL: Integration of solar array and power conditioning electronics
AUTH: A/SPRINGGATE, W. F.
71A38942
CNT#: NAS3-8995
71/00/00

UTTL: Nonequilibrium MHD generators in nuclear space power systems
AUTH: A/BERTOLINI, E.; B/HOFFMAN, M. A.
71A38930
71/00/00

UTTL: Multihundred watt radioisotope thermoelectric generator /MHW-RTG/
AUTH: A/ARKER, A. J.; B/MORROW, R. B.; C/PITROLO, A. A.
71A38927
CNT#: AT/29-2/-2831
71/00/00

UTTL: An isotope-Brayton modular power system for the space station
AUTH: A/MCCARTY, L. H.
71A38922
71/00/00

UTTL: Reactor power system application to the earth orbital space station
AUTH: A/COGGI, J. V.; B/MCGRATH, R. E.
71A38919
71/00/00

UTTL: Nuclear systems for space power and propulsion
AUTH: A/KLEIN, M.
CORP: Office of Space Nuclear Systems (AEC), Washington, D. C.
72N25612
RPT#: NASA-TM-X-68341 A/CONF-49/P/56 CONF-710901-8
71/00/00

UTTL: The radio complex, control systems, and electric power supply
AUTH: A/PUCHKOV, V. P.; B/PUCHENKO, L. L.; C/BABKOV, F. I.; D/BELOVA, R. O.; E/IVANOV, O. G.; F/MALIN, V. I.; G/MAKOV, A. S.; H/MERKOV, I. B.; I/UZKIY, Y. G.; J/ZHELEZNOV, N. A.
CORP: Academy of Sciences (USSR), Moscow.
72N18245
71/00/00

UTTL: Atom in space and on earth. Lunokhod Furnace
AUTH: A/BERESTOV, IU.
CORP: Lockheed Missiles and Space Co., Palo Alto, Calif.
71N21579
71/00/00

UTTL: Conceptual design study of nuclear Brayton cycle heat exchanger and duct assembly /HXDA/, phase 1
AUTH: A/COOMBS, M. G.; B/MORSE, C. J.; C/RICHARD, C. E.
CORP: AiResearch Mfg. Co., Los Angeles, Calif.
71N14037
RPT#: NASA-CR-72783 AIRESEARCH-70-6691
CNT#: NAS3-13453
70/12/04

UTTL: Spacecraft power
CORP: Jet Propulsion Lab., California Inst. of Tech., Pasadena.
71N16678
70/10/31

UTTL: Technological problems anticipated in the application of fusion reactors to space propulsion and power generation
AUTH: A/RAYLE, W. D.; B/REINMANN, J. J.; C/ROTH, J. R.
CORP: National Aeronautics and Space Administration. Lewis Research Center, Cleveland, Ohio.
70N42521
RPT#: NASA-TM-X-2106 E-5575
CNT#: 129-02
70/10/00

UTTL: TOPS - Solar-independent power
AUTH: A/WICK, H. M.
70A41802
70/09/00

UTTL: Spacecraft power - Guidance and Control Division
CORP: Jet Propulsion Lab., California Inst. of Tech., Pasadena.
71N10258
70/08/31

UTTL: Power conditioning equipment for a thermoelectric outer planet spacecraft Quarterly technical reports
AUTH: A/ANDREWS, R.; B/ANDRYCZYK, R.; C/CAPODICI, S.; D/EBERSOLE, T.; E/KIRPICH, A.; F/PELLMANN, R.
CORP: General Electric Co., Philadelphia, Pa.; Jet Propulsion Lab., California Inst. of Tech., Pasadena.
70N39509
RPT#: NASA-CR-113603 REPT-1J86-TOPS-555 QTR-1 QTR-2
CNT#: NAS7-100 JPL-952536
70/08/01

UTTL: High voltage solar arrays with integral power conditioning
AUTH: A/HERRON, B. G.; B/OPJORDEN, R. W.
70A41787
RPT#: AIAA PAPER 70-1158
70/08/00

UTTL: Review of SERT II power conditioning
AUTH: A/BAGWELL, J. W.; B/HOFFMAN, A. C.; C/LESER, R. J.; D/READER, K. F.; E/STOVER, J. B.; F/VASICEK, R. W.
70A40216
RPT#: AIAA PAPER 70-1129
70/08/00

UTTL: Space electric rocket test solar array power system
AUTH: A/FALCONER, J. C.; B/SHAW, G. A. D.
70A40202
RPT#: AIAA PAPER 70-1159
70/08/00

UTTL: High voltage solar array configuration study Final report
AUTH: A/CREED, D. E.; B/HERRON, B. G.; C/OPJORDEN, R. W.; D/TODD, G. T.
CORP: Hughes Aircraft Co., El Segundo, Calif.
71N11048
RPT#: NASA-CR-72724
CNT#: NAS3-8996
70/07/00

UTTL: Development and testing of a flight prototype ion thruster power conditioner
AUTH: A/BENSON, G. C.; B/GARTH, D. R.; C/MULDOON, W. J.
70A33615
RPT#: AIAA PAPER 70-649
70/06/00

UTTL: Space electric power R and D program, part 1 Quarterly status report, period ending 30 Apr. 1970
CORP: Los Alamos Scientific Lab., N. Mex.
70N39996
RPT#: LA-4446-PT-1
CNT#: W-7405-ENG-36
70/05/00

UTTL: Research and advanced concepts
CORP: Jet Propulsion Lab., California Inst. of Tech., Pasadena.
70N36896
70/04/30

UTTL: Possible space application of nuclear power supply, particularly for direct TV-broadcasting
AUTH: A/KLEINKAUF, W.; B/KRUPSTEDT, U.; C/QUAST, A.; D/RASCH, W.; E/SCHARF, W.
CORP: Deutsche Forschungs- und Versuchsanstalt fuer Luft- und Raumfahrt, Brunswick (West Germany).
70N30407
RPT#: BMBW-FB-W-70-16
70/04/00

UTTL: Technology for nuclear dynamic space power systems
AUTH: A/ENGLISH, R. E.
70A29492
70/04/00

UTTL: The synthesis of the optimal control systems of the power and the energetic plants for space vehicles using nuclear energy
AUTH: A/BODNER, V. A.; B/BUGROVSKY, V. V.; C/KANIOVSKY, S. S.; D/MARTIANOVA, T. S.; E/PETROV, B. N.; F/RYASANOV, J. A.; G/SHEVYACOV, A. A.; H/ULANOV, J. M.
70A28436
70/03/00

UTTL: Conceptual design of a 10-MWe nuclear Rankine system for space power
AUTH: A/PITTS, J. H.; B/WALTER, C. E.
70A26123
70/03/00

UTTL: Steady-state analysis of a Brayton space- power system
AUTH: A/KLANN, J. L.
CORP: National Aeronautics and Space Administration. Lewis Research Center, Cleveland, Ohio.
70N18954
RPT#: NASA-TN-D-5673 E-5281
CNT#: 120-27
70/02/00

UTTL: Thermionic spacecraft design study, phase 1
CORP: General Electric Co., Philadelphia, Pa.; Jet Propulsion Lab., California Inst. of Tech., Pasadena.
73N71875
RPT#: NASA-CR-131106 GESP-7031
CNT#: NAS7-100 JPL-952381
70/01/00

UTTL: Closed Brayton cycle system optimization for undersea, terrestrial, and space applications
AUTH: A/MOCK, E. A.
CORP: AiResearch Mfg. Co., Phoenix, Ariz.
79N22096
70/00/00

UTTL: Advanced techniques of spacecraft electrical power transformation and control
AUTH: A/YAGERHOFER, F. C.
71A13049
70/00/00

UTTL: Nuclear safety of space nuclear power systems
AUTH: A/DIX, G. P.
70A43192
70/00/00

UTTL: ZrH reactor and thermoelectric conversion system
AUTH: A/WILSON, R. F.
70A43190
CNT#: AT/04-3/-701
70/00/00

UTTL: Technology for nuclear dynamic space power systems
AUTH: A/ENGLISH, R. E.
70A43189
70/00/00

UTTL: Rotary transformer design
AUTH: A/LANDSMAN, E. E.
70A41222
70/00/00

UTTL: Integrated circuit requirements for high power space power conditioning equipment
AUTH: A/BIESS, J. J.; B/GOLDIN, D. S.
70A41211
70/00/00

UTTL: Solid state power controller circuits and their effect upon power conditioning requirements
AUTH: A/HEINZMAN, H. W.; B/JONES, C. M.
70A41210
70/00/00

UTTL: Communications satellite power conditioning systems
AUTH: A/DUNLOP, J. D.
70A41207
70/00/00

UTTL: Institute of Electrical and Electronics Engineers, Power Conditioning Specialists Conference, Nasa Goddard Space Flight Center, Greenbelt, Md., Apr. 20, 21, 1970, Record
70A41206
70/00/00

UTTL: Functional and physical design of a flight prototype ion engine power conditioner
AUTH: A/BENSON, G. C.; B/GARTH, D. R.; C/MULDOON, W. J.
70A41006
CNT#: JPL-952297
70/00/00

UTTL: Erosion testing of a three-stage potassium turbine
AUTH: A/KAPLAN, G. M.; B/SCHNETZER, E.
70A41005
CNT#: NAS3-10606
70/00/00

UTTL: Nuclear power supplies
AUTH: A/HOMEYER, W.
70A31147
70/00/00

UTTL: A modern spacecraft power system concept with power adaptation, using a "maximum power point tracker'
AUTH: A/FROEHLICH, H.; B/MUELLER, W.
CORP: Dornier-Werke G.m.b.H., Friedrichshafen (West Germany).
72N15995
70/00/00

UTTL: Low input voltage conversion from unconventional primary /RTG'S/ and secondary /battery/ sources
AUTH: A/PASCIUTTI, E. R.
CORP: National Aeronautics and Space Administration. Goddard Space Flight Center, Greenbelt, Md.
71N25309
70/00/00

UTTL: Spacecraft power
CORP: Jet Propulsion Lab., California Inst. of Tech., Pasadena.
70N25235
69/12/31

UTTL: Electrical power systems for solar probes - Some general considerations
AUTH: A/DESAUTELS, A. N.
70A14753
RPT#: ASME PAPER 69-WA/SOL-5
69/11/00

UTTL: Progress in the design of electronic circuits for satellite power systems
AUTH: A/CAPART, J. J.
CORP: European Space Agency. European Space Research and Technology Center, ESTEC, Noordwijk (Netherlands).
71N12580
69/11/00

UTTL: Auxiliary circuits and power system performance analysis
AUTH: A/PREUKSCHAT, A. W.
CORP: European Space Agency. European Space Research and Technology Center, ESTEC, Noordwijk (Netherlands).
71N12579
69/11/00

UTTL: Power distribution
AUTH: A/LE HERITTE, B.
CORP: Sogam-Electronique, Poissy (France).
71N12578
69/11/00

UTTL: Proceedings of the sixth ESRO summer school, volume 11 - Space power systems - Power conditioning and control
CORP: European Space Agency, Paris (France).
71N12576
RPT#: ESRO-SP-50
69/11/00

UTTL: Space power systems, part 2 Lecture series
CORP: Advisory Group for Aerospace Research and Development, Paris (France).
70N16222
RPT#: AGARDOGRAPH-123-PT-2
69/11/00

UTTL: Nuclear space power systems
AUTH: A/DIECKAMP, H. M.
CORP: Advisory Group for Aerospace Research and Development, Paris (France).
70N16220
69/11/00

UTTL: Power conditioning equipment for the thermoelectric outer planet spacecraft Quarterly technical report, 17 Apr. - 30 Jun. 1969
AUTH: A/ANDRYCZYK, R. W.; B/BARRY, F. R.; C/EBERSOLE, T. J.; D/JEREMENKO, A.; E/PELLMAN, R. R.; F/SCHERER, P. R.
CORP: General Electric Co., Philadelphia, Pa.; Jet Propulsion Lab., California Inst. of Tech., Pasadena.
70N12070
RPT#: NASA-CR-107013 REPT-1J86-TOPS-479
CNT#: NAS7-100 JPL-952536
69/10/15

UTTL: Space electric power R and D program /U/ Quarterly status report for the period ending 31 Jul. 1969
CORP: Los Alamos Scientific Lab., N. Mex.
79N77411
RPT#: LA-4232-MS
CNT#: W-7405-ENG-36
69/08/21

UTTL: Isotope reentry vehicle design study preliminary design - Phase 2 Final report
AUTH: A/GRAHAM, J. W.; B/RYAN, R. L.
CORP: Avco Corp., Wilmington, Mass.
69N34989
RPT#: NASA-CR-72555 AVSD-0306-69-RR
CNT#: NAS3-10938
69/08/00

UTTL: The influence of variable thermal conductivity and variable electrical resistivity on thermoelectric generator performance.
AUTH: A/LEE, J. S.
69A40131
69/08/00

UTTL: Development of a high-efficiency cascaded thermoelectric module.
AUTH: A/ROCKLIN, S. R.
69A37706
CNT#: AF 33/615/-67-C-1822
69/07/00

UTTL: Solar cell power systems on US satellites. Part 1 - Satellites designed by the NASA, Goddard Space Flight Center
AUTH: A/MAC KENZIE, C. M.
CORP: National Aeronautics and Space Administration. Goddard Space Flight Center, Greenbelt, Md.
70N12694
69/07/00

UTTL: Power sources for European satellites other than those of the European Space Research Organization
AUTH: A/BOCHET, J. C.
CORP: European Space Agency. European Space Research and Technology Center, ESTEC, Noordwijk (Netherlands).
70N12693
69/07/00

UTTL: Power systems in ESRO satellites
AUTH: A/PREUKSCHAT, A. W.
CORP: European Space Agency. European Space Research and Technology Center, ESTEC, Noordwijk (Netherlands).
70N12692
69/07/00

UTTL: Proceedings of the Sixth ESRO Summer School. Volume 7 - Space power Systems - Application
CORP: European Space Agency, Paris (France).
70N12691
RPT#: ESRO-SP-46
69/07/00

UTTL: Nuclear reactors as a source of power in space
AUTH: A/SHEPHERD, L. R.
CORP: Atomic Energy Establishment, Winfrith (England).
70N11305
69/07/00

UTTL: Isotopic energy sources
AUTH: A/DASPET, H.
CORP: Centre National d'Etudes Spatiales, Bretigny-sur-Orge (France).
70N11304
69/07/00

UTTL: Primary energy sources and conversion systems
AUTH: A/HEFFELS, K. H.
CORP: European Space Agency. European Space Research and Technology Center, ESTEC, Noordwijk (Netherlands).
70N11303
69/07/00

UTTL: Proceedings of the sixth ESRO summer school, Volume 6 - Space power systems - Introduction
CORP: European Space Agency, Paris (France).
70N11301
RPT#: ESRO-SP-45
69/07/00

UTTL: Power systems in ESRO satellites
AUTH: A/PREUKSCHAT, A. W.
CORP: European Space Agency. European Space Research and Technology Center, ESTEC, Noordwijk (Netherlands).
70N17621
RPT#: ESRO-TN-83
69/07/00

UTTL: Mariner Venus 67 power subsystem modification - Test and flight operation
AUTH: A/KRUG, A.
CORP: Jet Propulsion Lab., California Inst. of Tech., Pasadena.
70N20751
RPT#: NASA-CR-109033 JPL-TM-33-423
CNT#: NAS7-100
69/06/30

UTTL: Nuclear reactor systems for space electric power applications
AUTH: A/WITZE, C. P.
CORP: Bellcomm, Inc., Washington, D. C.
79N73200
RPT#: NASA-CR-106691 B69-06033
CNT#: NASW-417
69/06/09

UTTL: Applications and development of space nuclear electric power systems.
AUTH: A/LAFLEUR, J. D., JR.; B/SCHULMAN, F.
69A42865
RPT#: AAS PAPER 69-305
69/06/00

UTTL: Space electric power R and D program /U/ Quarterly status report for the period ending 30 Apr. 1969
CORP: Los Alamos Scientific Lab., N. Mex.
79N77410
RPT#: LA-4183-MS
CNT#: W-7405-ENG-36
69/05/28

UTTL: Low power nuclear energy conversion for long duration space missions.
AUTH: A/BJERKLIE, J. W.
69A31748
69/05/00

UTTL: The 1968 results from BMwF supported studies of the IKE. Part 1 - Continuation of basic research studies on thermionic reactors for space flight purposes. Part 2 - Studies on neutron and gamma ray interactions with matter. Calculations for compact reactors, especially with plutonium fuel
AUTH: A/HOECKER, K. H.
CORP: Technische Hochschule, Stuttgart (West Germany).
71N14209
RPT#: K-12
69/05/00

UTTL: Hydrogen-oxygen fired thermionic generators and thermionic diodes
CORP: Thermo Electron Corp., Waltham, Mass.
69N30871
RPT#: NASA-CR-101745 TE-5045-145-69
CNT#: NAS9-4282
69/04/03

UTTL: Space electric R and D program, part 1 Quarterly status report, period ending 31 Jan. 1969
CORP: Los Alamos Scientific Lab., N. Mex.
69N28827
RPT#: LA-4109-MS-PT-1
CNT#: W-7405-ENG-36
69/02/26

UTTL: Higher outputs and efficiencies for nuclear batteries.
AUTH: A/MATHESON, W. E.
69A37288
69/02/00

UTTL: Analysis of an out-of-core thermionic space power system.
AUTH: A/LOEWE, W. E.
69A19856
69/01/00

UTTL: Guidebook for the application of Space Nuclear Power Systems
70A10942
69/00/00

UTTL: Power conditioning development for the Sert II ion thrustor.
AUTH: A/BAUER, S. F.; B/BRIGGS, R. W.; C/HOFFMAN, A. C.; D/SWIDERSKI, E. F.; E/WEGER, R. M.
69A42301
69/00/00

UTTL: Modularization of high-power inverters and converters.
AUTH: A/GOURASH, F.; B/HEINS, J. F.; C/PITTMAN, P. F.
69A42292
69/00/00

UTTL: Parametric charge studies for aerospace nickel-cadmium batteries.
AUTH: A/BETZ, F. E.; B/PREUSSE, K. E.; C/SHAIR, R. C.; D/SYLVIA, J.
69A42282
69/00/00

UTTL: 25 kwe reactor-thermoelectric power system for manned orbiting space stations.
AUTH: A/BRANTLEY, L. W.; B/DUVAL, R. A.; C/GYLFE, J. D.; D/JOHNSON, R. A.
69A42256
69/00/00

UTTL: Status report on small reactor-thermoelectric power systems for unmanned space applications.
AUTH: A/GYLFE, J. D.; B/VANOSDOL, J. H.
69A42255
69/00/00

UTTL: Thermal model of a 75 watt
AUTH: A/PARKER, A. J., JR.; B/WEST, W. S.
69A42254
CNT#: NAS5-0441
69/00/00

UTTL: Impactable power subsystems for Mars landers.
AUTH: A/SWERDLING, M.
69A42253
69/00/00

UTTL: Performance analysis of satellite electric power systems by computer simulation.
AUTH: A/SCHWARTZBURG, M.
69A42241
69/00/00

UTTL: American Institute of Chemical Engineers, Intersociety Energy Conversion Engineering Conference, 4th, Washington, D.C., September 22-26, 1969, Proceedings.
69A42236
69/00/00

UTTL: Power distribution characteristics for overload protection.
AUTH: A/PELLMANN, R. R.
69A34088
CNT#: JPL-952150
69/00/00

UTTL: Application of thermionic energy conversion in the USSR.
AUTH: A/DANILOV, IU. L.
69A29279
69/00/00

UTTL: Out-of-core thermionic space power.
AUTH: A/LOEWE, W. E.
69A29188
69/00/00

UTTL: America in space, the first decade - Spacecraft power
AUTH: A/CORLISS, W. R.
CORP: National Aeronautics and Space Administration, Washington, D.C.
71N10585
RPT#: NASA-EP-59
69/00/00

UTTL: A heat pipe thermionic reactor concept.
AUTH: A/FIEBELMANN, P.; B/NEU, H.; C/RINALDINI, C.
69A29187
69/00/00

UTTL: Design and dimensioning of a nuclear power supply installation with an in-core thermionic reactor
AUTH: A/QUAST, A.; B/RASCH, W.
69A20871
68/12/00

UTTL: A silicon-germanium solar thermoelectric generator.
AUTH: A/BERLIN, R. E.; B/RAAG, V.
69A15674
CNT#: NAS3-10600
68/12/00

UTTL: An in-core thermionic reactor for powering space vehicles
AUTH: A/ANDRAE, H.; B/BUDNICK, D.; C/GROSS, F.; D/JAHNS, W.; E/JANNER, K.; F/JESTER, A.
69A12666
68/12/00

UTTL: Parametric study of space power systems. Volume 2 - Technical report Final report
AUTH: A/TONELLI, A. D.
CORP: McDonnell-Douglas Corp., Huntington Beach, Calif.
69N14760
RPT#: NASA-CR-73280 DAC-62304-VOL-2
CNT#: NAS2-4482
68/11/00

UTTL: Impact of the thermionic reactor on advanced space vehicles.
AUTH: A/BREUER, F. D.; B/POWELL, D. J.
68A44249
RPT#: IAF PAPER SD-111
68/10/00

UTTL: A SNAP-8 breadboard system. Operating experience.
AUTH: A/HODGSON, J. N.; B/MACOSKO, R. P.
CORP: National Aeronautics and Space Administration. Lewis Research Center, Cleveland, Ohio.
68N33238
RPT#: NASA-TM-X-61161 REPT.-3511
68/08/00

UTTL: Power systems.
AUTH: A/BORETZ, J. E.; B/JONES, I. R.
68A38506
68/07/31

UTTL: SNAP 19, phase 3. Volume 1. Power supply system Final report
CORP: Martin Co., Baltimore, Md.
68N38006
RPT#: MND-3607-239-1, V. 1
CNT#: AT/30-1/-3607
68/05/00

UTTL: Evaluation of the am/ows electrical power system using solar array modules form the atm electrical power system
AUTH: A/MOSS, B. W.
CORP: Bellcomm, Inc., Washington, D. C.
79N72949
RPT#: NASA-CR-95450
CNT#: NASW-417
68/04/04

UTTL: Out of core thermionic space power
AUTH: A/LOEWE, W. E.
CORP: California Univ., Livermore. Lawrence Radiation Lab.
68N36908
RPT#: UCRL-70816 CONF-680508-1
CNT#: W-7405-ENG-48
68/03/08

UTTL: Design study electrical component technology for 0.25 to 10.0 megawatt space power systems Final report, 1 Sep. 1966 - 29 Feb. 1968
AUTH: A/KING, A. E.
CORP: Westinghouse Electric Corp., Lima, Ohio.
68N37438
RPT#: SAN-679-8
CNT#: AT/04-3/-679
68/02/01

UTTL: A reactor concept for space power employing thermionic diodes and heat pipes.
AUTH: A/HEATH, C. A.; B/LANTZ, E.
68A17540
RPT#: AIAA PAPER 68-122
68/01/00

UTTL: Results of studies on thermionic reactor systems
AUTH: A/DAGBJARTSSON, S.; B/EMENDOERFER, D.; C/GROLL, M.; D/HAUG, W.; E/PRUSCHEK, R.
CORP: Technische Hochschule, Stuttgart (West Germany).
68N21856
RPT#: REPT.-68-007

68/00/00

UTTL: Flat plate thermoelectric generators for solar probe missions
AUTH: A/BERLIN, R. E.; B/BIFANO, W. J.; C/RAAG, V.
CORP: National Aeronautics and Space Administration. Lewis Research Center, Cleveland, Ohio.
68N31018
RPT#: NASA-TM-X-52451
68/00/00

UTTL: Aerospace nuclear safety.
AUTH: A/BLAKE, V. E.
68A25647
68/00/00

UTTL: Energy in space - Program planning for space power system technology.
AUTH: A/WOODWARD, W. H.
68A40071
68/00/00

UTTL: New developments in the space isotope power program.
AUTH: A/CLARK, A. J., JR.
68A37739
68/00/00

UTTL: Optimization of thermionic generator systems of high reliability.
AUTH: A/DE WINTER, F.; B/SHIMADA, K.
68A37738
68/00/00

UTTL: Nuclear power supplies for space.
AUTH: A/POLAK, H.
68A37252
68/00/00

UTTL: Thermionic energy sources and their applications
AUTH: A/LANGPAPE, R.
69A25869
68/00/00

UTTL: Power requirements and power supply of spacecraft
AUTH: A/OLDEKOP, W.
69A25863
68/00/00

UTTL: Deutsche Gesellschaft fuer Flugwissenschaften, Lectures on Astronautics, 7th, Technische Unversitaet Braunschweig, Braunschweig, West Germany, October 7-11, 1968, Proceedings. Volume 2 - Energy Sources
69A25862
68/00/00

UTTL: Development of high temperature thyratrons for large nuclear electrical space power systems.
AUTH: A/JONES, N. D.
69A24744
CNT#: NAS3-8525
68/00/00

UTTL: Nuclear reactors in space flight technology
AUTH: A/NAUMANN, H. D.
69A19739
68/00/00

UTTL: Nuclear organic Rankine/thermoelectric systems.
AUTH: A/HOWARD, J. M.
68A42558
68/00/00

UTTL: The development of a 28-volt 500-watt thermionic power generator.
AUTH: A/HARBAUGH, W. E.; B/LONGSDERFF, R. W.; C/TURNER, R. C.
68A42557
CNT#: AF 33/615/-5095
68/00/00

UTTL: SNAP 29 system design and development.
AUTH: A/SCHEVE, M. R.
68A42552
68/00/00

UTTL: SNAP 11 radioisotope thermoelectric generator.
AUTH: A/BRITTAIN, W. M.
68A42551
CNT#: AT/30-1/-2952
68/00/00

UTTL: Development of a two watt/lb radioisotope fueled space thermoelectric generator.
AUTH: A/DESCHAMPS, N. H.; B/REXFORD, H. E.
68A42549
68/00/00

UTTL: 2 to 10 kilowatt solar or radioisotope Brayton power system.
AUTH: A/KLANN, J. L.
68A42544
68/00/00

UTTL: SNAP 29 heat source design and development.
AUTH: A/WACHTL, W. W.
68A42528
68/00/00

UTTL: Studies of thermionic materials for space power applications
AUTH: A/YANG, L.
CORP: General Dynamics Corp., San Diego, Calif.
73N70352
RPT#: NASA-CR-54779 GA-6717
CNT#: NAS3-6471
67/12/20

UTTL: Design study /of/ electrical component technology for 0.25 to 10.0 megawatt space power systems. Parametric design study of canned ac induction motors
AUTH: A/ALLEN, T. C.
CORP: Westinghouse Electric Corp., Lima, Ohio.
68N31544
RPT#: SAN-679-5 WAED-67-52E
CNT#: AT/04-3/-679
67/12/15

UTTL: New developments in the space isotope power program
AUTH: A/CLARK, A. J., JR.
CORP: Sandia Corp., Albuquerque, N. Mex.
68N22898
RPT#: SC-DC-67-2119 CONF-680301-1
CNT#: AT/29-1/-789
67/12/00

UTTL: Isotopic thermoionic generator
AUTH: A/CLEMOT, M.; B/DEVIN, B.; C/DURAND, J.-P.
CORP: Commissariat a l'Energie Atomique, Saclay (France).
68N22701
RPT#: CEA-R-3418
67/12/00

UTTL: S2 childown inverter /P-66/ qualification test, Saturn program Test reprot, 8 Aug. - 25 Oct. 1967
AUTH: A/HAGINO, I.
CORP: Douglas Aircraft Co., Inc., Santa Monica, Calif.
70N76240
RPT#: NASA-CR-113240 TM-DSV4B-EE-R6065
67/11/29

UTTL: Space vehicle missile power supplies Annotated bibliography
AUTH: A/BENTON, M.
CORP: National Aeronautics and Space Administration. Marshall Space Flight Center, Huntsville, Ala.
68N17223
RPT#: NASA-TM-X-60877 RSIC-743
CNT#: DAAH01-67-C-1036/Z/
67/11/00

UTTL: Review of the radiator design completed at the Institute for Nuclear Energy
AUTH: A/GROLL, M.; B/WEISSER, TH. W.
CORP: Technische Hochschule, Stuttgart (West Germany).
68N15042
RPT#: REPT.-5-39
67/07/00

UTTL: Comparison study of RTG and solar powered Voyager spacecraft
CORP: General Electric Co., Philadelphia, Pa.
75N78228
RPT#: NASA-CR-145783 TID/SNG-16
67/06/01

UTTL: Studies of thermionic materials for space power applications
AUTH: A/YANG, L.
CORP: General Dynamics Corp., San Diego, Calif.
73N70351
RPT#: NASA-CR-72247 GA-7710
CNT#: NAS3-6471
67/05/14

UTTL: Fuel produced from spacecraft material
AUTH: A/SEGAL, H. M.
CORP: Boeing Co., Seattle, Wash.
68N17358
67/03/03

UTTL: SNAP power system for Dodge-M satellite, technical description
CORP: Martin Marietta Corp., Baltimore, Md.
76N75243
RPT#: MND-3607-131-2
CNT#: AT(30-1)-3607
67/03/00

UTTL: Status of isotope thermionic module development program
AUTH: A/WILLIAMS, E. W.; B/HOWARD, R. C.
CORP: General Electric Co., Philadelphia, Pa.
73N73464
CNT#: AT(29-2)-2055
67/03/00

UTTL: Power conditioning for satellite systems /A system power conditioning primer/
AUTH: A/PRO, S.
CORP: Aerospace Corp., El Segundo, Calif.
68N12046
RPT#: TR-1001/2307/-6 SAMSO-TR-67-10 AD-660532
CNT#: AF 04/695/-1001
67/03/00

UTTL: RTG integration problem areas and parametric analysis
AUTH: A/SELWITZ, L.
CORP: Jet Propulsion Lab., California Inst. of Tech., Pasadena.
68N21204
RPT#: NASA-CR-94042 JPL-TM-33-321
CNT#: NAS7-100
67/02/01

UTTL: Research and development on fission-heated thermionic cells for application to nuclear space power systems
CORP: General Dynamics Corp., San Diego, Calif.
73N74397
RPT#: GA-7660
CNT#: AT(04-3)-167 PROJ. 278
67/01/27

UTTL: Thermally regenerative fuel cells
AUTH: A/HENDERSON, R. E.
CORP: General Motors Corp., Dayton, Ohio.
68N17825
67/00/00

UTTL: The development of thermionic isotope space power technology, appendix 1 Final technical report
CORP: Radio Corp. of America, Lancaster, Pa.
68N12989
RPT#: NASA-CR-91354
CNT#: NASW-1254
67/00/00

UTTL: Spacepower advanced technology planning
AUTH: A/WOODWARD, W. H.
CORP: National Aeronautics and Space Administration, Washington, D.C.
68N33173
67/00/00

UTTL: Future applications for static energy conversion devices
AUTH: A/WOODWARD, W. H.
CORP: National Aeronautics and Space Administration, Washington, D.C.
68N28748
67/00/00

UTTL: Advanced dynamic power generating systems for space vehicle applications.
AUTH: A/CORCORAN, E. G.; B/LEE, H. S.
68A42151
67/00/00

UTTL: Development of a thermally regenerative sodium-mercury galvanic system. III - Performance analysis for a nuclear reactor-powered, thermally regenerative sodium-mercury galvanic system.
AUTH: A/OLDENKAMP, R. D.; B/RECHT, H. L.
68A27640
67/00/00

UTTL: A thermionic reactor based on radiant heat transfer and demonstrated components.
AUTH: A/GREENBORG, J.; B/MAYER, M. S.; C/RASOR, N. S.
68A24402
67/00/00

UTTL: Thermally regenerative fuel cells.
AUTH: A/HENDERSON, R. E.
68A22544
RPT#: AGARDOGRAPH 81
67/00/00

UTTL: Working gas selection for the closed Brayton cycle.
AUTH: A/MASON, J. L.
68A22523
RPT#: AGARDOGRAPH 81
67/00/00

UTTL: Design and integration study of an RTG powered Voyager spacecraft.
AUTH: A/KIRPICH, A.
68A17137
67/00/00

UTTL: Reactors for space.
AUTH: A/FRAAS, A. P.
68A12299
67/00/00

UTTL: Studies of thermionic materials for space power applications
AUTH: A/YANG, L.
CORP: General Dynamics Corp., San Diego, Calif.
73N70348
RPT#: NASA-CR-72132 GA-7473
CNT#: NAS3-6471
66/12/20

UTTL: Spacecraft radiation mapping, Voyager task C
AUTH: A/PEDEN, J. C.
CORP: General Electric Co., Philadelphia, Pa.
76N70377
RPT#: NASA-CR-145886 TID/SNG-13 VOY-C1-TR8
CNT#: JPL-951112
66/12/15

UTTL: Studies of thermionic materials for space power applications
AUTH: A/YANG, L.
CORP: General Dynamics Corp., San Diego, Calif.
73N70349
RPT#: NASA-CR-72032 GA-7250
CNT#: NAS3-6471
66/09/06

UTTL: Design and development of a thermo-ionic electric thrustor Final report, 30 Apr. 1964 - 11 Jan. 1966
AUTH: A/DUCATI, A. C.; B/JAHN, R. G.; C/MUEHLBERGER, E.; D/TREAT, R. P.
CORP: Giannini Scientific Corp., Santa Ana, Calif.
68N26981
RPT#: NASA-CR-54703 FR-056-968
CNT#: NASW-968
66/05/00

UTTL: SNAP 10A
AUTH: A/STAUB, D. W.
CORP: Atomics International, Canoga Park, Calif.
73N74404
RPT#: NAA-SR-11693
CNT#: AT(11-1)-GEN-8
65/12/29

UTTL: Development of a nuclear thermionic fuel element
CORP: General Electric Co., Pleasanton, Calif.
73N74208
RPT#: GESR-2061 QPR-14
CNT#: AT(04-3)-189
65/11/30

UTTL: Research and development on fission-heated thermionic cells for application to nuclear space power systems
CORP: General Dynamics Corp., San Diego, Calif.
73N74334
RPT#: GA-6004

CNT#: AT(04-3)-167
64/10/31

UTTL: Engineering study of an advanced 250 watt (e) SR-90 fueled thermoelectric space power supply, volume 2
CORP: Hittman Associates, Inc., Baltimore, Md.
74N71621
RPT#: HIT-143-VOL-2
CNT#: AT(30-1)-3392
64/08/14

UTTL: Research on spacecraft and powerplant integration problems
AUTH: A/LARSON, J. W.
CORP: General Electric Co., Philadelphia, Pa.
71N76060
RPT#: NASA-CR-54159 GE-64SD892
CNT#: NAS3-2533
64/07/24

UTTL: Design study for an advanced space radioisotope thermoelectric power supply
AUTH: A/LARSON, T. J.
CORP: General Dynamics Corp., San Diego, Calif.
74N72273
RPT#: GA-5500
CNT#: AT(04-3)-167
64/07/17

UTTL: Studies of thermionic materials for space power applications
AUTH: A/YANG, L.
CORP: General Dynamics Corp., San Diego, Calif.
73N70373
RPT#: NASA-CR-63495 GA-5108
CNT#: NAS3-4165
64/05/20

UTTL: Development of electrical switchgear for space nuclear electrical systems
AUTH: A/EDWARDS, R. N.; B/GOLDBERG, L. J.; C/TRAVIS, E. F. ; D/KESSLER, G. W.
CORP: General Electric Co., Cincinnati, Ohio.
73N72213
RPT#: NASA-CR-54059 QPR-3
CNT#: NAS3-2546
64/04/16

UTTL: Propulsion and power generation
CORP: National Aeronautics and Space Administration, Washington, D.C.
73N71877
RPT#: NASA-TM-X-50121
63/07/00

UTTL: SNAP 2 nuclear auxiliary power unit development
AUTH: A/SHACKELFORD, M.
CORP: Atomics International, Canoga Park, Calif.
73N74216
RPT#: NAA-SR-7191
CNT#: AT(11-1)-GEN-8
62/09/15

UTTL: Research on reliable and radiation insensitive pulse-drive sources for all-magnetic logic systems
AUTH: A/BAER, J. A.; B/HECKLER, C. H., JR.
CORP: Stanford Research Inst., Menlo Park, Calif.
85N74053
RPT#: DE85-900318 NP-5900318
62/06/00

UTTL: An appraisal of the advanced electric space power systems
CORP: National Aeronautics and Space Administration. Lewis Research Center, Cleveland, Ohio.
83N71701
RPT#: NASA-TM-85185 NAS 1.15:85185
62/05/00

UTTL: Spacecraft power generation
AUTH: A/COOLEY, W. C.
CORP: National Aeronautics and Space Administration, Washington, D.C.
69N76845
RPT#: NASA-TM-X-61813
60/08/26

Record.
212 p. illus. 28 cm.
73V21522

SEARCH TITLE: SPACECRAFT RADIATORS

DESCRIPTION:

1. Space Power Reactors
2. Thermoelectric Power
3. Thermionic Power Generation
4. Nuclear Electric Power
5. Spacecraft Radiators

The above entries were combined using Boolean logic to refine a search strategy, and it was used with the above set numbers only.

Logic Statement: (1+2+3+4)*5

PRINT 09/4/1-54 TERMINAL=45

UTTL: Trends and limits in the upgrading of SP-100 baseline design of nuclear powered space system
AUTH: A/EL-GENK, MOHAMED S.; B/SEO, JONG-TAE
87A21831
CNT#: F29601-82-K-0055
87/00/00

UTTL: Analysis of alkali liquid metal Rankine space power systems
AUTH: A/YODER, G. L.; B/GRAVES, R. L.
87A21826
CNT#: DE-AC05-84OR-21400
87/00/00

UTTL: Space reactor/organic Rankine conversion - A near-term state-of-the-art solution
AUTH: A/NIGGEMANN, R. E.; B/LACEY, D.
87A21821
87/00/00

UTTL: A review of test options for SP-100 system designs
AUTH: A/SCHMIDT, GLEN L.
87A21817
87/00/00

UTTL: Optimization of a heat-pipe-cooled space radiator for use with a reactor-powered Stirling engine
AUTH: A/MORIARTY, MICHAEL P.; B/FRENCH, EDWARD P.
CORP: Rockwell International Corp., Canoga Park, Calif.
87A21815
CNT#: JPL-956935
87/00/00

UTTL: Heat transfer studies on the liquid droplet radiator
AUTH: A/MATTICK, A. T.; B/NELSON, M.
CORP: Washington Univ., Seattle.
87A21813
CNT#: AF-AFOSR-83-0367 NAG1-327
87/00/00

UTTL: Integration considerations of a dynamic power conversion system for spacecraft applications
AUTH: A/BLAND, T. J.; B/CIACCIO, M. P.; C/ELIASON, J.; D/FISHER, M.; E/TOLLEFSON, S.
87A18168
86/00/00

UTTL: Powering future space systems
AUTH: A/HASLETT, R. A.
86A46181
86/00/00

UTTL: Design of a nuclear electric propulsion orbital transfer vehicle
AUTH: A/BUDEN, D.; B/GARRISON, P. W.
CORP: Los Alamos Scientific Lab., N. Mex.; Jet Propulsion Lab., California Inst. of Tech., Pasadena.
85A23394
85/02/00

UTTL: Reactor/organic Rankine conversion - A sota solution to near term high power needs in space
AUTH: A/NIGGEMANN, R. E.; B/LACEY, D.
86A24825
85/00/00

UTTL: Radiator concepts for high power systems in space
AUTH: A/FEIG, J. R.
86A20767
85/00/00

UTTL: Thermal management of high power space based systems
AUTH: A/HWANGBO, H.; B/MCEVER, W. S.
CORP: MRJ, Inc., Fairfax, Va.
86A20766
85/00/00

UTTL: Rotary radiators for reduced space powerplant temperatures
AUTH: A/ELLIOTT, D. G.
CORP: Jet Propulsion Lab., California Inst. of Tech., Pasadena.
86A20764
85/00/00

UTTL: Liquid droplet radiator technology issues
AUTH: A/MATTICK, A. T.; B/HERTZBERG, A.
CORP: Washington Univ., Seattle.
86A20762
CNT#: NAG1-327 F04611-81-K-0040
85/00/00

UTTL: Space nuclear power system and the design of the nuclear electric propulsion OTV
AUTH: A/BUDEN, D.; B/GARRISON, P. W.
CORP: Los Alamos Scientific Lab., N. Mex.; Jet Propulsion Lab., California Inst. of Tech., Pasadena.
84A37655
RPT#: AIAA PAPER 84-1447
84/06/00

UTTL: Advanced and nontraditional concepts working group report
AUTH: A/HERTZBERG, A.
CORP: Washington Univ., Seattle.
85N13909
84/04/00

UTTL: The liquid droplet radiator - an ultralightweight heat rejection system for efficient energy conversion in space
AUTH: A/MATTICK, A. T.; B/HERTZBERG, A.
CORP: Washington Univ., Seattle.
85N13900
84/04/00

UTTL: Advanced concepts liquid droplet radiator
AUTH: A/HERTZBERG, A.
CORP: Washington Univ., Seattle.
85N13899
84/04/00

UTTL: Multi-megawatt space power thermal management system requirements
AUTH: A/TAUSSIG, R. T.
84A21284
RPT#: AIAA PAPER 84-0056
84/01/00

UTTL: Promises and problems of Liquid Droplet Radiators for megawatt applications
AUTH: A/FULLWOOD, R. R.; B/FRAGOLA, J. R.; C/POWELL, J. R.
85A45431
84/00/00

UTTL: Review of the Tri-Agency Space Nuclear Reactor Power System Technology Program
AUTH: A/AMBRUS, J. H.; B/WRIGHT, W. E.; C/BUNCH, D. F.
CORP: National Aeronautics and Space Administration, Washington, D.C.; Defense Advanced Research Projects Agency, Arlington, Va.; Department of Energy, Washington, D. C.
85A45428
84/00/00

UTTL: Liquid droplet radiator collector development
AUTH: A/CALIA, V.; B/HASLETT, R.; C/KONOPKA, W.; D/KOSSON, R.
85A45376
84/00/00

UTTL: Nuclear space power systems for orbit raising and maneuvering
AUTH: A/BUDEN, D.; B/SULLIVAN, J. A.
84A32070
84/00/00

UTTL: Organic Rankine Cycle power conversion systems for space applications
AUTH: A/BLAND, T. J.; B/NIGGEMANN, R. E.; C/WREN, P. W.
84A30112
83/00/00

UTTL: Thermionic space reactors overview
AUTH: A/WETCH, J. R.; B/RASOR, N. S.; C/BRITT, E. J.; D/FITZPATRICK, G. O.
84A30033
83/00/00

UTTL: Long titanium heat pipes for high-temperature space radiators
AUTH: A/GIRRENS, S. P.; B/ERNST, D. M.
CORP: Los Alamos Scientific Lab., N. Mex.
83N24819
RPT#: DE82-014069 LA-UR-81-1054 CONF-820814-2
CNT#: W-7405-ENG-36
82/00/00

UTTL: Thermal management of large pulsed power systems
AUTH: A/HASLETT, B.
CORP: Grumman Aerospace Corp., Bethpage, N.Y.
83N15889
82/00/00

UTTL: Effects of reactor design, component characteristics and operating temperatures on direct conversion power systems
AUTH: A/FITZPATRICK, G. O.; B/BRITT, E. J.
CORP: Rasor Associates, Inc., Sunnyvale, Calif.
83N15857
82/00/00

UTTL: Long titanium heat pipes for high-temperature space radiators
AUTH: A/GIRRENS, S. P.; B/ERNST, D. M.
CORP: Los Alamos Scientific Lab., N. Mex.; Thermacore, Inc., Lancaster, Pa.
83A27127
CNT#: JPL-955935 NAS7-100
82/00/00

UTTL: Spacecraft radiative transfer and temperature control
AUTH: A/HORTON, T. E.
82A39949
82/00/00

UTTL: Heat pipes for NEP spacecraft radiators
AUTH: A/ERNST, D. M.
82A11748
81/00/00

UTTL: Titanium heat pipes for space power systems
AUTH: A/MEIER, K. L.; B/GIRRENS, S. P.; C/DICKINSON, J. M.
80A48261
80/00/00

UTTL: Experimental results for space nuclear power plant design
AUTH: A/RANKEN, W. A.
80A48259
80/00/00

UTTL: System tradeoffs in space reactor design
AUTH: A/COOPER, K. C.; B/PALMER, R. G.
80A48258
80/00/00

UTTL: 100-kWe nuclear space electric power source
AUTH: A/BUDEN, D.
80A10397
RPT#: AIAA PAPER 79-2089
79/10/00

UTTL: Optimisation of powerful energy supply systems for application in space
AUTH: A/BLUMENBERG, J.
79A53333
RPT#: IAF PAPER 79-169
79/09/00

UTTL: Nuclear-pumped lasers for space application
AUTH: A/NAFF, W. T.; B/FRENCH, F. W.
80A17450
79/00/00

UTTL: NEP heat pipe radiators
AUTH: A/ERNST, D. M.
79A51985
CNT#: NAS7-100
79/00/00

UTTL: Baseline design of the thermoelectric reactor space power system
AUTH: A/RANKEN, W. A.; B/KOENIG, D. R.
79A51932
79/00/00

UTTL: Selection of power plant elements for future reactor space electric power systems
AUTH: A/BUDEN, D.
79A51930
RPT#: CONF-790803-11 LA-UR-79-1239
79/00/00

UTTL: Heat pipe nuclear reactors for space applications
AUTH: A/KOENIG, D. R.; B/RANKEN, W. A.
78A35629
RPT#: AIAA 78-454
78/00/00

UTTL: Conceptual design of a heat pipe radiator
AUTH: A/BENNETT, G. A.
CORP: Los Alamos Scientific Lab., N. Mex.
78N20471
RPT#: LA-6939-MS
CNT#: W-7405-ENG-36
77/09/00

UTTL: General Electric preliminary design review data package for BIPS-ERDA PDR
CORP: AiResearch Mfg. Co., Phoenix, Ariz.
78N75242
RPT#: GE-BIPS-30-001
76/06/01

UTTL: Radioisotope power systems.
72A10387
RPT#: SAE AIR 1213
71/07/30

UTTL: Heat-rejection radiator mass and its influence in space power systems
AUTH: A/BONNEVILLE, J. M.
71A28597
71/03/00

UTTL: A 120 kWe thermionic reactor ion propulsion spacecraft for the Comet Halley rendezvous mission
AUTH: A/PRICKETT, W. Z.
71A25896
CNT#: JPL-952381
70/00/00

UTTL: The development of a 28-volt 500-watt thermionic power generator.
AUTH: A/HARBAUGH, W. E.; B/LONGSDERFF, R. W.; C/TURNER, R. C.
68A42557
CNT#: AF 33/615/-5095
68/00/00

UTTL: Application of heat pipes to SNAP 29.
AUTH: A/BIENERT, W. B.; B/FRANK, S.; C/HANNAH, R.; D/PETERS, J. T.
68A42553
68/00/00

UTTL: SNAP 29 system design and development.
AUTH: A/SCHEVE, M. R.
68A42552
68/00/00

UTTL: Review of the radiator design completed at the Institute for Nuclear Energy
AUTH: A/GROLL, M.; B/WEISSER, TH. W.
CORP: Technische Hochschule, Stuttgart (West Germany).
68N15042
RPT#: REPT.-5-39
67/07/00

UTTL: Summary
AUTH: A/GROVER, G. M.
CORP: Los Alamos Scientific Lab., N. Mex.
74N71731
66/07/08

UTTL: Integrated system
AUTH: A/BLACKSTOCK, A. W.
CORP: Los Alamos Scientific Lab., N. Mex.
74N71728
66/07/08

UTTL: Moving belt radiators
AUTH: A/FENSTERMACHER, C. A.
CORP: Los Alamos Scientific Lab., N. Mex.
74N71724
66/07/08

UTTL: Lectures on nuclear thermionic electric propulsion for space
AUTH: A/SALMI, E. W.
CORP: Los Alamos Scientific Lab., N. Mex.
74N71718
RPT#: LA-3412-MS
CNT#: W-7405-ENG-36
66/07/08

SEARCH TITLE: SPACECRAFT RELIABILITY

DESCRIPTION:

1. Lunar Spacecraft
2. Space Power Reactors
3. Thermonuclear Power
4. Thermoelectric Power
5. Thermionic Power Generation
6. Nuclear Electric Power
7. Spacecraft Shielding
8. Spacecraft Reliability

The above entries were combined using Boolean logic to refine a search strategy, and it was used with the above set numbers only.

Logic Statement: (1+2+3+4+5+6+7)*8

Proceedings of Eighth Aerospace Testing Seminar, Los Angeles, California, 21-23 March, 1984 /
xiv, 237 p. : ill. ; 28 cm.
85V16808

UTTL: SP-100 missions overview
AUTH: A/WALLACE, RICHARD A.
CORP: Jet Propulsion Lab., California Inst. of Tech., Pasadena.
87A21808
87/00/00

UTTL: Space nuclear power systems 1985; Proceedings of the Second Symposium, Albuquerque, NM, Jan. 14-16, 1985. Volumes 3 & 4
AUTH: A/EL-GENK, MOHAMED S.; B/HOOVER, MARK D.
87A21801
87/00/00

UTTL: An approach to space reactor system selection and design
AUTH: A/BUDEN, D.; B/LEE, J. H., JR.
86A20737
85/00/00

UTTL: Space reactor safety
AUTH: A/BUNCH, D. F.
85A45433
84/00/00

UTTL: Aerospace Testing Seminar, 8th, Los Angeles, CA, March 21-23, 1984, Proceedings
85A38251
84/00/00

UTTL: Radiation hardened package for integrated electronics
AUTH: A/MERKER, M.; B/SCHMID, A.; C/SPRATT, J.; D/STROBEL, D.
85A32189
CNT#: F29601-82-C-0023
83/00/00

UTTL: Large discharges and arcs on spacecraft
AUTH: A/ROSEN, A.
75A32453
CNT#: F04701-69-C-0091
75/06/00

UTTL: Fusion power for space propulsion.
AUTH: A/ROTH, R.; B/RAYLE, W.; C/REINMANN, J.
72A35953
72/04/20

UTTL: Heat transfer and spacecraft thermal control
AUTH: A/LUCAS, J. W.
71A25360
71/00/00

UTTL: Navigating the grand tours
AUTH: A/BALL, J. E.; B/DUXBURY, T. C.
70A41799
70/09/00

UTTL: Quality and reliability for moon launch vehicles
AUTH: A/PENO, R. E.; B/SENN, G. A.
70A42384
70/08/00

UTTL: Relation of meteoroid protection to the luminous efficiency
AUTH: A/VORREITER, J. W.
70A32518
70/06/00

UTTL: TOPS' trails to outer planets map a new route to reliability
AUTH: A/ROSENBLATT, A.
70A25368
70/03/30

UTTL: Meteoroids and the safety of spacecraft
AUTH: A/MARCINEK, J. B.
70A42524
70/00/00

UTTL: Simulation of space corpuscular radiation
AUTH: A/WOHLLEBEN, K.
70A38284
70/00/00

UTTL: Conclusions
AUTH: A/HOLLY, F.; B/JANNI, J.
70A17273
69/12/00

UTTL: Study of structural-thermal insulation-meteoroid protection integration
AUTH: A/ARMSTRONG, W. H.; B/CORNETT, D. W.
CORP: Boeing Co., Huntsville, Ala.
70N12537
RPT#: NASA-CR-102364 D5-17525
CNT#: NAS8-21430
69/05/15

UTTL: Compact ZrH reactor development status and reactor thermoelectric space power systems.
AUTH: A/KITTERMAN, W. L.; B/WILSON, R. F.
69A31723
CNT#: AT/30-3/-701
69/05/00

UTTL: Impact of the thermionic reactor on advanced space vehicles.
AUTH: A/BREUER, F. D.; B/POWELL, D. J.
68A44249
RPT#: IAF PAPER SD-111
68/10/00

UTTL: Effectiveness of multisheet structures for meteoroid impact protection.
AUTH: A/SENNETT, R. E.
68A27107
68/05/00

UTTL: Optimization of thermionic generator systems of high reliability.
AUTH: A/DE WINTER, F.; B/SHIMADA, K.
68A37738
68/00/00

UTTL: Design and integration study of an RTG powered Voyager spacecraft.
AUTH: A/KIRPICH, A.
68A17137
67/00/00

UTTL: Jupiter flyby application - Advanced planetary probe
CORP: Jet Propulsion Lab., California Inst. of Tech., Pasadena.
68N88679
RPT#: NASA-CR-97384 JPL-EPD-358
CNT#: NAS7-100
66/05/02